# THE SEPARATION OF VISUAL AXES IN APPOSITION COMPOUND EYES

By G. A. HORRIDGE, F.R.S.

*Department of Neurobiology, Australian National University, Canberra, Australia* 2600

(*Received* 7 *September* 1977)

[Plates 1–8]

## CONTENTS



 [Published 5 December 1978

Measurements of the interommatidial angle ($\Delta\phi$) and facet diameter ($D$) *of the same ommatidia* in a number of insects and crustaceans with large eyes have been related to the effective intensity at which the eye functions by the following theory. The highest spatial frequency which the eye is able to reconstruct as a pattern is limited by the interommatidial angle $\Delta\phi$, which is the sampling angle, because two ommatidia are required to cover each cycle of the pattern. At the same time, the absolute modulation of light in the receptors caused by the pattern depends on three interdependent factors.

(*a*) The theoretical minimum angular sensitivity function, which has a width of $\lambda/D$ at the 50% level. The wavelength $\lambda$ is taken as 0.5 μm. This component is not only the limiting angular resolving power of the lens: it reduces modulation caused by all patterns, with greater loss at higher spatial frequencies. Larger lenses increase resolution and sensitivity.

(*b*) The effective light catching area of the rhabdom. This is the angular subtense of the rhabdom area (the receptor) as seen in the outside world (i.e. subtended through the posterior nodal point of the lens), and is the equivalent of the grain size in a film. Large receptors favour sensitivity at the expense of resolution.

(*c*) The $F$ value or focal ratio $f/D$, as in the camera, where $F$ is the distance from the focal plane to the posterior nodal point. Larger $F$ values increase sensitivity.

The modulation resulting from these three factors is then set so that it exceeds the noise caused by the random arrival of photons at each ambient intensity. From this, the optimum value of the product $D\Delta\phi$ (known as the eye parameter) can be calculated for eyes adapted to any ambient intensity. The same result is reached by a recent theory of Snyder, Stavenga & Laughlin (1977) who calculate the value of $D\Delta\phi$ which allows the eye to reconstruct the maximum number of pictures despite photon noise. The eye parameter (divided by half the wavelength) is the ratio of the highest spatial frequency passing the lens to the highest spatial frequency reconstructed by the eye. Compound eyes should have larger facets and interommatidial angles than predicted by diffraction theory alone because photon noise must be exceeded at all intensities. Theoretically, $D\Delta\phi$ lies in the range 0.3 to 0.5 for bright light insects and is increased to 2.0 or more for those active in dim light. As well as depending on intensity, $D\Delta\phi$ should depend on factors such as the typical angular velocity and level of intensity discrimination at which the eye is used. As $D\Delta\phi$ can be measured from the outside of the eye, the theoretical predictions can be compared with measured values.

Most of this paper consists of maps of the values of $D\Delta\phi$ for eyes of a variety of arthropods from different habitats. The maps are made by a new convention in which the minimum theoretical field of each ommatidium is placed in angular coordinates

as a circle of diameter $\lambda/D$ with centre on the axis at the place where it lies on the eye. To do this, a value of $\lambda$ must be assumed. Every fifth facet is taken on most maps with the fields magnified five times. The overlap or separation of these circles of diameter $\lambda/D$ shows the local value of $D\Delta\phi$ for any direction for each part of the eye. The method is independent of horizontal and vertical axes, of directions of facet rows, of regularity of facets and of eye radius. The problem of mapping a surface with double curvature upon a flat sheet was solved approximately by working with strips taken along the eye surface. Equal distances on the map then represent equal angles in any direction; with this projection there are no poles, and axes are arbitrary.

Maps of $D\Delta\phi$ reveal that compound eyes differ according to the intensity of light they normally encounter; eyes of animals which are active in bright light have smaller values of $D\Delta\phi$. The smallest value of about 0.3 is found in the forward facing acute zone of the sand wasp *Bembix*, which hovers while hunting in bright sunshine. The absolute limit set by diffraction of 0.25 (for square facets) is approached but never reached. Values of $D\Delta\phi$ up to about 2.0 or even 4.0 are found in crepuscular animals which have apposition eyes. The interpretation is that the values of $D$ and $\Delta\phi$ are the result of a compromise between contrast sensitivity and resolution. An increase in aperture provides increased modulation and therefore increased sensitivity, but the additional angular resolving power which comes with the increased aperture is not used because sensitivity is also enhanced by an increase in the receptor size. The ommatidium then detects only the lower spatial frequencies (wider stripes) from the range which passes the lens. In an ommatidium optimized for any but the highest known intensities, both $\Delta\phi$ and $D$ (and therefore $D\Delta\phi$) are larger than they would have to be if set at the diffraction limit.

The maps also reveal that many apposition compound eyes have one or more regions of smaller $\Delta\phi$, called acute zones. None of the eyes are spherically symmetrical; all have gradients of both $D$ and $\Delta\phi$, and all have regions where $\Delta\phi$ varies in different directions on the eye surface. The acute zone is usually forward looking, but is upward looking in some insects which catch prey or mate in flight. In addition, some dragonflies have a lateral acute zone. In the acute zone the facet pattern is always more regular than elsewhere.

Some acute zones, as in the locust (*Locusta*), the mantid *Orthodera* and the ghost crab *Ocypode*, are formed by reduction in $\Delta\phi$ with little compensatory increase in $D$. Others such as the native bee *Amegilla*, the dragonfly *Austrogomphus*, and the mantid shrimp *Odontodactylus* have larger values of $D$ which match the decreasing $\Delta\phi$ towards the centre of the acute zone, so that $D\Delta\phi$ remains constant. Others again, particularly the wasp *Bembix*, the dragonflies *Hemicordulia*, *Orthetrum* and several mantids, show an increase in $D$ which is insufficient to compensate for the large decrease in $\Delta\phi$, so that $D\Delta\phi$ is smaller in the acute zone. A reduced $D\Delta\phi$ in the acute zone may imply that it requires brighter light or more time than the rest of the eye in order to make full use of its increased sampling density.

Mapping the regional differences of the theoretical resolving power of the ommatidia, and of the potential spatial resolution of different parts of the eye is only the first step towards understanding the functions of the different eye regions. The anatomical basis of the optics, the actual field sizes of receptors as measured physiologically, the part played by binocular overlap, the regional differences in the mechanisms of integration behind the eye, and the patterns of behaviour that are dependent on each eye region, remain to be elucidated.

## Introduction

The form of the compound eye lends itself to the interpretation of the basic optics and density of sampling stations in terms of function, and a number of attempts have been made in this direction (Mallock 1894; Zänkert 1939; Barlow 1952; Kirschfeld 1976). It is indeed an attractive proposition to suggest that the sizes of facets and interommatidial angles can be related to

function for a wide variety of species and eye regions. However, the optical axes of even the commonest insect's eyes are undescribed except for a few limited regions in two or three species, and both theory and observations available in the literature are rudimentary. In particular, where a compound eye has large facets, or a region of the eye has facets larger than elsewhere, we do not know whether the facets are larger to improve the resolution of each ommatidium or to catch more light to overcome photon noise at low light levels. Seeing maximum detail implies a minimum angle between ommatidial axes, but because the area of eye surface is limited, larger facets imply correspondingly fewer of them. Recently however a comprehensive theory has appeared which shows the optimum compromise between having maximum numbers of ommatidia and also facets of maximum size (Snyder 1977; Snyder *et al.* 1977). This theory predicts, for example, that an ommatidium used in bright light will have a rhabdom with a narrow tip to preserve all the resolution of the lens because sensitivity can be sacrificed. On the other hand an ommatidium adapted to dimmer light will have a broad rhabdom that gives it a broad receptive field, even though the aperture may be large. We can distinguish between the two cases without examining the rhabdom or measuring the physiological field size because the narrow field ommatidia have to be at smaller angles to each other so that the density of sampling points is sufficient to reconstitute all the detail that the individual ommatidia can resolve. The dim light eye, on the other hand, will have large interommatidial angles even though the facets are large, because otherwise there would be too much overlap of the larger visual fields that are caused by larger rhabdoms. A perfectly adapted eye or eye region will not have more sampling stations than is justified by the diameter of the field of each. The work which follows is a summary of this theory, followed by systematic measurements of actual eyes in the form of maps which illustrate these principles. Needless to say, the analysis can be carried much farther than the two measurements of interommatidial angle and facet diameter which appear in the elementary theory (Horridge 1977*a*).

The most convenient method of producing maps of the directions of the visual axes is to use the pseudopupil as described below. The pseudopupil is the black spot seen in the eye always facing the observer. Although the value of the pseudopupil has been recognized for almost a century as giving the direction of the optical axes of the ommatidia at each place on the eye (Exner 1891), only recently has it been used for making maps in angular coordinates (Beersma, Stavenga & Kuiper 1975) in a way that can be related to visual behaviour and the function of different parts of the eye. Regional differences in interommatidial angle have been discussed from time to time in relation to function (Dietrich 1909; Demoll 1910 (p. 480 onwards); Baumgärtner 1928; Friedrichs 1931; del Portillo 1936) but the angles described were from histological sections and were inaccurate because the axis is not perpendicular to the corneal surface and refraction at the two surfaces of the cornea is difficult to estimate.

Quite recently it was a valid inference from the literature to say that 'Among insects other than flies, a distinct region of high acuity (large facet size, low curvature) is uncommon, but is found in some predatory species like praying mantids' (Collett & Land 1975). However, as mapping of visual axes proceeded, it quickly became evident that large compound eyes in many insects with complex visual behaviour are far from uniform in interommatidial angle. Regions are revealed where the pseudopupil is larger than elsewhere, or it changes in shape, and these eye regions clearly differ in function. The most obvious special areas, called here acute zones, have a smaller interommatidial angle than elsewhere, and frequently they have larger facets than elsewhere. To confuse the issue, a fovea has been recently described in a

mantid eye (Barros-Pitá & Maldonado 1970) in which the region essential for the strike behaviour turned out to be a horseshoe shaped area encircling the central region of smallest interommatidial angle and not the acute zone of maximum sampling density as the acute zone is defined here (Levin & Maldonado 1970). The term fovea has also been used for the forward looking acute zone of the eye of the male hoverfly *Syritta* where smaller interommatidial angles, measured from the pseudopupil, were correlated with larger facet diameters (Collett & Land 1975). In the present work the term fovea has been abandoned in favour of 'acute zone' because in compound eyes the gradients of sampling angle take all shapes, sizes, accentuation and direction in a way quite unlike the foveas of vertebrate eyes. Indications of possible acute zones can be found in many systematic works of insects and Crustacea in which the size or arrangement of facets is a systematic character, for example Smart & Clifford (1965) on simuliid flies and Kemp (1913) on mantid shrimps. Despite his wide experience, Hesse (1908) mentioned that in the the central regions, the ommatidia with larger facets are inclined at smaller angles to each other only in mantid eyes. Regions of larger facets are mentioned in many groups of insects, with partial descriptions, but the whole subject of the optics, anatomy and function of acute zones and their integration in the optic lobe is unexplored. Therefore, measurements of the interommatidial angle ($\Delta\phi$) and the diameter ($D$) of the same facets, to provide data to test the new theories based on photon noise, quickly become a study of different kinds of acute zones.

## Definitions

Many of the terms used in particular ways in this account are newly applied to compound eyes as extensions from other branches of science. The intended meanings are as follows.

### (*a*) *Terminology*

*Aperture and facet diameter.* Because facets are rarely circular and the effective optical aperture may be smaller than the diameter on the corneal surface (or even larger where the refracting surface is on the *inside* of the cornea), the aperture and facet diameter have been defined as the centre to centre separation of the facets at the corneal surface.

*Binocular overlap:* the angle between the midline of the head and the most extreme median visual axis. Stated binocular overlaps always refer to the edge of the eye in proximity to the dorsal or anterior fovea; ventral overlaps have not been studied.

*Focal ratio:* the ratio $f/D$ ($= F$ stop in photography), where $f$ is the distance of the focal plane from the posterior nodal point of the lens and $D$ is the lens diameter.

*Acute zone:* a region where the angles between the *optical axes* of receptors ($\Delta\phi$) are less than the general average for the eye or for surrounding regions of the eye.

*Types of acute zones:* descriptive terms for acute zones of different shape are *deep* versus *shallow* and *small* versus *broad*. A deep zone is one with considerable local reduction in $\Delta\phi$, a broad one spreads over a large solid angle on the eye. To have an acute zone which is both broad and deep requires a physically large eye.

*Interommatidial angle* $\Delta\phi$*:* the angle between the *optical axes* of adjacent ommatidia. This angle depends on which nearest neighbours are selected. Although facets are squares or regular hexagons the interommatidial angle depends on the direction of the row that is selected. Usually there is a two dimensional gradient of $\Delta\phi$ at every point on the eye, as shown in maps of the optical axes of ommatidia in angular coordinates.

*Isopupil lines:* the track of the pseudopupil *centre* as it moves across the surface of a compound eye which is tilted in a series of steps about a defined axis. An isopupil line is a line of optical axes in one plane and does not, in general, correspond to a line of facets. The baselines (0° on the maps) are usually through the centre of the acute zone. Often one baseline looks forwards parallel to the median plane through the head (0° H) and the other (0° V) is parallel to the horizontal when the eye is in its normal position.

*Optical axis:* the direction of rays that are best focused on the rhabdom and therefore the direction of maximum sensitivity to a distant point source. It has been assumed that the optical axis of an ommatidium is the direction in space at which that ommatidium is in the centre of the pseudopupil.

*Optical radius (R):* the length of the optical axis of an ommatidium when it is continued into the eye until it meets the optical axis of the neighbouring ommatidium. This is the eye radius measured optically.

*Posterior nodal point* (p.n.p.). Rays drawn through this point are parallel outside the eye to their path inside the eye. When taken relative to the p.n.p., therefore, angles inside the eye can be directly related to angles measured outside the eye without further reference to the optics or refractive index of the internal medium. For a single spherical refracting surface, the p.n.p. is at the centre of curvature.

*Resolution, resolving power and acuity.* For compound eyes it is essential to have two clearly separate terms, one for the properties of a single lens, and another for the ability of several ommatidia together to reconstruct the separate parts of a pattern. The term (*limiting*) *angular resolving power* (of the lens) has been reserved for the theoretical optimum performance when a single lens is optically perfect. At the focus, the spatial frequency cut-off is $D/\lambda$ rad$^{-1}$ and the width of the Airy disk at 50 % intensity is $\lambda/D$ rad, subtended at the posterior nodal point, where $\lambda$ is the vacuum wavelength and $D$ is the diameter of the aperture. For an eye immersed in water, the width of the Airy disk is reduced by a factor of 1/1.33, if the lens remains focused on the rhabdom, so that theoretical resolution is improved.

The term *spatial resolution* (of a region of the eye) is the sampling interval which determines the ability to reconstruct a pattern. For the special case of regular stripes and sufficient modulation to reach the threshold signal, the minimum stripe period that can be reconstructed is twice the interommatidial angle ($2\Delta\phi$). The maximum spatial frequency reconstructed, given perfect optics, sufficient light and small enough fields, is only dependent on interommatidial angle, and is equal to $1/2\Delta\phi$ rad$^{-1}$.

We still have available the term *acuity*, which can be reserved for the performance of animals in behavioural tests. The acuity of the eye then depends not only on $D$ and $\Delta\phi$ but also on light intensity, angular velocity of the object relative to the eye, duration of seeing, contrast, colour and so on. As will be seen, these factors can be analysed only when the resolving power and spatial resolution have been defined, that is when the maps of $D$ and $\Delta\phi$ are available.

### (*b*) *Notation*

Angles in the optics of a single ommatidium are measured about the posterior nodal point (p.n.p.). This has the result that angles measured outside the eye (e.g. $\Delta\phi$, $\Delta\rho$) are unaffected by the value of the internal refractive index when compared with or calculated from angles inside the eye (e.g. $\Delta\alpha$, $\Delta\sigma$) as in figure 2. When the eye moves from air to water the position of the p.n.p. moves back within the eye.

The following notation appears throughout this paper:

$\Delta\alpha$ angular diameter of the Airy disk measured at 50 % intensity

$\Delta\sigma$ angular diameter of the effective light capture cross section of the rhabdom subtended at the p.n.p.

$\Delta\rho$ angular diameter of the angular sensitivity function at 50 % sensitivity

$\Delta\rho_{LA}$ value of $\Delta\rho$ stressing the state of adaptation at which the eye is used (usually light adapted)

$\Delta\theta$ period of regular striped pattern of sinusoidal intensity modulation, measured as the angle subtended at the eye

$\Delta\tau$ angular radius of the Airy disk to the first minimum, subtended at the p.n.p.

$\Delta\phi$ interommatidial angle, measured between optical axes

$\Delta\phi_H$ the angle between the axes of adjacent ommatidia of a row when rows of optical axes are horizontal

$\Delta\phi_V$ similar to $\Delta\phi_H$, but for the axes of ommatidia in vertical rows (Note that the pattern of *axes* is usually not hexagonal and therefore $\Delta\phi_V$ is not equal to $\frac{\sqrt{3}}{2}\Delta\phi_H$.)

$d$, $d_1$, $d_2$, $d_3$ linear diameters of the rhabdom tip

$D$ centre to centre distance between facets

$f$ distance from rhabdom tip to posterior nodal point

$F$ focal ratio or $F$ value of the lens, $f/D$

$\phi$ angles measured round the eye

$\lambda$ wavelength, vacuum

$M$ peak to peak modulation of intensity in a sinusoidal pattern of period $\Delta\theta$

$m$ peak to peak modulation of intensity at the rhabdom tip, arising from $M$

$\bar{N}$ average photon flux at the rhabdom tip caused by an extended object

$I_{max}$ and $I_{min}$ the maximum and minimum photon flux during the modulation $m$

$R$ local optical radius. This is the distance from the surface of the eye to the point where the optical axes of two adjacent ommatidia cross. At any point on the eye, $R = D/\Delta\phi$

$s$ sensitivity to a point source, measured at the peak of the angular sensitivity curve. Sensitivity is measured as the reciprocal of the number of photons/(cm$^2$ s$^{-1}$) of parallel light on the optical axis at optimum wavelength which give a response of 50 % saturation (Laughlin 1976*a*, for dragonfly retinula cells)

$S$ sensitivity to a diffuse source, and therefore dependent upon the width of the field as well as upon $s$

## Theory

### (*a*) *The need for maps of compound eyes*

A method is required to map the optical features of the eye in a way that relates to theory, but which also acts as a description of the measurable parameters of the eye. The optical axis of each ommatidium can be represented by a dot in two dimensional angular coordinates. Ideally this would be done on the surface of a spheroid which varies in radius according to the optical radius of the eye at each point. However, as for maps of the world, the practical requirement is a two dimensional representation on paper and in this case the particular projection selected is the natural consequence of the method of collecting the data (see below).

When we consider how the ommatidia are put together to make an eye, we see that some measurements are critical. These are:

(*a*) The angle between the optical axes of neighbouring ommatidia measured along a known axis: in two dimensions this angle fixes the density of optical axes per unit solid angle.

(*b*) The field width of the receptors, which together with (*a*), determines the overlap of visual fields.

(*c*) The aperture of the lens of each ommatidium which influences (*a*) by anatomical and (*b*) by optical constraints.

By definition of $R$,

$$\Delta\phi = D/R \text{ rad}, \tag{1}$$

where $\Delta\phi$ is the local interommatidial angle, $D$ is the lens diameter, and $R$ is the local optical radius. This equation applies at each point on the eye surface, but $\Delta\phi$, and therefore also $R$, can be different along the various axes at the same point on the eye: also the lens diameter is not necessarily equivalent to the facet diameter, which in turn is not circular. It is assumed that, in eyes that have been optimized for excellent vision by a long period of natural selection, the effective aperture is as large as possible. Therefore, unless otherwise stated, it is assumed that the aperture $D$ is the same as the centre to centre spacing of the facets and that facets are circular. It is a general observation that minimal space is wasted on the surface of the eye. Maps of the eye could show the field size of the receptors in each ommatidium. The relation between interommatidial angle $\Delta\phi$ and the width of the field $\Delta\rho$ would then illustrate the overlap of the fields at each point and in each direction on the eye. Some day perhaps this will be, but at present the best that can be done is to map the theoretical minimum field of each ommatidium as limited by the aperture of its facet. Maps of the narrowest possible field ($\lambda/D$ rad), interommatidial angle ($\Delta\phi$) or the local optical radius of the eye ($D/\Delta\phi$) can be made from a series of photographs of the pseudopupil taken at different angles from outside the eye.

### (*b*) *The question of focus*

It is assumed that the Airy disk is focused sharply by the corneal lens on the end of the rhabdom because a poor focus throws away resolution with no compensatory gain in sensitivity. Many demonstrations of small fields indicate a sharp focus, for example in the locust (Wilson 1975), in large flies (Kuiper 1966; Horridge, Mimura & Hardie 1976) and in dragonflies (Laughlin 1976*b*). The same may be inferred from numerous experiments on antidromic illumination of the eyes of flies (Franceschini & Kirschfeld 1971) or from the light reflected from the eyes of butterflies, beautifully illustrated by Miller & Bernard (1968). For most of the eyes to be described, the only relevant observation is one made on the pseudopupil as follows. When observed with a microscope of long focal length (3 cm) and numerical aperture of about 0.05, the pseudopupil stays in focus over a considerable distance when the compound eye surface is defocused. This property of the pseudopupil is explained by supposing that the rhabdom tip and surrounding screening pigments which absorb light and give rise to a pseudopupil are near the optical axis in the focal plane of the corneal lens, so that the pseudopupil is formed by the lack of rays reflected from near the optical axis in the focal plane. For a single facet, these missing rays form a narrow cone outside the eye. As one moves across the retina from the centre of the pseudopupil, a decreasing proportion of missing rays from each facet enters the observing instrument. Therefore *the contrast of the pseudopupil* is less affected than that of the eye surface by defocusing the observing instrument. This test, first outlined to me by Professor Kirschfeld,

with reference to antidromic illustration of the bee eye, suggests that all of the large diurnal insects which have apposition eyes and depend on good vision have lenses that are focused upon the rhabdom. The same probably does not apply in general to compound eyes that are small or have large rhabdoms.

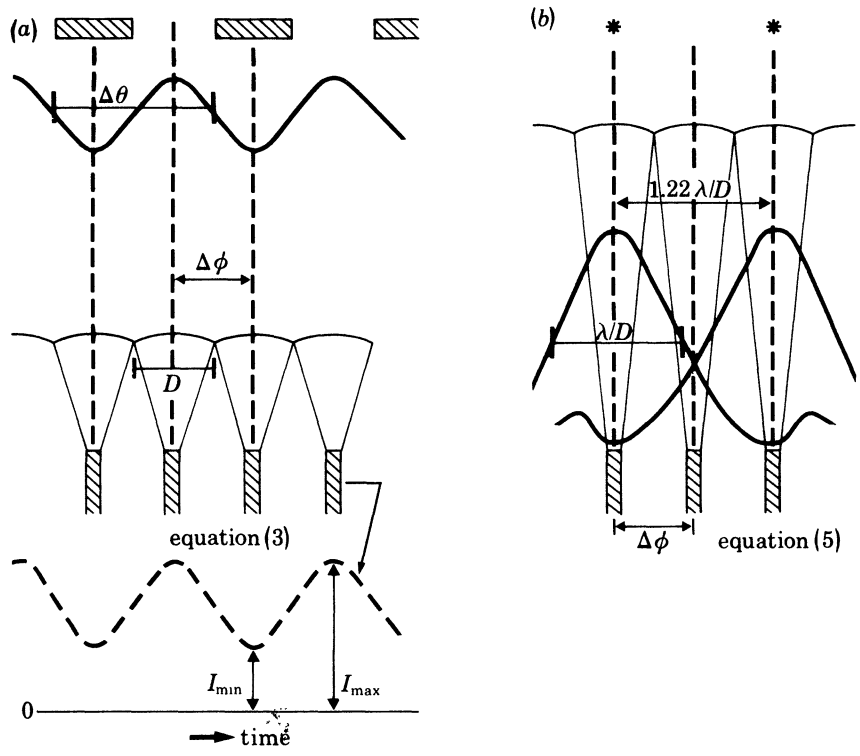


FIGURE 1. Diagram matching the sampling angle to the minimum angular resolving power so that an object which can be resolved can also be reconstructed by the eye. (*a*) Sinusoidal spatial pattern as an example of an extended object; (*b*) two point sources, by the Raleigh criterion. Note that both of these situations assume that an abundance of photons is available at the receptor.

### (*c*) *The sampling criterion*

With a striped pattern of sinusoidal intensity distribution in front of a compound eye there is a minimum sampling density of ommatidia in that the interommatidial angle has to be half of the period of the pattern, as shown in figure 1*a*. If there is a greater density of ommatidia, some are superfluous and if the interommatidial angle is greater than this maximum, the pattern as a whole cannot be reconstructed within the eye.

With an infinitely extended sinusoidal pattern there is a minimum period which an aperture $D$ can resolve. By diffraction theory, this minimum pattern period is given by

$$\Delta\theta = \lambda/D \text{ rad}. \tag{2}$$

When $\Delta\theta < \lambda/D$, a sinusoidal pattern generates no modulation at all. For the same eye in water, if focus is retained,

$$\Delta\theta_W = \lambda/nD, \tag{2a}$$

where $n$ is the refractive index of water. Angular resolving power is therefore better underwater than in air.

There is no point in having a sampling density of ommatidia greater than is required to reconstruct the finest pattern that can pass the lens. Let us put the required interommatidial angle:

$$\Delta\phi = \tfrac{1}{2}\Delta\theta \tag{3}$$

together with the diffraction limit in one dimension for square facets:

$$\Delta\theta = \lambda/D$$

so that

$$D\Delta\phi = \tfrac{1}{2}\lambda = 0.25\ \mu\text{m} \quad \text{when } \lambda = 0.5\ \mu\text{m}. \tag{4}$$

The eye parameter $D\Delta\phi$, which is measurable from the outside of the eye, should be 0.25 for square facets and 0.3 for hexagonal facets (Snyder 1977) but we will see in the next section that a different set of assumptions yields a different result when the intensity at which the eye functions is taken into account.

### (*d*) *The Raleigh criterion*

Instead of an extended regular pattern, consider the task of a compound eye which is designed to see as separate two small points of light. For this task, Lord Raleigh set out an arbitrary criterion that agrees with the human ability to separate two points for an unstated intensity of bright light. The two point sources can be resolved when the peak of the Airy disk caused by one alone falls on or outside the ring of the first dark minimum of the Airy disk of the other. The *radius* of the Airy disk to the first dark ring is:

$$\Delta\tau = 1.22\,\lambda/D \text{ rad.} \tag{5}$$

As illustrated in figure 1*b*, in order to separate the two points and also see the dark space between, there have to be *three* ommatidia participating, so that $2\Delta\phi = \Delta\tau = 1.22\,\lambda/D$ from which $D\Delta\phi = 0.305\ \mu\text{m}$.

The eye parameter $D\Delta\phi$ is larger on the Raleigh criterion than on the diffraction cut off criterion because the former allows for some modulation if applied to an extended sinusoidal pattern, whereas the cut off criterion can never be reached because it is the limit at which the modulation of light at the receptor disappears. We have therefore introduced the idea that the eye parameter $D\Delta\phi$ can be adapted to a required level of signal modulation; and at a subsequent step in the theory the required signal:noise ratio is substituted for the modulation level.

The exact minimum value of $D\Delta\phi$ at the absolute cut off cannot in fact be inferred from the size and pattern of the facets, despite what has been said, for the following reasons. If resolution along only one direction of the rows of visual axes is paramount then the minimum $D\Delta\phi = 0.25$, as calculated. However if all directions have equal weight, the limit is near 0.3 for a hexagonal array and 0.25 for a square array. As will be shown, even when the facets are superficially regular hexagons, there is often quite a different, sometimes square, array of *visual axes*. The pattern of axes is not constant over the eye and the directions of the functionally significant correlations between axes are usually unknown.

### (*e*) *The origin of the acceptance angle* $\Delta\rho$

The diameter of the Airy disk at its 50 % intensity contour, from tables of Bessel functions, turns out to be almost exactly $\lambda/D$ radians

$$\Delta\alpha = \lambda/D. \tag{6}$$

This is a more convenient measure than the usual one (which is: angular *radius* of Airy disk to 1st dark ring $= 1.22\,\lambda/D$) because field widths ($\Delta\rho$) of photoreceptors of insects are also

measured as the diameter at the 50 % sensitivity contour, and because $\lambda/D$ coincides with the theoretical cut off.

The field of the photoreceptor is defined as the sensitivity towards a point source as a function of angle, and sensitivity is the reciprocal of the number of photons required to make a criterion response. The optical axis is defined as the axis of symmetry of the field. Usually it is the direction from which the light has maximum effect.

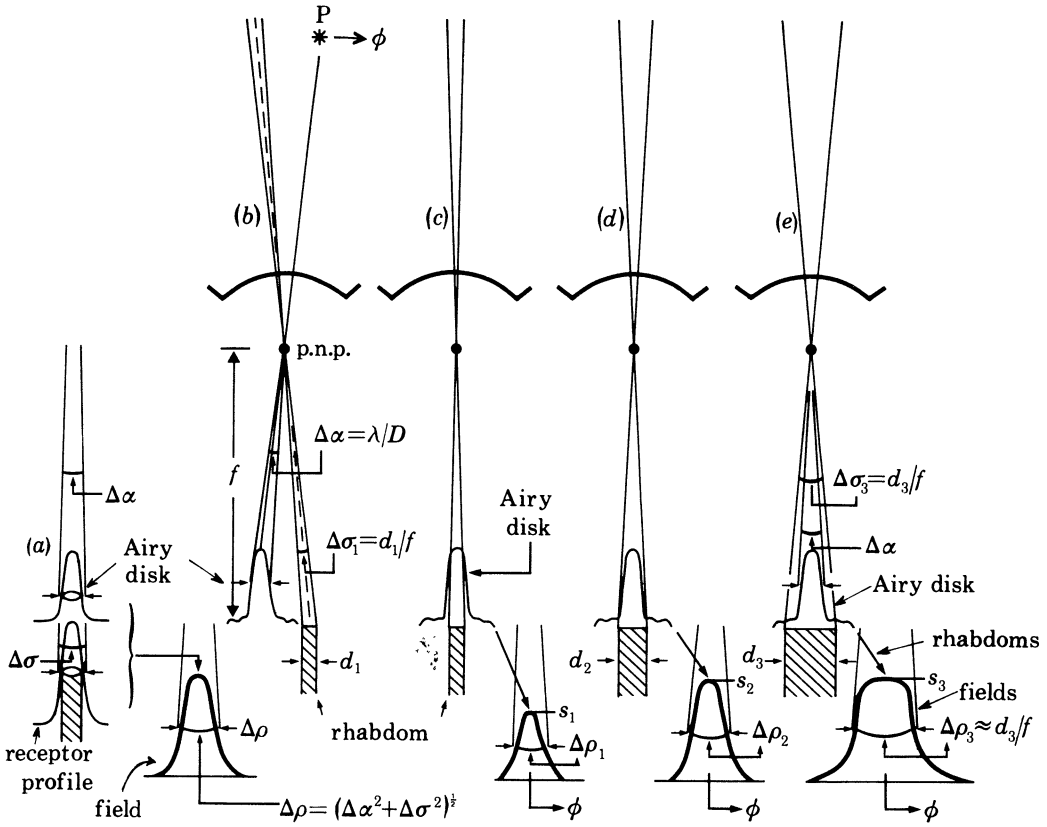


FIGURE 2. Origin of the angular sensitivity function of a receptor behind a small lens, in a single focused ommatidium. (*a*) In this model the angular sensitivity is Gaussian of width $\Delta\rho$, formed by convulution of a Gaussian shaped Airy disk and a Gaussian shaped rhabdom profile, as in equation (7). (*b*) A point source P, moving through an angle $\phi$, generates an Airy disk which moves across the cross section of the rhabdom. At the posterial nodal point (p.n.p.) the Airy disk subtends an angle $\Delta\alpha = \lambda/D$, whereas the rhabdom subtends an angle $\Delta\sigma_1 = d_1/f$. (*c*) (*d*) and (*e*) Increase in the rhabdom width causes increased sensitivity ($s_2$, $s_3$ compared to $s_1$), and increasing width of the angular sensitivity function ($\Delta\rho_{1-3}$) which progressively becomes flat topped ($s_3$).

The structure which catches the light is the rhabdom tip. As the Airy disk moves across it, the top of the rhabdom cuts off progressively more light up to a maximum when the Airy disk is centred on the rhabdom, then progressively less as the Airy disk moves off (figure 2*b*, *c*). In this way, the angular sensitivity of the receptor cell is a two dimensional bell shaped surface which is formed by the convolution of the Airy disk with the shape of the end of the rhabdom. The Airy disk can be approximated by a Gaussian function of width $\lambda/D$ at the 50 % intensity contour (figure 2*a*).

If the rhabdom tip is a circular disk of diameter $d$ and if geometrical optics are assumed, the convolution yielding the field shape is given by standard tables of the offset circle probabilities for the normal distribution function, as done by Horridge, Mimura & Hardie (1976). As the

rhabdom diameter $d$ increases in the range $\frac{1}{2}\Delta\alpha f < d < 2\Delta\alpha f$ the field width increases only slowly, but the sensitivity (the height of the peak, $s$ in figure 2*c*, *d*, *e*) increases with the increasing area of the rhabdom tip. In the range $2\Delta\alpha < d/f < \infty$, the value of $\Delta\rho$ becomes independent of $\lambda$ or $D$ and approximates to $d/f$. The angular sensitivity curves become progressively more flat topped (figure 2*d*, *e*). These field shapes are awkward because only numerical methods are available for the further calculations required to give the intensity modulation caused by various patterns.

A more amenable method is to approximate the light capturing properties of the rhabdom by a Gaussian surface of angular width $\Delta\sigma$ subtended at the posterior nodal point (figure 2*a*). The field size is then given by the convolution of two Gaussian functions which gives a third Gaussian of width $\Delta\rho$ at 50 % sensitivity, according to the relation:

$$\Delta\rho^2 = \Delta\alpha^2 + \Delta\sigma^2 = (\lambda/D)^2 + (d/f)^2. \tag{7}$$

The two factors $\Delta\alpha$ and $\Delta\sigma$ both contribute to $\Delta\rho$ when they are nearly equal. This means that when the rhabdom is small compared to the Airy disk the angular sensitivity curve approximates closely to the Airy disk in width and when the rhabdom is comparatively large its angular subtense ($d/f$) dominates the angular sensitivity (figure 2*e*), in which case:

$$\Delta\rho = \Delta\sigma = d/f \text{ rad}. \tag{8}$$

The relation between the facet diameter $D$ (and therefore $\lambda/D = \Delta\alpha$) and the rhabdom diameter $d$ depends on the compromise reached by natural selection between *resolution* and *sensitivity*. To make full use of the resolution of the lens the rhabdom must be small, in which case $\Delta\rho \approx \Delta\alpha$. To increase sensitivity towards a point source to a maximum, without further throwing away resolution, the rhabdom must catch most of the light in the Airy disk. The best match of $\Delta\alpha$ and $d$ is then

$$d/f = 2\Delta\alpha \quad \text{and} \quad \Delta\rho = 2\Delta\alpha \text{ rad}. \tag{8a}$$

Matching the Airy disk width with the rhabdom width is valid however only for point source objects. As the rhabdom diameter is increased beyond $2\Delta\alpha$ there is increasing sensitivity to a diffuse source, but only by sacrifice of resolution, so that only larger objects can be seen.

### (*f*) *Modulation*

When a pattern of stripes with sinusoidal intensity distribution in angular space is passed across a receptive field there is a modulation of the total light falling on the receptor. This modulation above and below a mean intensity is *the only indication of the pattern* which the receptor receives. Assuming that the receptive field is Gaussian in shape and that the contrast of the stripes ($M$, figure 3*a*) is 100 %, the fractional modulation $m$, defined as in figure 3, from Götz (1964, 1965) is given by

$$m = \exp\left[-3.56\left(\frac{\Delta\rho_{\text{LA}}}{\Delta\theta}\right)^2\right], \tag{9}$$

where $\Delta\rho_{\text{LA}}$ is the width of the field of the receptor when it is *light adapted to the mean intensity of the stimulus*, not of the dark adapted receptor, which is the measurement usually available. To give the absolute modulation at the receptor, which is the signal from the stimulus to the eye, the fractional modulation $m$ must be multiplied by the mean intensity (see below).

Values of $m$ are plotted in figure 3. There is a range of values of modulation for different stripe periods from $\Delta\theta = \Delta\rho$ to $\Delta\theta = 8\Delta\rho$ beyond which there is no further increase in modulation. The value of the eye parameter, $D\Delta\phi$, depends on which point in this range is set to be

the threshold modulation for seeing. At whatever value the threshold modulation is set to detect the stripes, there is no point in having a smaller interommatidial angle than is necessary to reconstruct stripes of the threshold period. For a given value of $m$ in equation (9) we can obtain $D\Delta\phi$ with the aid of equations (3), (6) and (8$c$). The minimum $m$ for vision depends as follows on the intensity.

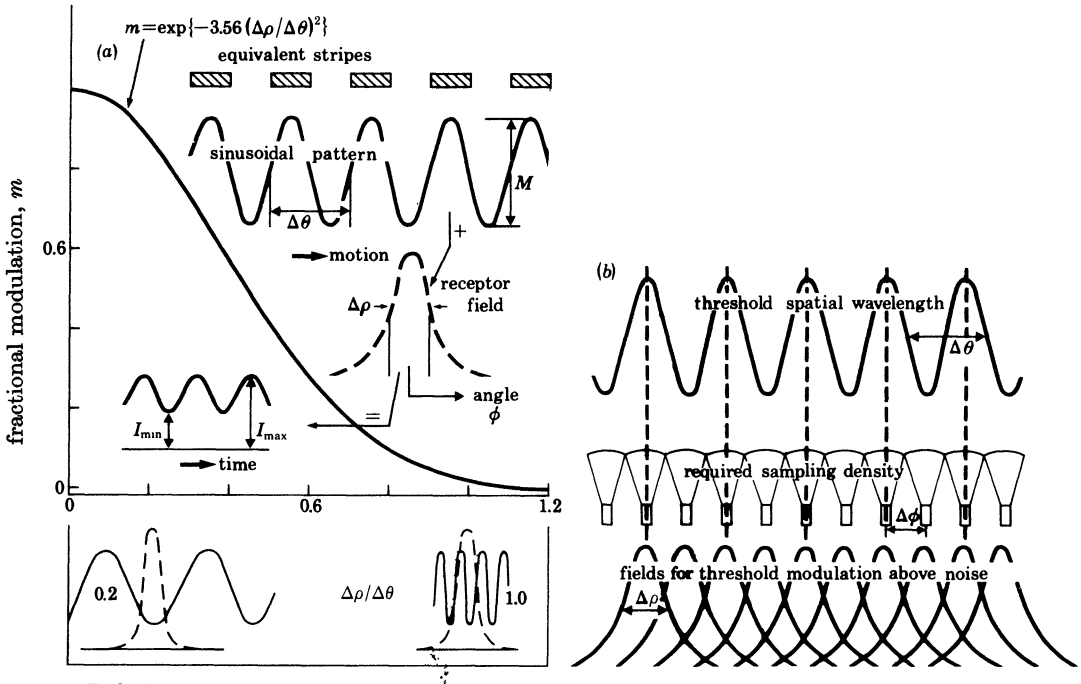


FIGURE 3. Relative modulation of light intensity in the rhabdom as a result of movement of a sinusoidal striped pattern of period $\Delta\theta$ across a visual field of width $\Delta\rho$ at 50% intensity. (*a*) The graph shows values of the fractional or relative modulation of $m$, defined as shown, for various ratios of $\Delta\rho$ and $\Delta\theta$. Two examples show the relative angular widths of pattern period and visual field width, for $\Delta\rho = 0.2\Delta\theta$ and $\Delta\rho = 1.0\Delta\theta$. (*b*) A particular solution of the relation between $\Delta\theta$, $\Delta\phi$ and $\Delta\rho$. In this case $\Delta\rho$ is approximately equal to $\Delta\phi$ and therefore to $0.5\Delta\theta$, where $\Delta\theta$ is the threshold stripe period. According to the graph, at $\Delta\rho/\Delta\theta = 0.5$ we find a modulation of 0.41. Such a large modulation at threshold period would be necessary only for an eye that operates at relatively low intensity.

### (*g*) *Absolute sensitivity and modulation*

The total amount of light caught by a receptor is a function of the $F$ value of the lens and the grain size of the catching area, as in camera theory. The effective area for catching light is proportional to the area of the rhabdom tip subtended at the posterior nodal point, multiplied by the area of the lens through which it looks:

$$S = k'D^2(d/f)^2 = k'D^2\Delta\sigma^2 = \frac{k'd^2}{F^2} \qquad (10)$$

where $F$ is the focal ratio, or $F$ value of the lens. Equation (10) shows how changes in the anatomical features $D$, $f$ and $d$, affect the sensitivity to a large source. Therefore the number of photons caught per unit time is

$$N = kID^2\Delta\sigma^2, \qquad (10a)$$

where $k$ is a constant depending on the units of intensity and $I$ is the photon flux per unit area per unit time. As before, in typical compound eyes, when $d$ is greater than about 2 μm, $\Delta\sigma = \Delta\rho$ (as in equation 8 and figure 2$e$).

The absolute modulation caused by a sinusoidal pattern is therefore

$$Nm = kD^2\Delta\sigma^2 \exp\left[-3.56(\Delta\rho/\Delta\theta)^2\right]. \quad (11)$$

Values of this modulation are plotted in figure 4*a*, assuming $\Delta\sigma \approx \Delta\rho$ and $D$ is constant. There are numerous possible combinations of $D$ and $d/f = \Delta\sigma \approx \Delta\rho$, in different eyes or eye regions (see figure 4*b*). The curves in figure 4 show three things: (*a*) narrow stripes, only seen at all by receptors with narrow fields, are always seen with low modulation; (*b*) for objects large enough to fill the field, sensitivity is proportional to the square of the field width and (*c*) each value of the field width is better than any other for seeing stripes in a narrow range, which is when $\Delta\theta = 2\Delta\rho$. This family of curves illustrates that the eye can be optimized to see objects over

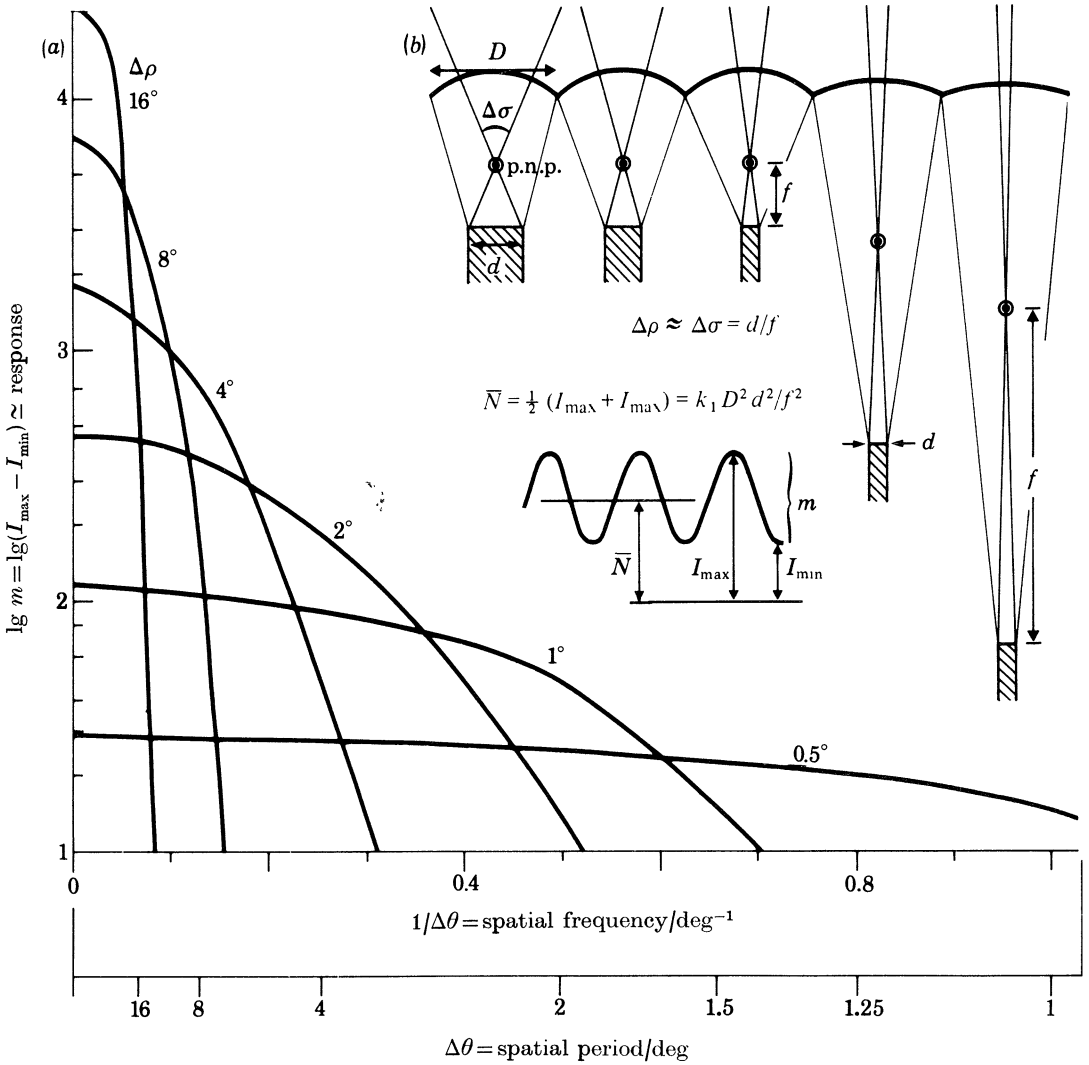


FIGURE 4. (*a*) Absolute modulation, its origin and consequences. Modulation of light at the receptor (defined as $I_{max} - I_{min}$) plotted as a function of spatial frequency for different values of the field width $\Delta\rho$. Note the logarithmic scale, so that ommatidia with $\Delta\rho = 16°$ are 256 times more sensitive to objects which fill the field than ommatidia with $\Delta\rho = 1°$. (*b*) Variation of the visual fields and sensitivity to large objects in different ommatidia or in different eyes. There is a progressive decrease of $\Delta\rho$ as we go towards the right, first by reduction in the rhabdom width $d$, then by increase in the distance $f$ to the posterior nodal point (p.n.p.). These anatomical differences, together with changes in $D$ and $\Delta\phi$, are the basis of the acute zones and other optical differences between eye regions.

a maximum range of sizes, or some favoured range. The theory presented below assumes that the eye is adapted to see the maximum range of spatial frequencies.

### (*h*) *Modulation in relation to photon noise*

Some time has elapsed since Fermi & Reichardt (1963) found that the relation between intensity and vision of a moving striped pattern of a fly suggests that the limiting factor in vision is the random arrival of photons. They also found that absolute intensities where vision fails are in the range where photon noise is comparable to the modulation in the signal.

The standard deviation in the photon counts in any one period across an array of photoreceptors is $\sqrt{\bar{N}}$ where $\bar{N}$ is the mean number of photons captured by the individual receptors per integration time of the eye. This is because photon arrivals obey the Poisson distribution (Barlow 1964; Rose 1973). The signal is the absolute modulation, which is fractional modulation multiplied by the average number of photons caught per integration time by the receptor:

$$\text{signal} = m\bar{N}. \tag{12}$$

Therefore,

$$\text{signal:noise ratio} = m\sqrt{\bar{N}}. \tag{13}$$

We can give the required signal:noise ratio an arbitrary value to ensure that a signal can be recognized with reasonable probability above the noise. If the required signal is put equal to the noise, we have $m\sqrt{\bar{N}} = 1$ as the threshold for sensing the modulation. When the average intensity of a threshold signal falls by a factor of 4, the absolute modulation must be doubled for the signal to remain at threshold. As the intensity is lowered the eye therefore sees only larger and larger stripes. The optimum interommatidial angle is that just necessary for the eye as a whole to reconstruct the minimum period that yields sufficient modulation at threshold. Therefore the interommatidial angle will be larger for eyes adapted to dim light; the larger $\Delta\phi$ in turn makes possible larger facets.

In very bright light let us suppose that only 3 % modulation is required to make the signal: noise ratio = 1. Then from equation (9) $\Delta\rho = \Delta\theta$, and from equation (3) $\Delta\theta = 2\Delta\phi$ so that $\Delta\rho = 2\Delta\phi$. We now return to the compromise dependence of $\Delta\rho$ upon $\Delta\alpha$, remembering that when light is abundant the rhabdom may be so small that $\Delta\rho$ can equal $\Delta\alpha$. Then $\Delta\rho = \Delta\alpha = \lambda/D$ so that $\lambda/D = 2\Delta\phi$ and $D\Delta\phi = \lambda/2 = 0.25$ μm. More likely, the rhabdom diameter is matched to the width of the Airy disk, so that from equation (7) $\Delta\rho = \sqrt{2}\Delta\alpha = \sqrt{2}\lambda/D = 2\Delta\phi$ making $D\Delta\phi = 0.7\,\lambda = 0.35$ μm. If conditions are so dark that 80 % modulation is required, then from equation (9), $\Delta\theta = 4\Delta\rho$ so that $\Delta\phi = 2\Delta\rho$. For these conditions, with large receptors which are adapted only for seeing patterns of large period, we might have $\Delta\rho = 4\Delta\alpha = 4\lambda/D$ so that $\Delta\phi = 8\lambda/D$; now $D\Delta\phi = 4.0$. The eye parameter $D\Delta\phi$ therefore lies between about 0.3 and 4.0 for apposition compound eyes, and depends on the ambient intensity for which the eye is selected.

When the stimulus moves relative to the eye, the effect is to reduce the effective modulation on each ommatidium because the receptor cell has less time to respond. The optimum values of $D\Delta\phi$ in eyes adapted to different light levels have been worked out by Snyder (1977). Similar results have been obtained by Snyder, Stavenga & Laughlin (1977) by use of the assumption that compound eyes are adapted to see the maximum number of different pictures. Eyes differ because they function at various light intensities (figure 5). These are the theories which make it of interest to map the regional distribution of $D\Delta\phi$ on the compound eyes of crustaceans and insects with a variety of habits.

*(i) The mapping and meaning of the eye parameter $D\Delta\phi$*

A circle of diameter $\lambda/D$ is drawn with its centre at each ommatidial optical axis on a map of axes in angular coordinates. Larger circles imply smaller facets. Then, if the circles exactly touch we have $\lambda/D = \Delta\phi$ so that $D\Delta\phi = \lambda = 0.5$ μm. If the centre of a circle falls on the neighbouring circle, we have $\lambda/D = 2\Delta\phi$ so that $D\Delta\phi = \lambda/2 = 0.25$ μm. The overlap of separation of the circles can be read as the local value of the eye parameter $D\Delta\phi$ (figure 5).

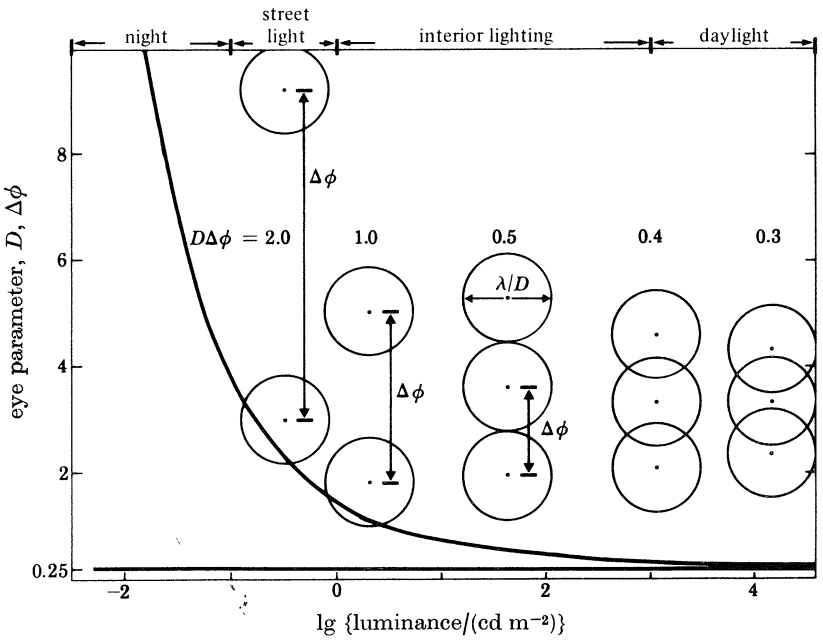


FIGURE 5. Predicted optimum values of the eye parameter $D\Delta\phi$ for eyes adapted to function at different ambient intensities (from Synder 1977). This curve is calculated for objects of 100% object modulation, $M$, in figure 3. Circles of diameter $\lambda/D$ with their centres separated by $\Delta\phi$ have been superimposed at points along the curve corresponding to the different values of $D\Delta\phi$. By comparing the separation or overlap of the circles on the eye maps with the ones spread along the curve in this diagram, it is possible to read off the predicted optimum ambient intensity for which any eye region is adapted. $\Delta\phi$ = angle between axes (radians); $D$ = facet diameter; $\lambda = 0.5$ μm.

The virtue of this representation is that the map is independent of the axes of the eye in facet lines or head symmetry and is applicable irrespective of facet shape and the regularity of facet rows. Where the facet rows are reasonably regular, clearer maps result when circles of diameter $5\lambda/D$ are drawn at every fifth ommatidial axis, as in many of the maps presented. The disadvantages of mapping the eye parameter in this way are that when the facet rows are irregular every axis must be drawn. In addition, one meets the usual difficulties of mapping a spheroid on a plane. The key to understanding maps of $D\Delta\phi$ is to remember that the circles of diameter $\lambda/D$ indicate the theoretical minimum field and that the finest pattern which the eye can reconstruct is fixed by the separation of the circles, $\Delta\phi$. One should imagine a striped pattern of period $2\Delta\phi$ superimposed on the map (equation (3)) with alternative circles coinciding with peaks in the pattern (figure 1*a*). To obtain maximum modulation from this spacing, the actual field widths ($\Delta\rho$) will obviously have to be larger than the circles of $\lambda/D$ in most examples. We can guess that where $D\Delta\phi > 0.3$, the receptor subtense $d/f$ and therefore

the acceptance angle $\Delta\rho$ is also increased. The extent of this increase depends on the required sensitivity to the finest pattern reconstructed as limited by $\Delta\phi$, on the required sensitivity to patterns of larger period and on factors such as eye tremor, variety of different field sizes within one ommatidium and the ability to change the field angle $\Delta\rho$ with intensity. The balance between these factors can only be known when $\Delta\rho$ is measured, although the angle $d/f$ subtended by the rhabdom at the posterior nodal point gives a first approximation to $\Delta\rho$.

To obtain good modulation from a sinusoidal pattern of period $\Delta\theta$, and from all larger periods, the acceptance angle $\Delta\rho$ must be about $\frac{1}{2}\Delta\theta$ (figure 3*b*). In this case, from equation (3) $\Delta\rho = \Delta\phi$, so that circles representing the acceptance angles $\Delta\rho$ would just touch. In perusing the maps one can, as a first approximation, imagine the circles expanded until they just touch. The amount by which they have to be expanded indicates the increase over the diffraction limit that has governed the eye parameter at that point on the eye. When the circles already overlap, the amount of overlap represents the pressure for increased spatial resolution at the expense of sensitivity at that point on the eye. A deeper understanding will come from study of the theories of Snyder (1977) and Snyder, Stavenga & Laughlin (1977). These theories however do not take into account the many variables which must contribute to the eye parameter of real eyes, such as different fields within one ommatidium, eye tremor or peering, binocular overlap, regional sensitivity to short wavelengths, or the possibility that the eye is adapted to see specialized features (such as a flash of light by a firefly, or a prey of constant size against the background of the sky) rather than generalized features (such as the maximum range of spatial wavelengths and the maximum number of random dot pictures). In brief, the eye parameter $D\Delta\phi$ (divided by half the wavelength $\lambda$) is the ratio of the maximum spatial frequency which passes the lens to the maximum spatial frequency which the eye can reconstruct.

## Methods

A series of photographs of the eye was taken with a camera mounted on a Zeiss Stereo 4 microscope. Maximum depth of focus was obtained by having the objective magnification as low as possible, together with an eyepiece at a magnification of $\times 20$. Objective magnifications of 0.8–3.0 can be adjusted for different sizes of eye. A diaphragm in the system close to the objective reduced the aperture of the microscope, which must be small to give the correct diameter and maximum contrast of the pseudopupil, but not so small that the resolution of the picture was seriously impaired. After numerous trials it was found best to make an exposure of about 0.2 s with Kodak TRI X film, and an overexposure of 1 stop. The film was then somewhat under developed in Microdol X developer and printed on Ilfospeed paper developed in Ilfospeed developer.

The eye of the whole animal can be mounted on a goniometer stage (figure 6) of the type used in crystallography, with angles in two planes measurable by vernier to one tenth of a degree. The eye is illuminated by two or three microscope lamps set at between 20 and 60° to the axis of the microscope, whichever setting happens to be most convenient for reducing reflexions on the eye surface. Heat filters on the lamps are necessary so that the light can be bright enough to bring the exposure time below 0.5 s, but the lamps are not kept on the eye for long periods. Chalk dust is blown on the eye to provide marks by which each facet can be recognized. First the axes of the head are lined up with the axes of the goniometer, then the eye is photographed from a series of clearly defined directions in angular coordinates; usually

the centre of the acute zone was selected for the zeros in both axes, and sometimes (0°, 0°) on the map looks straight ahead. Pictures are taken at intervals of 5 or 10° by rotating the eye in one particular plane, the dorso-ventral plane parallel to the main axis of the animal, or the main axis of the eyestalk. Each frame is numbered and the angle noted. When a row of pictures is completed another row is taken at an angle of 5 or 10° lateral to the first row. Intervals of 5° or less are essential at the acute zone but intervals of 10° are tolerable elsewhere. The changes in pseudopupil size are shown in many of the illustrations described in this paper. The movement of the pseudopupil centre relative to the dust markers is shown in figure 14. Errors in processing of the data are readily detected from the regularity of the sequence where the eye is uniform. All prints are made at the same magnification, which should be sufficient to make each facet several millimetres in diameter. Accurate maps cannot be made at smaller magnifications. A large eye, such as that of a ghost crab or dragonfly, requires two or three hundred pictures, so only regions of interest are mapped. Apart from the scale, all the rest of the work can be done by reference to the pictures.

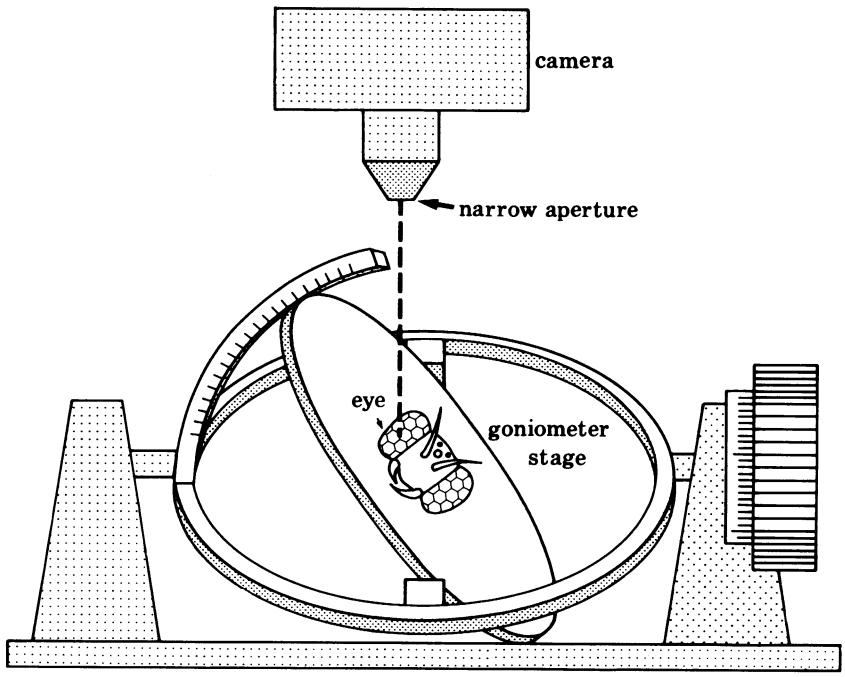


FIGURE 6. The essential equipment for mapping eyes is a camera of narrow aperture with a magnification of about × 10 upon the film. In practice, a binocular dissecting microscope with camera attachment was used. The eye is mounted on a goniometer stage with calibrated tilt in two planes at right angles to each other.

To make the preliminary map, which is a linear one and not an angular representation of the eye surface, one selects a row of pictures running right across the region of interest, as marked by a dashed line in the eye maps. Every facet, or more often every fifth facet, is then marked on the pictures along this row. It is unnecessary to mark every facet unless the pattern is irregular and every tenth facet is not sufficiently accurate. The marks provided by the chalk dust allow identification of corresponding facets between adjacent pictures. From a line of pictures across the eye, a long strip map is traced from successive frames. The projection is orthographic and can only be correct along two lines rolled out along a spheroidal surface. At an angular distance

$\phi$ away from the line along which the strip is developed, the error due to projection is given approximately by the equation:

$$\text{error} = (1-\cos\phi) \times 100\,\% \tag{14}$$

which is negligible up to 10° and reaches 10% at 25°.

When every fifth facet position has been transferred to paper, the positions of the pseudopupil centres are then traced from the whole set of photographs. Pseudopupil positions caused by tilting in a single plane are joined to give lines at intervals of 5 or 10°; these are called isopupil lines. Strips across the eye can be mapped accurately by this method but the maps are difficult to read. Centre to centre distances between facets are shown directly at each point on the map but the differences in facet size are not easily noticed. The isopupil lines cannot be directly interpreted in terms of function, although where the two orthogonal sets of isopupil lines are not equally spaced, they reveal that the interommatidial angle is different in different directions; where they are abnormally far apart they show the positions of the acute zones.

A second map in angular coordinates is then made from the map in linear coordinates, by plotting from the linear map the angular coordinates of each fifth facet. The effect is a transformation of the linear map by straightening out the isopupil lines, but these rows of axes are not straight lines on the eye and not necessarily the same as the rows of facets. Every facet or every fifth facet appears as a dot showing the position of its optical axis in angular coordinates. Ideally, the directions of all the optical axes should be represented on the surface of a sphere, but a flat map is the practical requirement. As before, a long strip across the eye can be mapped in angular coordinates on paper without serious error, and strips in other directions can be superimposed across the first strip. These maps have no poles, as a strip can start and end anywhere, but a large area cannot be mapped for obvious reasons. If, on the map of the world we proceed from the North Pole along the Greenwich Meridian by 90° then along the Equator by 90° then turn North again for 90° we arrive back at the starting point. Similarly on the eye, but on a flat map we finish up a quarter of the global circumference from the starting point. For this reason it is essential to show the dashed lines along which the first strips of the map have been developed, as in the figures. The alternative of using one of the geographer's standard projections of the sphere, such as the hemispherical, or polar projections, has not been followed because the interommatidial angle must have the same scale at every point and in every direction on the map. Also minimum field sizes are mapped at one scale over the whole eye, and represented as circles, of which the overlap is critical. Coordinates, which are lines of latitude and longitude as on a map of the globe with poles, are therefore not appropriate because the lines of latitude are closer together nearer the poles when measured in angular coordinates based on the centre. For the compound eye there are no poles and no single centre and only strips or small areas can be mapped. There is an optical centre for each pair of neighbouring ommatidia, so that there are three optical eye centres for each group of three neighbouring facets. For all of these reasons it was considered preferable to map the optical axes of ommatidia in strips with the angles in cartesian coordinates, and to tolerate the distortions when several strips across an eye are placed on one map.

The final state in the construction of a map is to measure $D$, the interval between facets in every part of the eye, and draw a circle of diameter $\lambda/D$ radians with centre on each ommatidial axis. The aperture is taken as the centre to centre distance between ommatidia on the photographs, for which the justification is that in the photographs of the eyes studied here (except the central band of rectangular facets in *Odontodactylus* and *Gonodactylus*), the apertures near the

pseudopupil appear as black disks which touch their neighbours (figure 14, 17, 20, 25, 31). The diameter of these disks is therefore the shorter diameter of the hexagonal facet, or the centre to centre separation. The peak wavelength $\lambda$ is usually taken as 500 nm, which is known to be a common spectral sensitivity peak, except in the dorsal parts of dragonfly eyes where $\lambda$ = 400 nm is more realistic. As $\lambda/D$ is the minimum field width of that facet and also the minimum angular resolving power, the map now shows the resolving power and sampling angle for each part of the eye, and the ratio between these two, which is the eye parameter.

## Results

### (*a*) *Hymenoptera*

(i) *The situation in the bee*, Apis mellifera

Measurements of the facet diameter and interommatidial angle of the honey bee *Apis mellifera* made by Baumgärtner (1928) have often been quoted despite the fact that del Portillo (1936) pointed out minor errors, notably that the ratio $\Delta\phi_H:\Delta\phi_V$ is 2.5:1 rather than Baumgärtner's 3:1. Their method of mapping gives only the angles between ommatidia along one section in various planes measured from sections. A considerable literature on the functional significance of this asymmetry has led to nothing except that the reconstruction of the image by the eye is compressed in the horizontal direction. Whether this is so, of course, depends on subsequent integration by the optic lobe; I do not know of behavioural evidence to suggest that horizontal stripes can be narrower than vertical ones and still be effective as a visual stimulus.

In the worker bee, $\Delta\phi$ in the vertical plane is given in these early papers as 1° to 1° 10′ over a considerable part of the eye looking at the horizon, both forwards and sideways, but 2° 40′ to 3° in the horizontal plane. The position of the minimum $\Delta\phi$ in the horizontal plane is said to be on the side of the eye. In the bee and the wasp *Vespa vulgaris*, according to del Portillo, $\Delta\phi$ *diminishes* from front to side along the horizontal equator on the eye. As these early results disagree sharply with the general findings in the present account, there is no doubt of the need for a revision of the bee's eye as a starting point for studies of its visual behaviour or optic lobe anatomy. However, the pseudopupil is not readily seen in *Apis* and another method must be found.

(ii) Amegilla *sp.* (*Anthophorinae*, *Apoidea*)

This Australian native bee was selected as it has a clearly visible pseudopupil, and it turns out to be a typical generalized eye with which others can be compared. This insect frequents wild flowers in gardens and scrub vegetation around Canberra in sunshine or shade. In the use of the eyes in foraging it resembles *Apis*.

There is a shallow forward looking acute zone with obvious binocular overlap between the two sides. In the acute zone the symmetrical, hexagonal pattern of facets becomes a vertically compressed pattern of visual axes, shown by the shaded circles in figure 7. The functionally significant relations between ommatidia may then be those indicated by the diamond pattern. This vertical compression continues from the acute zone laterally all around the equator of the eye, along which is a gradient of increasing $\Delta\phi$ from the front to the side of the eye. Along this band the pseudopupil is about 3 times as large in the vertical as in the horizontal direction. corresponding to a ratio of $\Delta\phi_H:\Delta\phi_V = 3:1$.

Figure 7, by the contact of the circles, shows that the eye parameter $D\Delta\phi$ is uniformly 0.5 over large parts of the eye. According to figure 5 this implies that the eye is adapted to vision of stationary objects in medium bright light and that the fovea operates at the same intensities as the rest of the eye. There is only a quarter of the number of facets possible if the eye were adapted to reconstruct the finest pattern each lens can theoretically resolve irrespective of intensity (as in equation (4)).

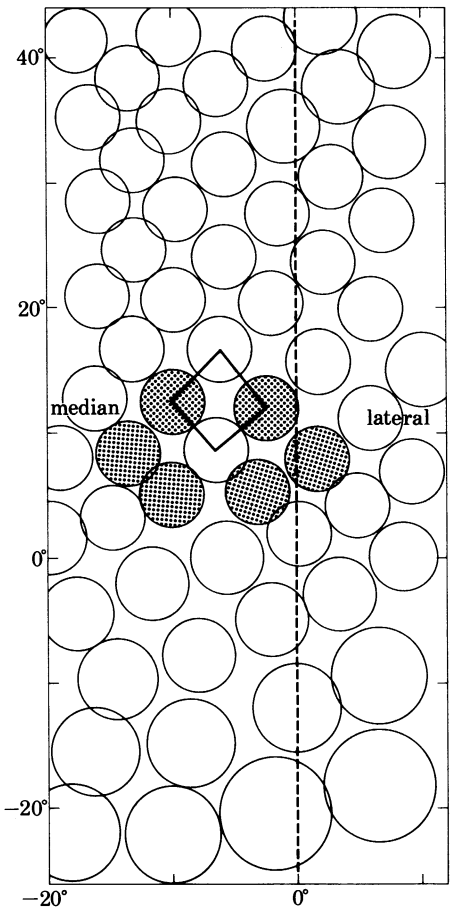


FIGURE 7. *Amegilla* sp. (Australian native bee), Hymenoptera. Type of map: every fifth ommatidial axis and its minimum visual field (magnified five times), in angular coordinates. Axes: arbitrary zero looking ahead on both axes. The acute zone, which looks directly forwards, is the region of the shaded circles. The dashed line is the base line of the map. Features: dorso-ventral compression which converts a hexagonal pattern of facets to a diamond pattern of axes, as indicated by stippled circles; very shallow acute zone; binocular overlap of 15°; $D\Delta\phi$ uniformly near 0.5.

### (iii) Bembix palmata *Smith* (*Sphecidae*)

The solitary wasp *Bembix palmata* hunts visually in bright sunlight. The female catches blowflies, such as *Lucilia*, in flight and carries them back in full sunshine to a nest dug in rather featureless hard sand or gravel. This creature possesses the ability to hover quite stationary and to fly at great speed and is very difficult to catch with a net. There is a large forward looking acute zone of astonishing clarity in the living insect (figure 8, plate 1), but not a corresponding large local increase in facet diameter.

A map of every facet in the acute zone (figure 9) shows the following features:

(*a*) the acute zone is formed by the curving inwards of the inclined rows of axes.

(*b*) There is 13° of binocular overlap between the acute zone and the ommatidial axes of the front margin of the eye.

(*c*) The eye parameter $D\Delta\phi$ decreases towards the centre of the acute zone to a minimum of about 0.3, depending on the direction selected.

(*d*) In the acute zone, the interommatidial angle, and also therefore $D\Delta\phi$, is much less (by a factor of 2:1) along the inclined rows of optical axes than along the horizontal rows. Away from the acute zone, but still on the equatorial band, this ratio exceeds 3:1.

(*e*) Where extra facet lines are introduced on the eye they never end or cause an irregularity in the acute zone.

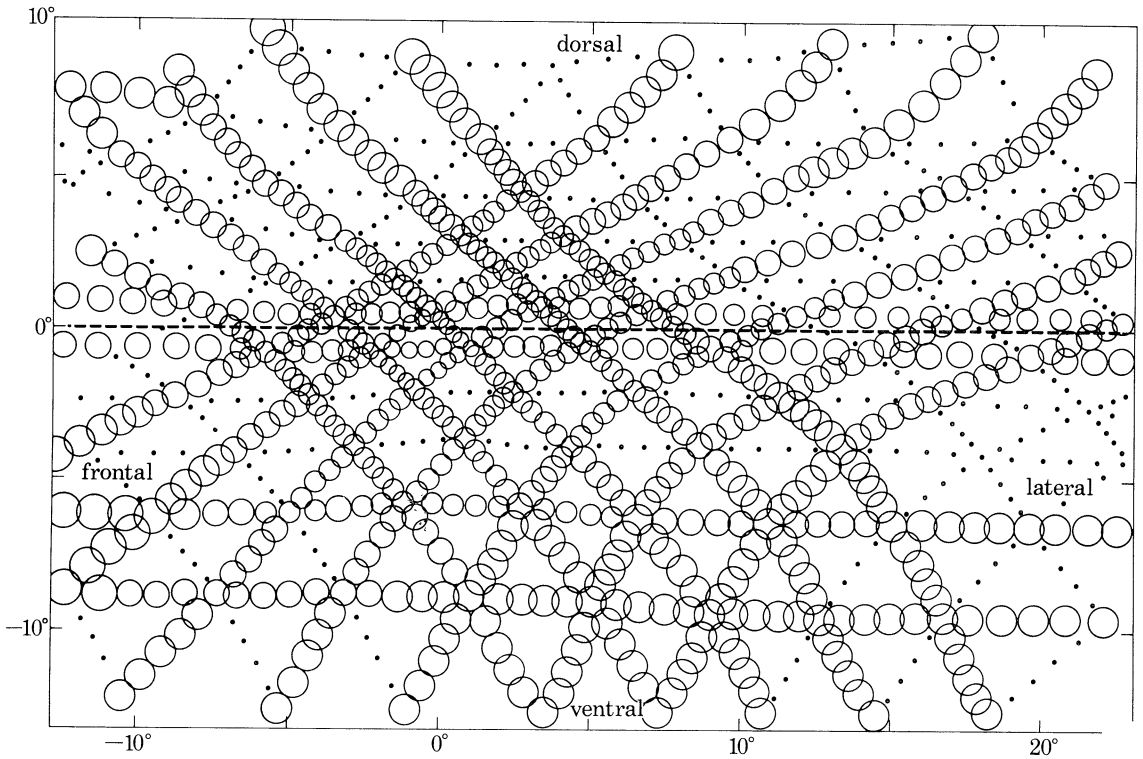


FIGURE 9. *Bembix palmata* Smith (sand wasp), Hymenoptera. Type of map: the location of every individual optical axis and its minimum field ($\lambda/D$) in each fifth row of ommatidia. In some places the axes are represented by dots to reduce the confusion. Axes: zeros at the centre of the acute zone on both axes. The dashed line is the base line of the map. Features: dorso-ventral compression of optical axes; large overlap of minimum fields in the acute zone, yielding an eye parameter $D\Delta\phi$ of minimum 0.3 μm in the acute zone along oblique rows; eye parameter about 0.5 μm in the acute zone along horizontal rows. Note the way the acute zone is formed by curvature of lines of optical axes. Habitat; visual predator, hunts large flies and hovers; active in open places in brightest sunlight over gravel and dried grass but also among trees.

*Bembix* provides the prime example of an acute zone of high resolution coupled with hovering habit and activity in bright sunshine. In the centre of the acute zone the interommatidial angle reaches a limit beyond which individual facets would not resolve the finest detail that the acute zone can reconstruct; the diffraction limit of $D\Delta\phi \approx 0.3$ is approached. In agreement with this, *Bembix* is active when the maximum intensity of light is available.

Species of *Bembix* differ, in *B. trepida* Handlirsch the facets are a little smaller and the values of $D\Delta\phi$ are greater than in *B. palmata* (figure 10, 11). Correspondingly *B. trepida* selects a habitat,

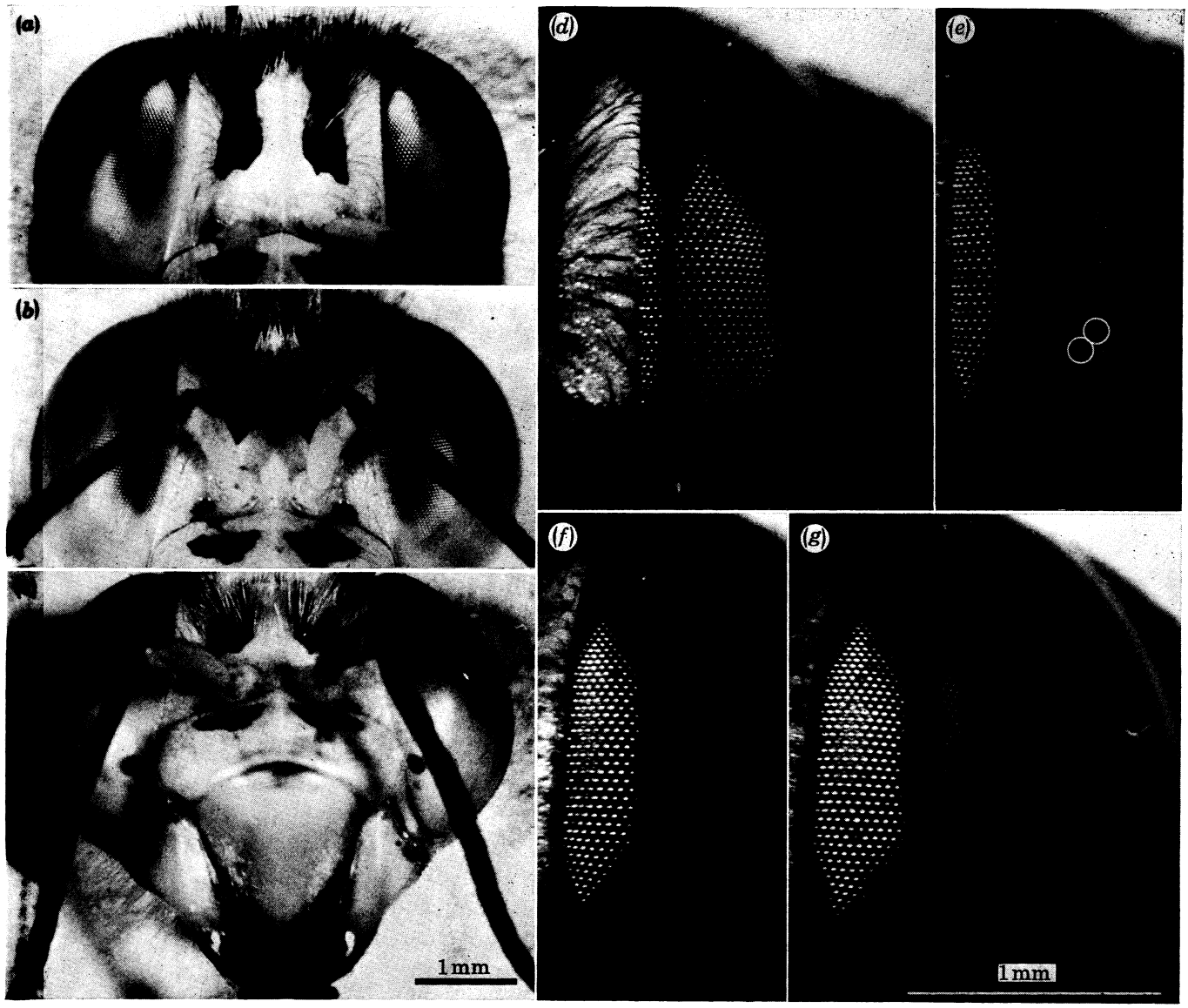


FIGURE 8. *Bembix palmata* Smith (sand wasp), Hymenoptera. (*a-c*) Living head seen from three angles: (*a*) from 5° to the side of the acute zone; (*b*) on the acute zone; (*c*) from 30° ventral to the acute zone. Features: large difference in size of the pseudopupil between (*b*) and (*c*); lateral shift of pseudopupil by about 8 facets for 5° horizontal shift; elongation of the pseudopupil in vertical direction at the level of the acute zone in (*a*) and (*b*) but not in (*c*); both acute zones look in the same direction, straight ahead. (*a*)–(*c*) are all the same magnification. (*d–g*) The pseudopupil at (*d*) −8°, (*e*) 0°, (*f*) 8°, (*g*) 16° relative to the acute zone, on the same horizontal line (the dashed line of figure 9). The circles show where additional facet lines begin, always *outside the acute zone*. (*d*)–(*g*) are all at the same magnification.

(*Facing p.* 22)

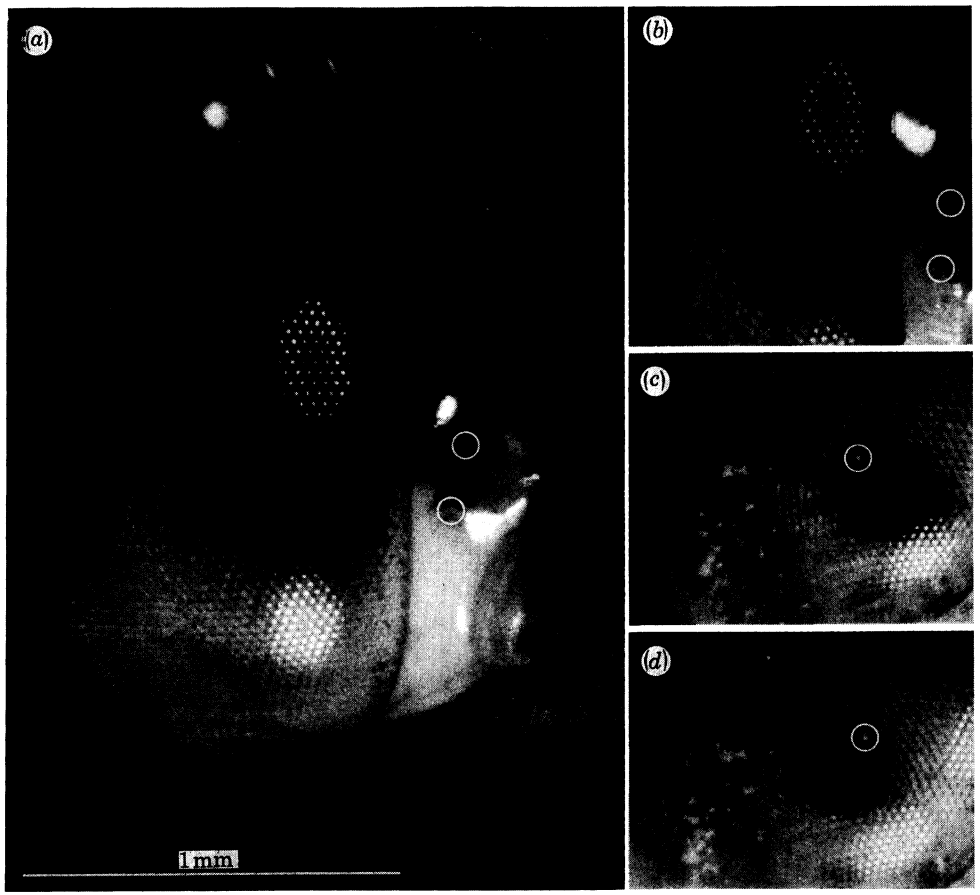


FIGURE 14. *Xanthagrion erythroneurum* Selys (damsel fly), Odonata. (*a*) The pseudopupil seen from the direction where it is largest, and axes are defined as 0°, 0°. Note the hemispherical eye, widely separated from its partner, which is characteristic of this group. (*b*) at 20° medial to (*a*) showing the large binocular overlap; axes 0° V, +20° H. (*c*) and (*d*) Movement of the pseudopupil relative to markers on the eye surface. Axes of (*c*) −15° V, 0° H: axes of (*d*) −15° V, +10° H. The coordinates are as in figure 16. Note the large differences in the size of the pseudopupil compared with the relatively small difference between the same regions on the map of the eye in figure 16. (*a*)–(*d*) are all at the same magnification.

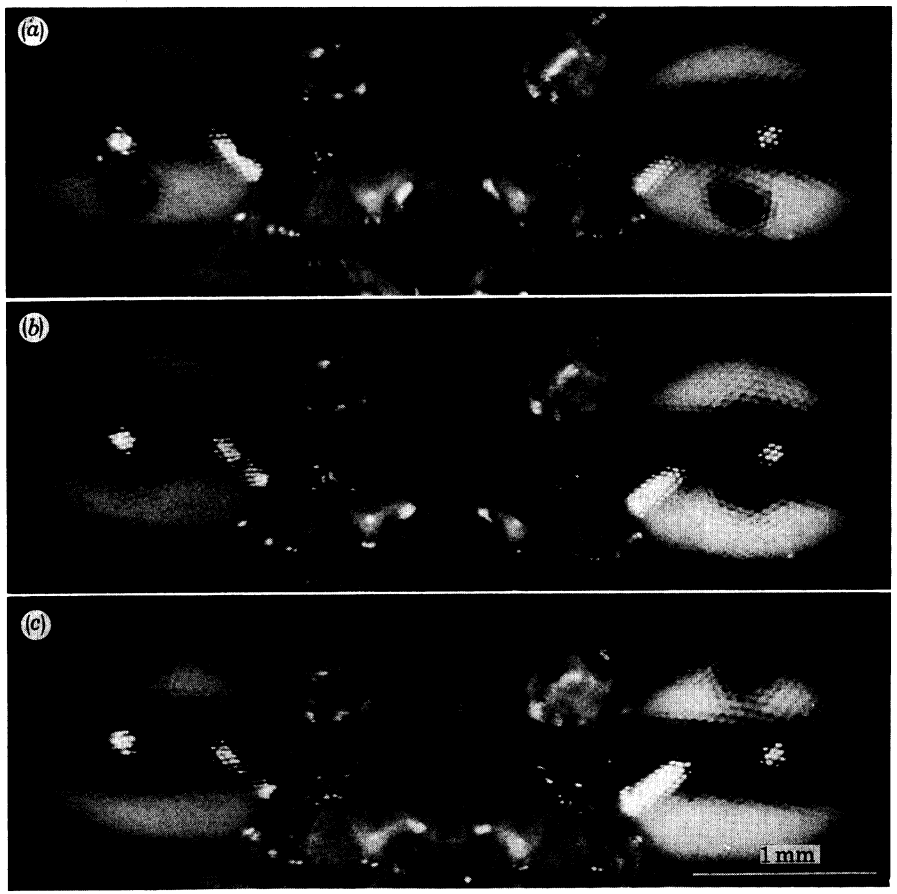


FIGURE 31. *Ciulfina* sp. probably *C. biseriata* (Westwood) (Iridopteryginae), Mantidae. Pseudopupils seen from the front at three inclinations of the head in the vertical plane; (*a*) 6° from fovea; (*b*) looking forwards; note pseudopupil extends beyond both sides of the line of pigment; (*c*) 6° below acute zone centre. Features: large binocular overlap and round, widely separated eyes, similar to those of Zygoptera (figure 14). (*a*), (*b*) and (*c*) are all the the same magnification.

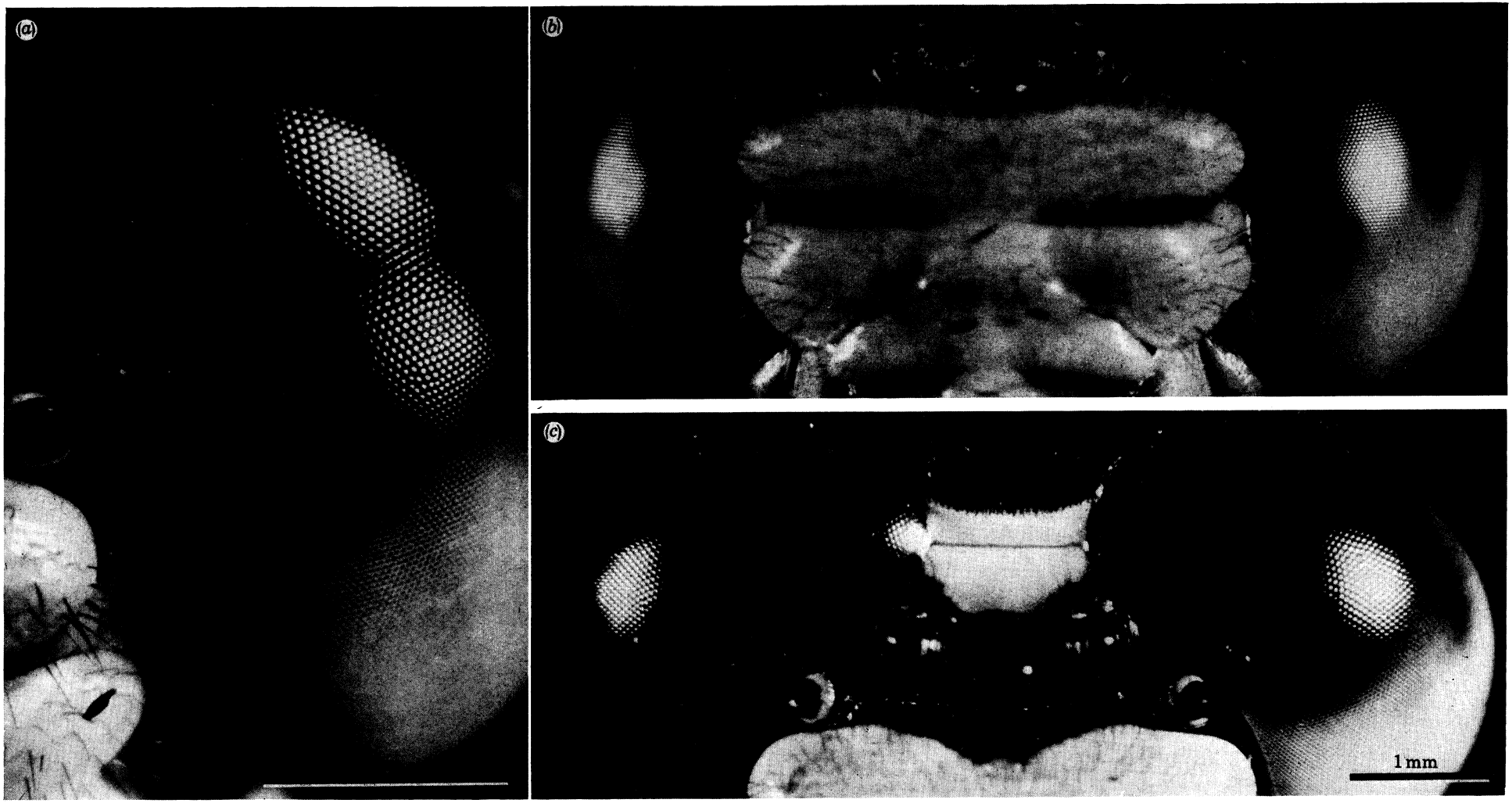


FIGURE 17. *Hemigomphus heteroclytus* Selys (gomphid), Odonata. (*a*) The great range of facet diameters, as in *Austrogomphus*. (*b*) The eyes, viewed from the front. The small forward looking acute zones are well separated, and the binocular overlap is small. (*c*) The large dorsal acute zones, which are also well separated, with at least 10° binocular overlap (see eye map, figure 18). Magnification of (*b*) the same as (*c*).

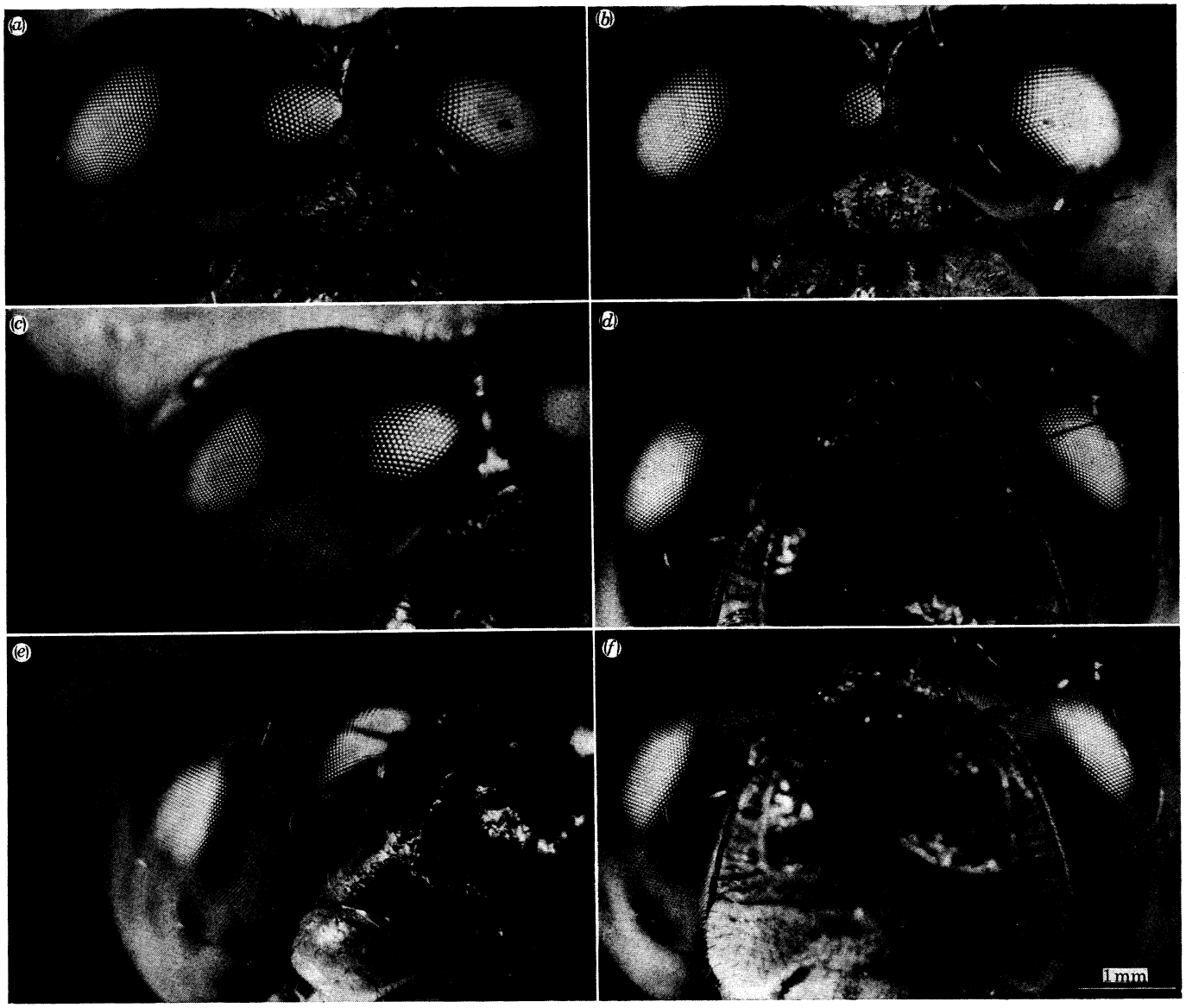


FIGURE 20. *Orthetrum caledonicum* (Brauer). The anterior regions of the eyes of a typical large dragonfly, photographed alive to show the different appearance of the pseudopupil and facets in different regions of the eye. (*a*), (*c*) and (*e*) are viewed from the right of the midline, (*b*), (*d*) and (*f*) are seen from on the midline. Axes as on figure 21; (*a*) 0° *D*V, 7.5° H (*b*) 0° *D*V, 0° H (*c*) 0° *D*V, 22.5° H (*d*) 25° *D*V, 0° H (*e*) 36° *D*V, 30° H (*f*) 36° *D*V, 0° H. (*a*)–(*f*) are all at the same magnification.

at least around Canberra, with more shade (Evans & Matthews 1973). Despite these differences, the acute zone is put together in exactly the same way in the two species.

### (*b*) *Orthoptera*

#### (i) Locusta migratoria

Surprisingly, for no one has noted it in this common laboratory animal, the locust has an inconspicuous acute zone at the front of the eye close to the lateral ocellus (illustrated by Horridge 1977*b*). The centres of the acute zones on the two sides coincide and they look straight ahead. As the acute zone could hardly be significant in jumping, because the locust rarely jumps straight, it is perhaps concerned with seeing ahead in level flight, or in the peering movement which may estimate distance (Wallace 1959). There are horizontal lines of facets on this part of the eye, and the corresponding rows of visual axes are approximately horizontal.

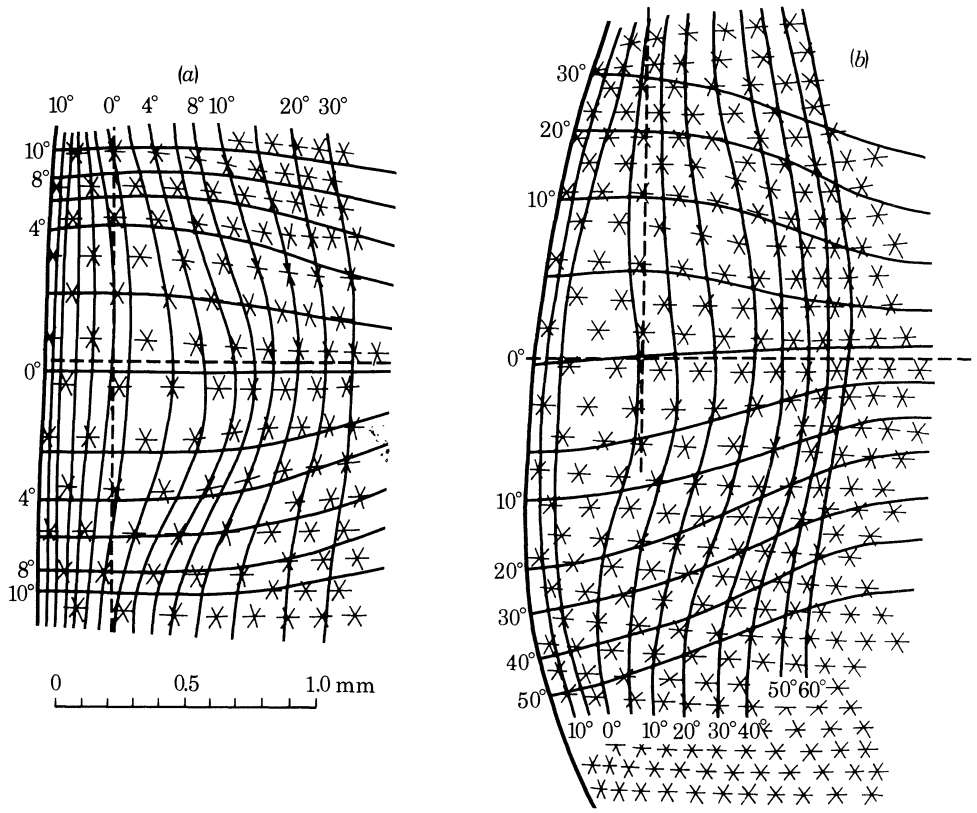


FIGURE 10. (*a*) *Bembix palmata* Smith, (*b*) *B. trepida* Handlirsch; sand wasps, Hymenoptera. Type of map: linear plot of every fifth facet and the isopupil lines, taken from the primary set of photographs. Axes: zeros looking forwards on vertical and horizontal axes. Features: facet rows horizontal at front of eye; facet centres and isopupil lines more separated near 0°, 0°; additional facet lines introduced away from the acute zone; inter-ommatidial angles less in *B. palmata* than in *B. trepida*.

On the linear map of this region, the isopupil lines spread out as they approach the edge of the eye (figure 12). On the map in angular coordinates the acute zone is an inward gathering of oblique rows of facets (figure 13), as in mantids. As in many other acute zones where there are horizontal facet lines, the acute zone of the locust shows a vertical compression of the hexagonal pattern of axes, which is more isotropic in other parts of the eye. This point is illustrated by the shaded circles in figure 13.

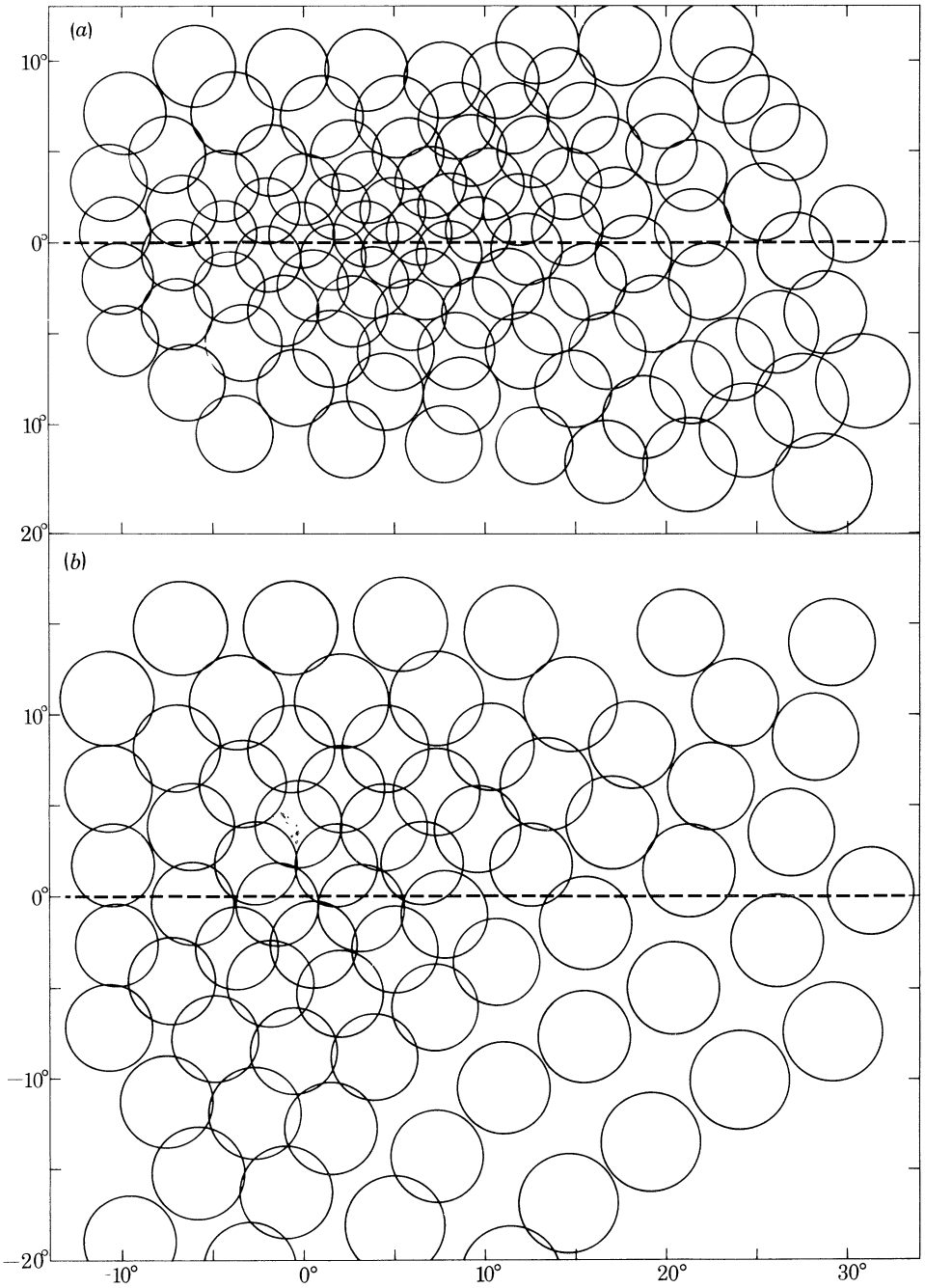


FIGURE 11. (*a*) *Bembix palmata*, (*b*) *B. trepida*; sand wasps, Hymenoptera. Type of map: the location of every fifth ommatidial axis and its minimum visual field magnified five times, in angular coordinates. Axes: from the isopupil lines of figure 10. Features: The two compound eyes are formed in the same way, with horizontal rows of facets having horizontal rows of optical axes, but the oblique rows of facets have curved rows of optical axes which are gathered together towards the acute zone. *B. palmata* has larger facets (smaller minimum fields) and a smaller eye parameter (more overlap) than *B. trepida*.

The acute zone is not marked by increased facet diameter. There is therefore a local decrease of $D\Delta\phi$ without change in the size of minimum possible fields. The interpretation of this type of acute zone is an interesting question. First let us take the light adapted field width $\Delta\rho$ determined electrophysiologically by Wilson (1975), who found $\Delta\rho_H = 1.5 \pm 0.2°$ s.d. and $\Delta\rho_V = 1.4 \pm 0.1°$ s.d. The minimum spatial frequency $\Delta\theta$ that can be reconstructed is $2\Delta\phi$, so $\Delta\theta$ is 2° at the centre of the acute zone where $\Delta\phi = 1°$, and $\Delta\theta$ is 2.5° for the surrounding area, where $\Delta\phi = 1.25°$.

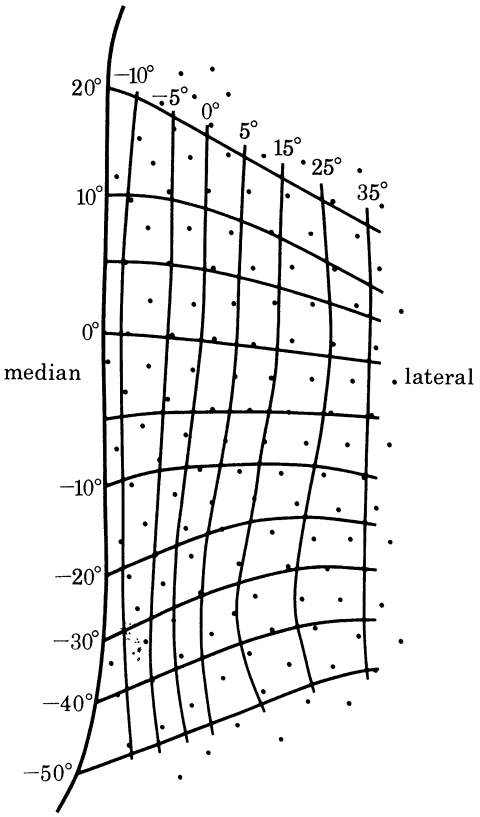


FIGURE 12. *Locusta migratoria*, Orthoptera. Type of map: linear plot of every fifth facet with isopupil lines, as taken from the primary sets of photos. Axes: horizontal zero through centre of maximum pseudopupil, vertical zero line looking directly ahead. Features: constant facet size, horizontal facet rows, more than 10° of binocular overlap, acute zone formed mainly by spreading of horizontal isopupil lines. The pseudopupil is illustrated by Horridge (1977*b*).

Assuming the above values of $\Delta\rho$ are valid within the acute zone as well as outside it, one can calculate from equation (9) or from figure 3 that stripes which can just be reconstructed by the eye, give a maximum fractional modulation of 28 % in the area adjacent to the acute zone, but only 13% at the centre of the acute zone. To work with the same effectiveness at the threshold of detail that each area can reconstruct, the acute zone therefore requires double the intensity to recover the same absolute modulation as the surrounding area. This calculation, although approximate, illustrates how the theory outlined above can be used in conjunction with the maps of compound eye.

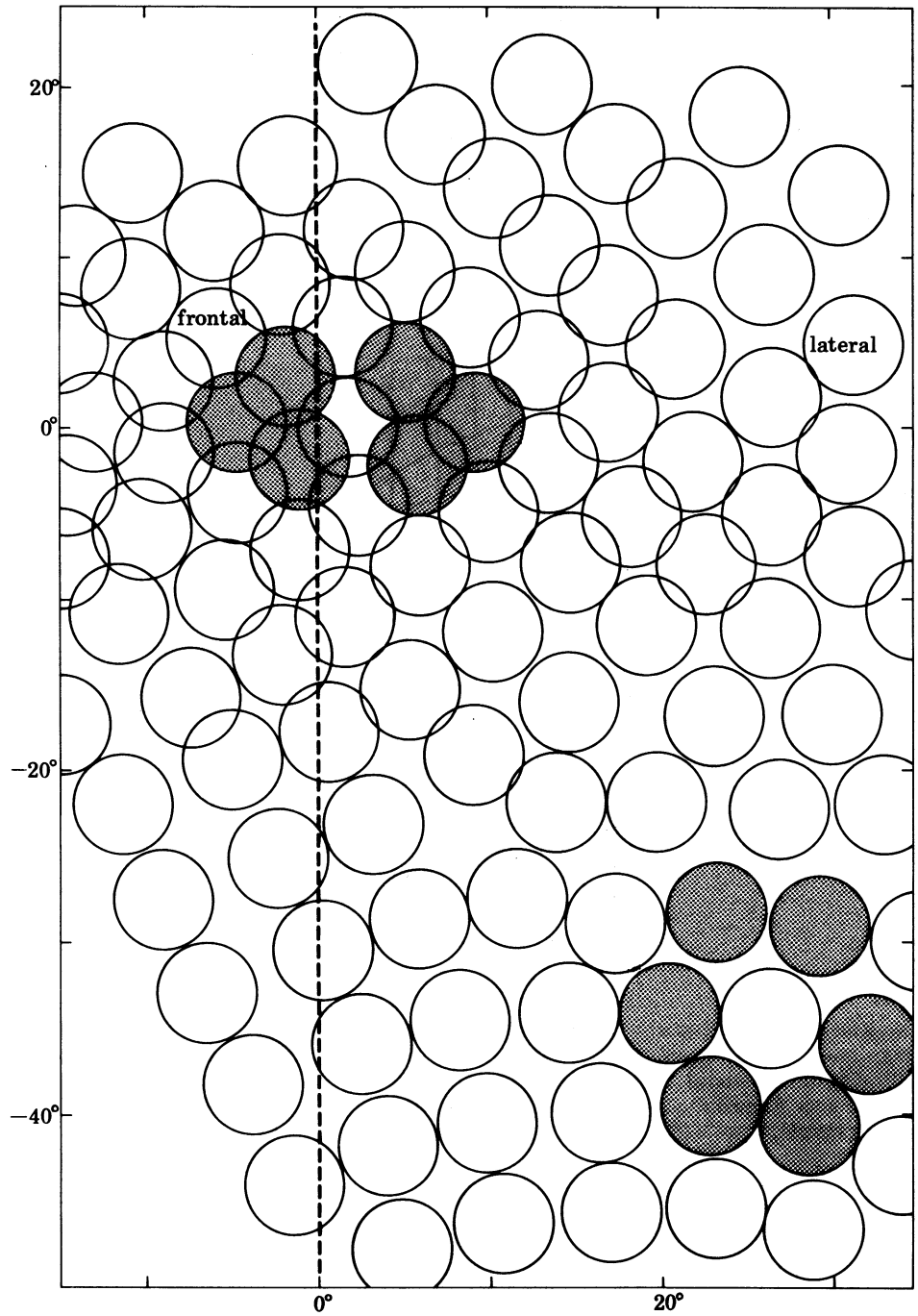


FIGURE 13. *Locusta migratoria*, Orthoptera. Type of map: every fifth ommatidial axis and its minimum visual field (magnified 5 times) in angular coordinates. Axes: from the isopupil lines of figure 12. Features: minimum visual fields ($\lambda/D$) all the same size; the acute zone, formed by curving of oblique lines of optical axes, is a region where the eye parameter $D\Delta\phi$ is smaller because $\Delta\phi$ is smaller. The pseudopupil is illustrated by Horridge (1977*b*).

### (*c*) *Odonata: dragonflies*

Dragonflies are so obviously dependent on vision that the eyes are likely to have been brought by natural selection to the optimum compromise which matches the visual habits. This is a very suitable group in which to investigate the eye parameter $D\Delta\phi$ because the habitat, behaviour, light intensity at the active period, and organization of acute zones are all widely varied in and between the different families.

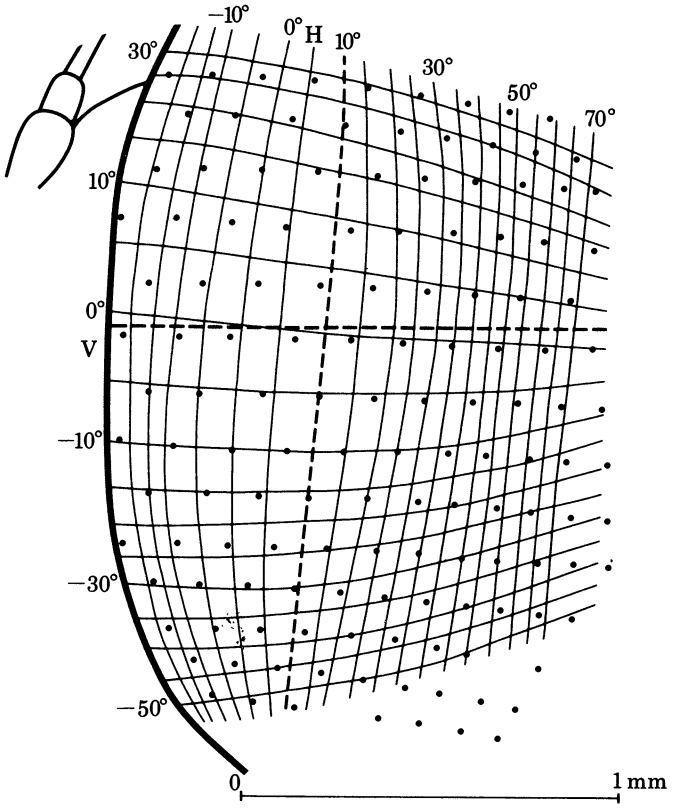


FIGURE 15. *Xanthagrion erythroneurum* Selys (damsel fly), Odonata. Type of map: linear plot on every 5th facet with isopupil lines. Axes: zero looking straight ahead. Features: one forward looking acute zone; facet rows near horizontal; gradient of facet sizes; binocular overlap of 20°.

#### (i) *Zygoptera: damselflies*

The common species examined, *Ishnura heterosticta* (Burmeister), *Xanthagrion erythroneurum* Selys and *Argiolestes griseus* Selys all have a broad and shallow forward looking acute zone, as illustrated in *Ishnura* by Horridge (1977*b*). When seen from directly in front, the pseudopupil fills a large part of the eye (figure 14, plate 2). Facet lines in this region are horizontal and regular. A typical example, *Xanthagrion*, is mapped in figure 15 and 16. Possibly some Zygoptera have an upward looking acute zone but I have seen no sign of it and the eye appears to be too small to have room for a second acute zone. In the Zygoptera available the upward looking part of the eye is black, so the pseudopupil cannot be seen. According to del Portillo (1936) the black colour is due to pigment between the crystalline cones. No explanation is available for the wide separation of the eyes or the large binocular overlap in Zygoptera. They catch prey or mate in the air and they also hover while inspecting reeds or twigs before landing on them.

The value of $D\Delta\phi$ for *Xanthagrion* is surprisingly large, ranging from about 0.6 along oblique rows in the acute zone to values exceeding 1.0 at 30° from the acute zone. This is not what we expect for a diurnal animal which flies slowly and appears to use its acute zones when it hovers. The eye is possibly adapted for working at optimum during a short period of twilight.

The acute zone of *Xanthagrion* (figure 16) is broad but shallow. Values of $D\Delta\phi$ decrease towards the middle of the acute zone, and facet sizes increase to 35 μm. The general impression is that the eye is small for a dragonfly, small to have an acute zone and much of the eye area is taken up by a binocular overlap of at least 25° (figure 15). Little is known of the visual behaviour or preferred intensity range.

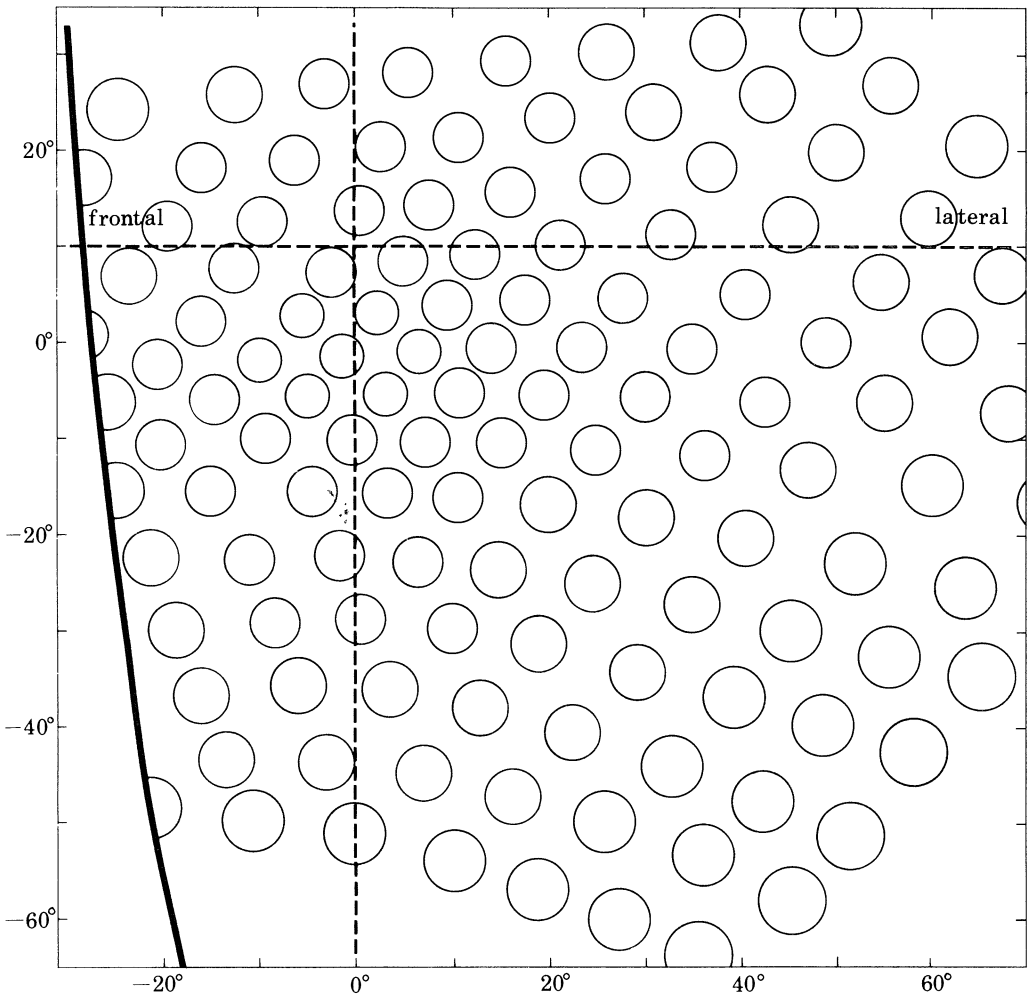


FIGURE 16. *Xanthagrion erythroneurum* Selys (damsel fly), Odonata. Type of map: every 5th ommatidial axis and its minimum field, magnified 5 times in angular coordinates. Axes: zero at centre of acute zone, looking straight ahead. The dashed lines are the base lines of the map. Features: regular lines of axes; no overlap of $\lambda/D$ circles; shallow acute zone. The shallow acute zone has an eye parameter $D\Delta\phi$ less than elsewhere, is formed by slight curving of the lines of optical axes and is well separated from the median edge of the eye. Habitat: predator on mosquitoes; hunts among foliage on lake edges, ponds and swamps.

(ii) *Anisoptera*

Here we find a diversity of habits and preferred intensities, some of which have been described (Tillyard 1917; Fraser 1960; Pritchard 1966) and a corresponding variety of eye forms which can be partially related to the habits. Several representative eyes have been mapped.

*Austrogomphus guerini* (Rambur) is a medium sized green-brown perching dragonfly which frequents the clear mountain streams of SE Australia. The males are often found sunning themselves on shingle beds by streams which are usually lined with river oaks (*Casuarina cunninghamiana*) or willows. The eye of *Austrogomphus* is similar to that of the related form *Hemigomphus heteroclytus* Selys, shown in figure 17, plate 3.

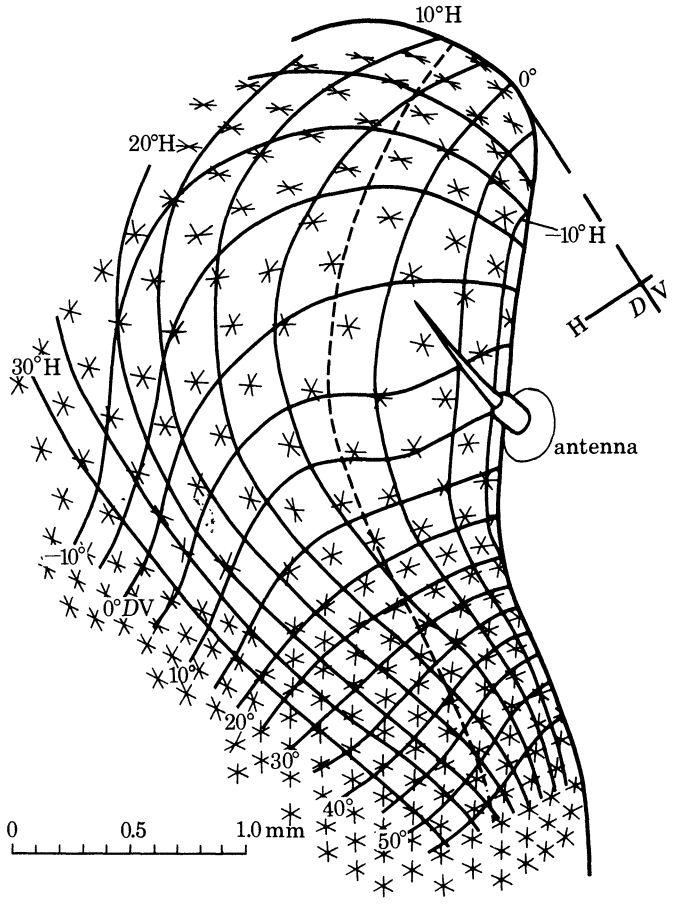


FIGURE 18. *Austrogomphus guerini* (Rambur) (gomphid), Odonata. Type of map: linear plot of the location of every 5th facet, and the isopupil lines at regular intervals, taken from the primary sets of photos. Axes: zero at upward looking acute zone; note obliquity of vertical and horizontal axes of the head. Features: facet lines are very regular in acute zones and around the equator of the eye, which is near the 50° *D*V line; binocular overlap of 5°–10°.

The eye is remarkable in having an upward looking acute zone of relatively enormous facets (up to 75 μm diameter, as noted by Tillyard (1926)). Between the well separated dorsal acute zones is a region of binocular overlap of 15°. The forward looking acute zone is poorly developed. Maps of the acute zone (figure 18 and 19) show pronounced gradients of $\Delta\phi$ and also of facet diameter, with the result that their product, the eye parameter, is approximately constant.

This finding can be interpreted by the theory presented above to suggest that the acute zone has an improved resolution which is available at the moderate intensities for which the rest of the eye is also adapted. To achieve this homogeneity of the eye parameter, relatively enormous facets are required at the centre of the acute zone.

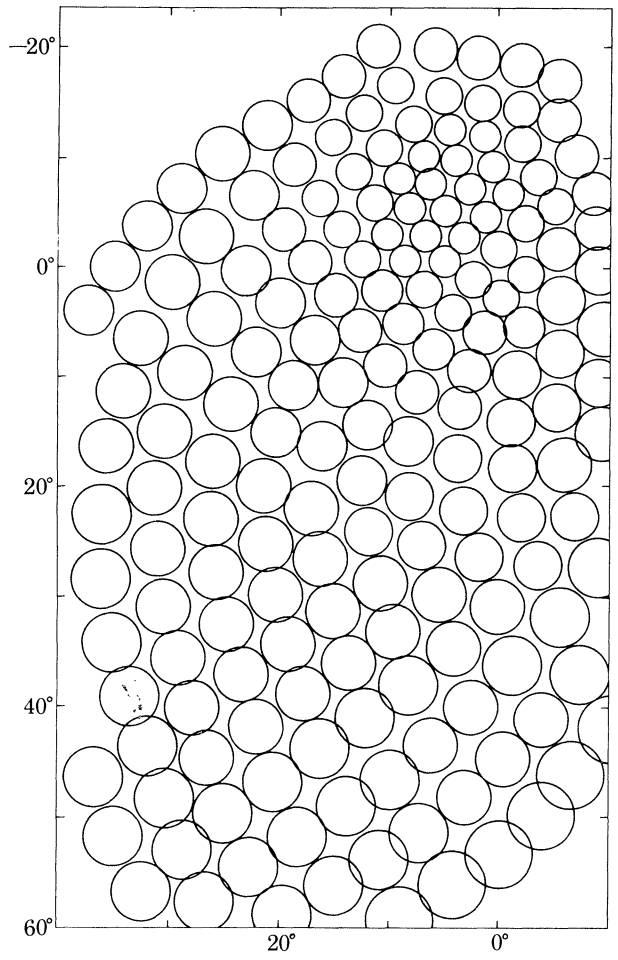


FIGURE 19. *Austrogomphus guerini* (Rambur) (gomphid), Odonata. Type of map: the location of every 5th ommatidial axis and its minimum theoretical visual field (magnified 5 times) in angular coordinates. Axes: zero at upward looking acute zone. Features: regular rows of optical axes; deep acute zone but uniform eye parameter $D\Delta\phi$, as indicated by the constant spacing of circles. Dorso-ventral lines of axes are regular but a few irregularities occur along other directions. Habits: the male perches on sand or gravel flats, usually in sunny patches along tree lined streams, and scans the sky for prey.

(iii) Orthetrum caledonicum (*Brauer*)

The males of this common, large libellulid are conspicuous by their bright blue abdomen. This species is a very fast flying acrobat and is usually found perching in open spaces near water, or defending a territory in bright sunlight. *Orthetrum* is also found hunting for mosquitoes at sunset and the eye is an example of a generalized large dragonfly eye.

As seen from the photographs (figure 20, plate 4) the eyes only just meet dorsally in the midline. In the dorsal acute zone the facets are larger than elsewhere; they are small in the area behind the antenna, but the acute zone which looks straight ahead (figure 20*f*) shows

little gradient in facet size. The absolute size of the eye is large; the largest dorsal facets approach 70 μm, and the largest forward looking facets approach 40 μm. The pseudopupil diameter reveals the positions of the acute zones, and the elongated pseudopupil along the equator of the eye reveals a region of dorsal compression of the visual axes, as shown in the map (figure 21).

The map of the eye in angular coordinates reveals a typical dragonfly eye. The facet lines are very regular except in the seam which lies between the dorsal and equatorial regions of high resolution. The directions of the lines of axes show a pattern found in many dragonflies.

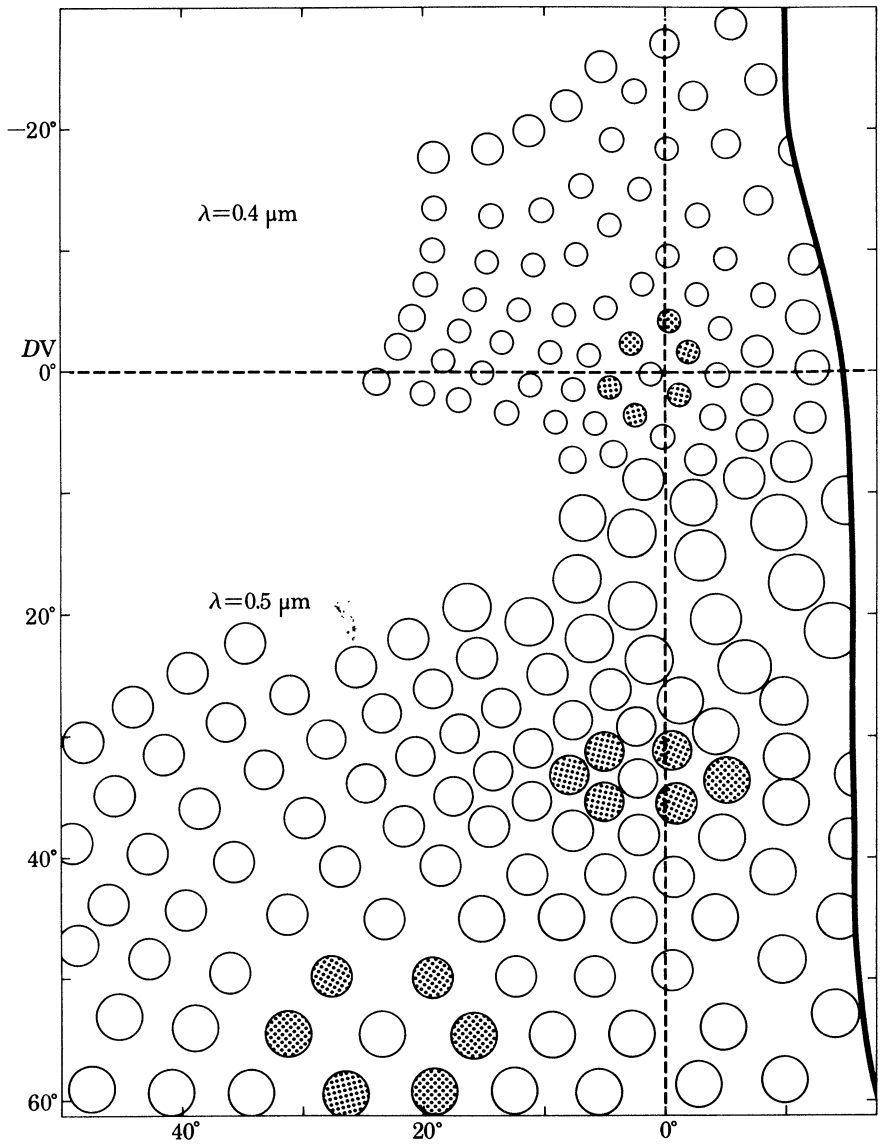


FIGURE 21. *Orthetrum caledonicum* (Brauer) male. Type of map: the location of every 5th ommatidial axis and its theoretical visual field (magnified 5 times) in angular coordinates; right eye. Axes: zero at upward looking acute zone. The dashed lines are the base lines of the map. Features: characteristic dragonfly pattern of axes. Values of $D\Delta\phi$ (as shown by the separation of the circles) suggest adaptation to low intensities or high angular flight velocity: vertical compression of optical axes along the equator of the eye (*D*V 30°–35°) shown by shaded circles: anterio-posterior rows of axes in dorsal acute zone; poor resolution in the region between the acute zones; 15° of binocular overlap. Habits: this is an aerial acrobat living in mixed shade and sunlight.

Interommatidial angles go down to 0.6° in the dorsal acute zone and along the oblique rows in the forward looking acute zone. The eye parameter $D\Delta\phi$ ranges from 0.5 to 1.0 in different parts of the eye. There is at most 15° of binocular overlap between the two dorsal acute zones. As in many examples of complex and regionally specialized compound eyes, there are patterns of visual axes with progressive changes in arrangement. These patterns would become geometrically untenable if continued indefinitely across a sphere. In this eye, e.g. at 30° *D*V–15° H in figure 21, the pattern reaches the limit just at the front edge, confirming that the facet pattern is a property related to the eye as a whole.

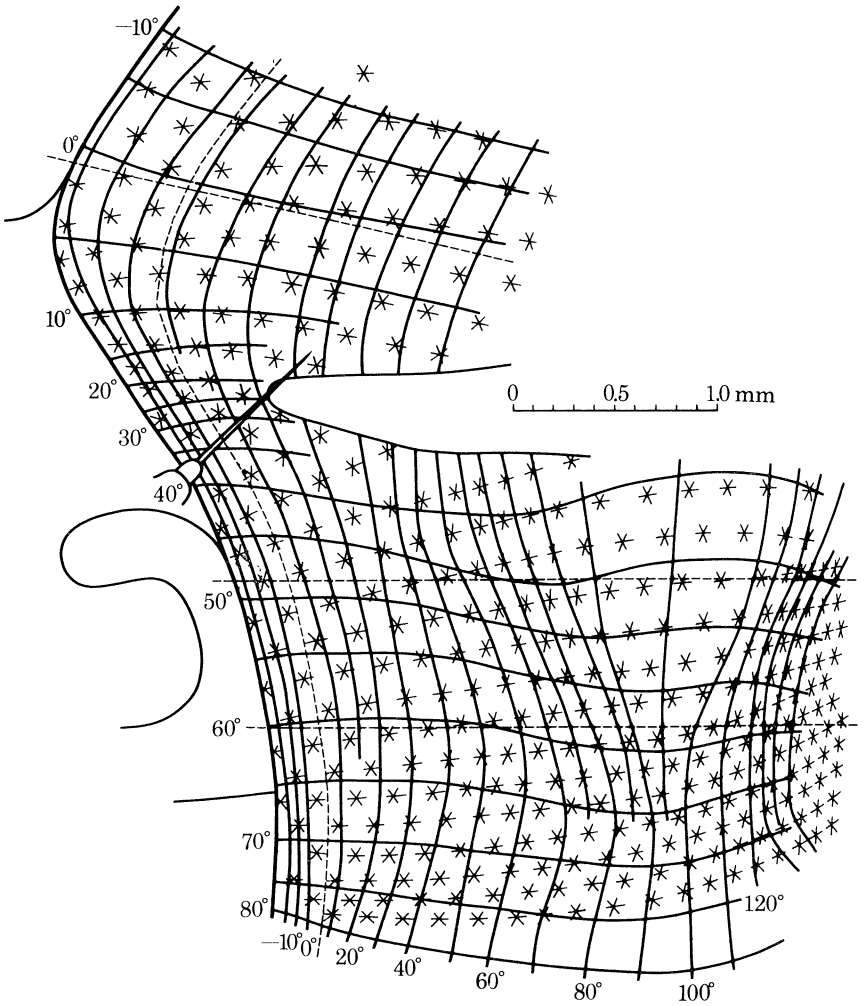


FIGURE 22. *Hemicordulia tau* Selys, (Cordulidae), Odonata, male. Type of map: linear plot of the location of every 5th facet with the isopupil lines taken from sets of photographs at different angles. Axes: zero at upward looking acute zone; left eye. Features: regularity of facet lines; complexity of eye. The dorsal and lateral acute zones are part of same dorso-lateral area with large facets, but are separated on this map on account of the way the rounded eye is rolled out on the paper (along the directions of the dashed lines).

(iv) Hemicordulia tau *Selys*

This species is taken as an example because it is found in large numbers around Canberra, and is physiologically the best known dragonfly retina (Laughlin 1976*b*). The eye is as complex as can be found among dragonflies. *Hemicordulia* is a strongly aerobatic and patrolling dragonfly; it perches when resting, unlike *Aeshna* and its relatives or the gomphid *Macromia* which hang.

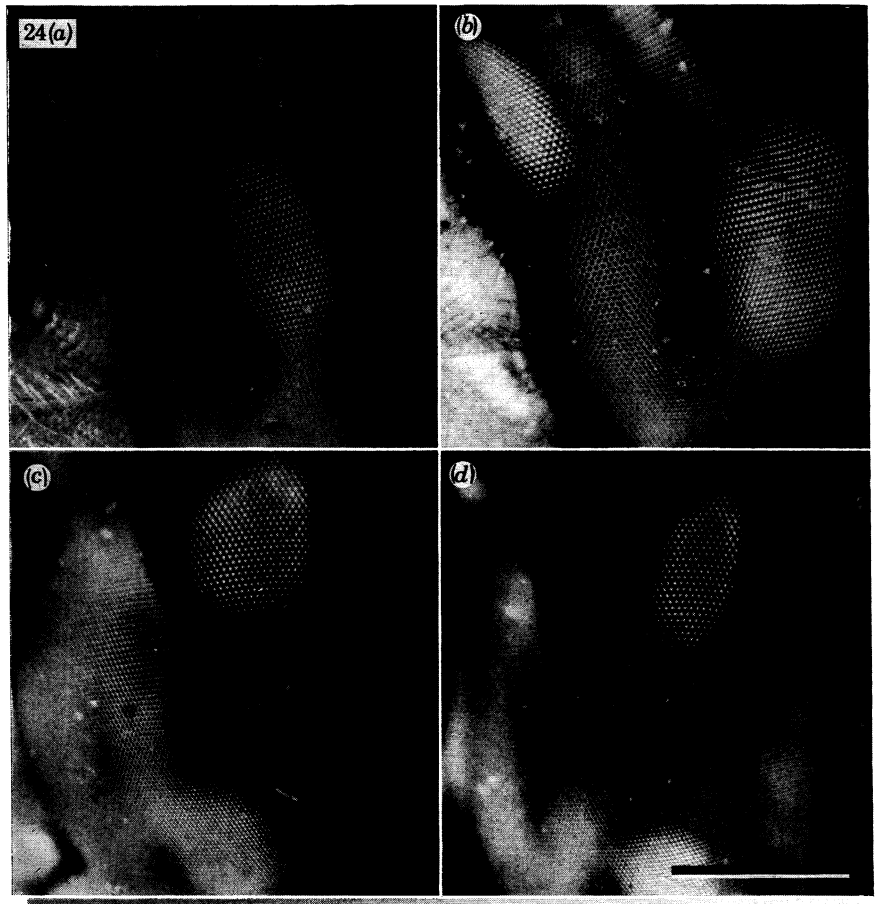


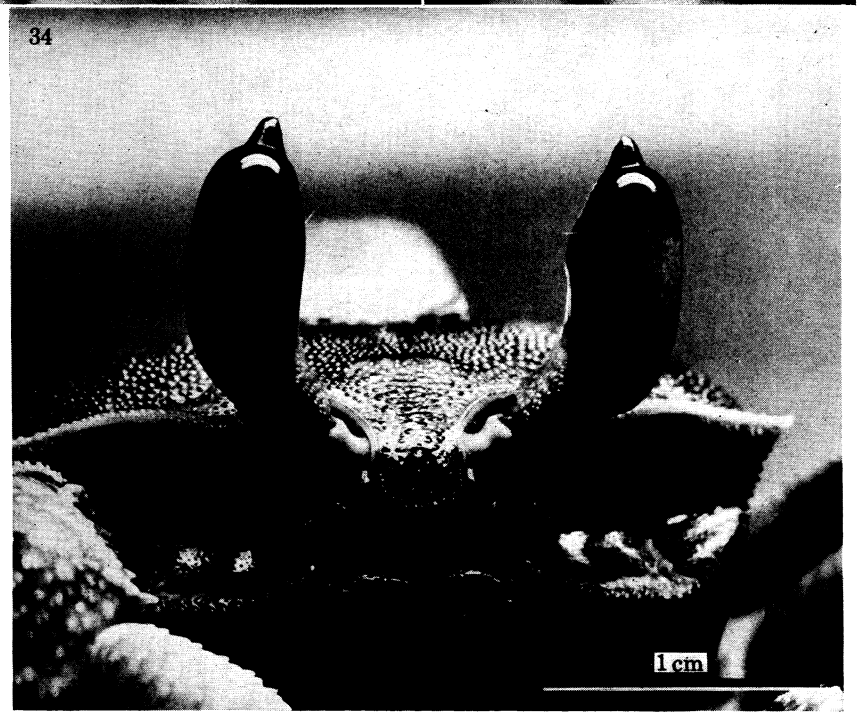


FIGURE 24. *Hemicordulia tau.* Selys (Corduliidae), Odonata, male. Change in shape of the pseudopupil as it moves along the part of the eye looking out at the horizon in level flight. (*a*) forward looking at 0° H, −60° V; (*b*) at 20° H, −60° V; (*c*) sideways looking at 90° H, −60° V, note the pseudopupil spreading across the lateral acute zone; (*d*) 100° H and −50° V, the pseudopupil is small, having now passed the acute zone. Note the changes in facet size. (*a*)–(*d*) are all at the same magnification. Angles as in figure 23.

FIGURE 34. *Ocypode ceratophthalma* female, from directly in front with the eyes erect and the camera on the same horizontal plane as the eyes. On this eye there are 160 horizontal rows of facets (Photograph W. Ribi).

(*Facing p.* 32)

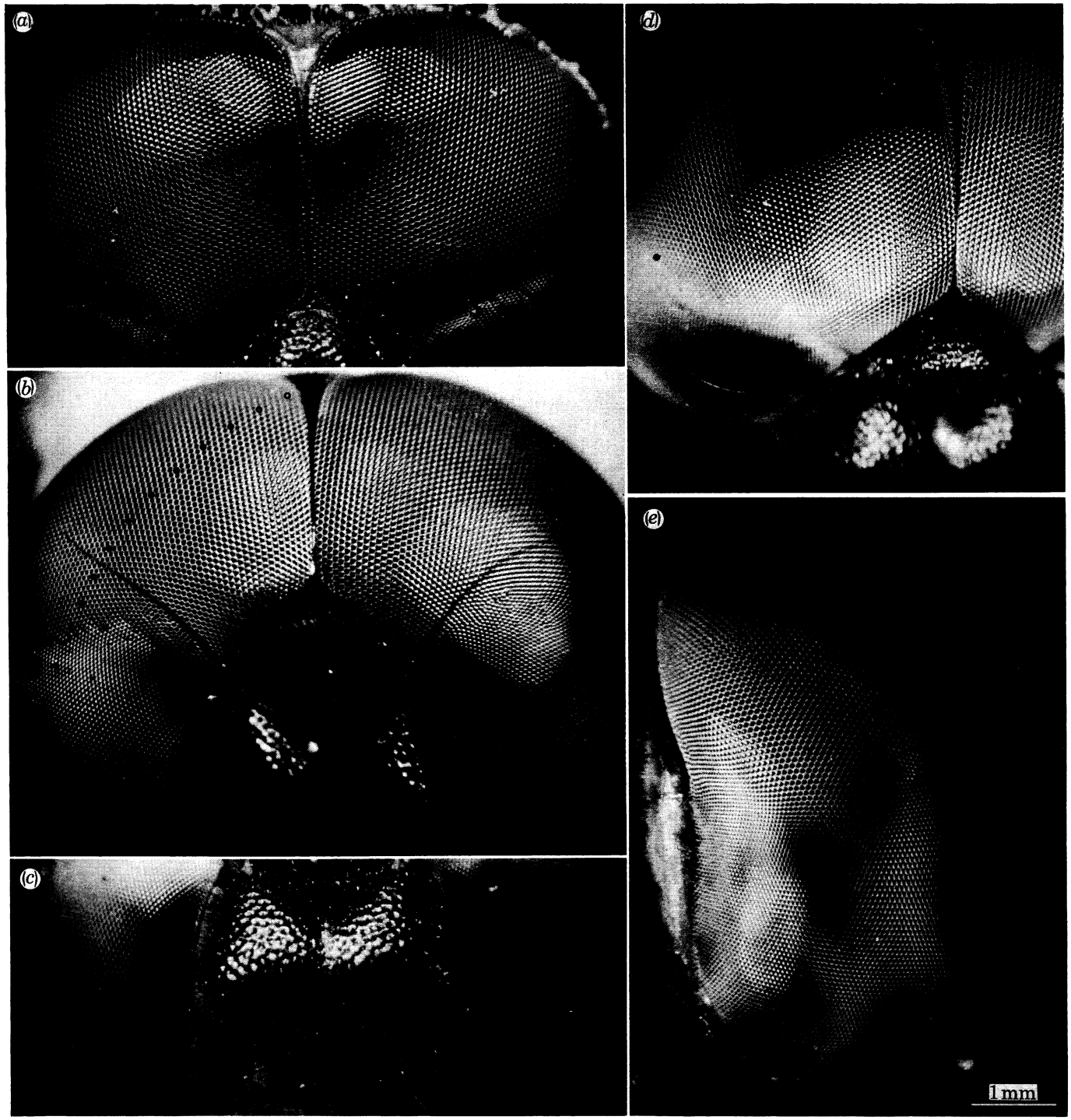


FIGURE 25. *Zyxomma obtusum* Albarda (Libellulidae), Odonata. The appearance of the pseudopupil in different regions of the living eye. Axes as figure 26; (*a*) lack of binocular overlap where the eyes meet dorsally, at 0° H, 55° *D*V; (*b*) the minimum pseudopupil at 0° H, 30° *D*V; (*c*) The forward looking pseudopupil near 0° H, 0° *D*V on the map; (*d*) part of the upward looking acute zone at 5° H, 60° *D*V; (*e*) the side of the eye lacks the sharply differentiated region of large facets, compare with *Hemicordulia*, figure 24). Features: eyes fused in the midline; facets large on absolute scale but no sharp gradients of facet size; region of obvious faults in the lines of facets behind the antenna in (*a*) and (*b*) but not on the side of the eye (*e*); uniform light colour of the eye, with pseudopupil visible in all regions. (*a*)–(*e*) are all at the same magnification.

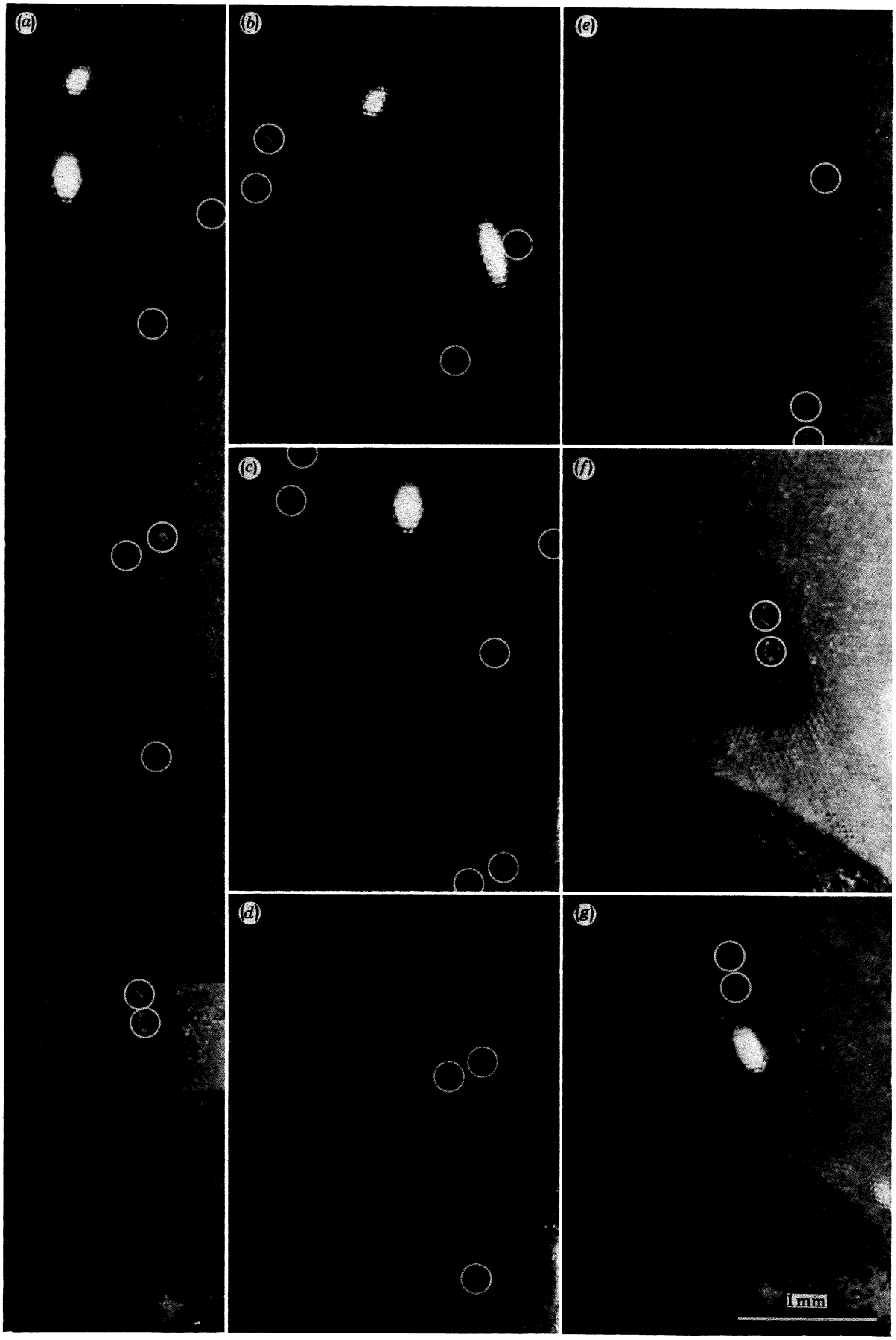


FIGURE 35. Pseudopupils of *Ocypode ceratophthalma*. (*a*) Assembled montage of 6 photographs of the eye at different angles, also shown in (*b*)–(*g*), along one vertical axis. (*b*) 30° above the acute zone, (*c*) 10° above the acute zone, (*d*) centred on the acute zone, (*e*) 5° below, (*f*) 30° below, (*g*) 60° below the acute zone. These pictures therefore cover a total of 90° in the vertical plane. Further axes, not shown, extend dorsally beyond an angle of 60° to the horizontal. Note that the facets are hexagonal, not square as in some crustaceans. (*a*)–(*g*) are all at the same magnification. The circles show the facet markers.

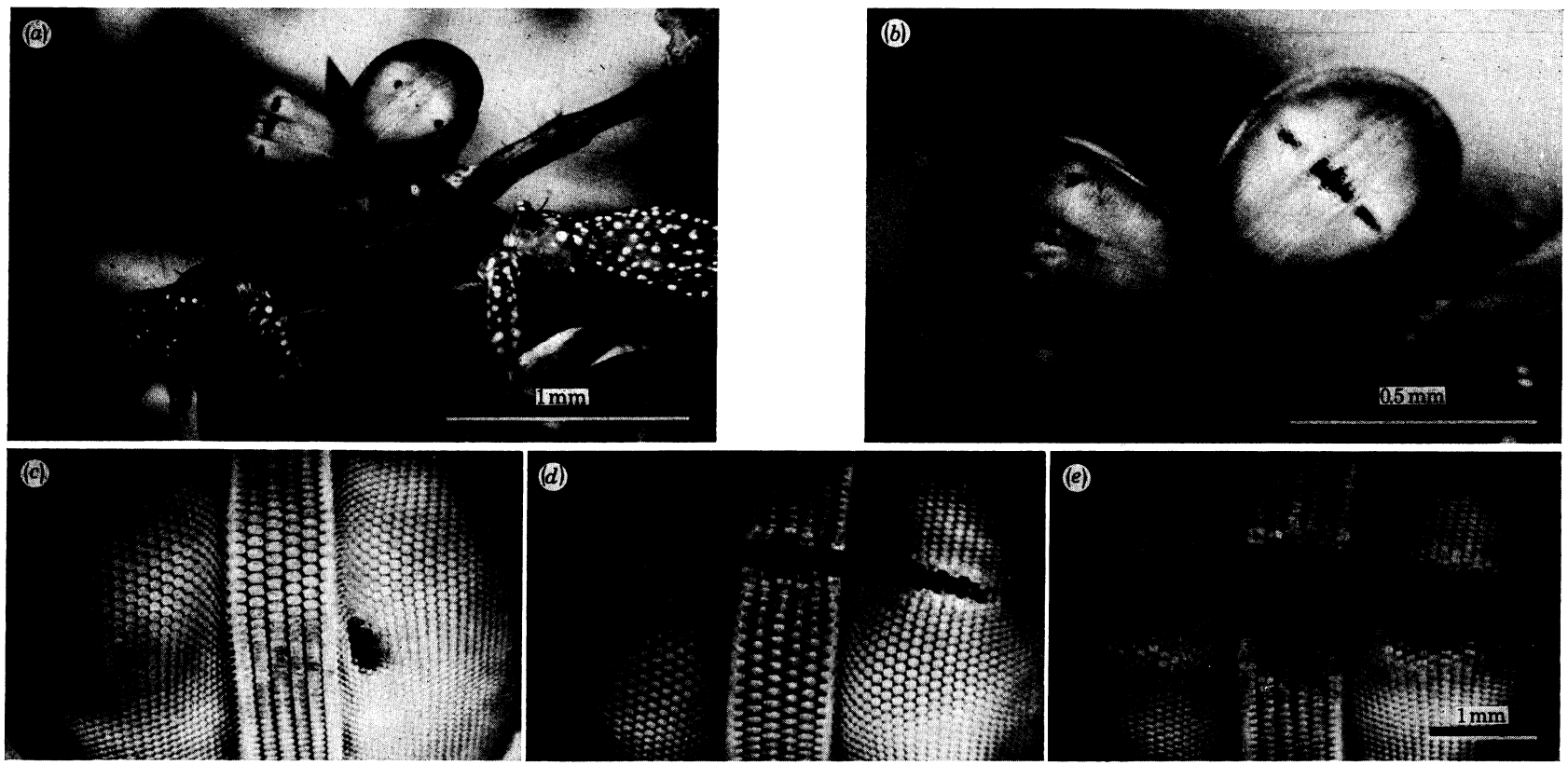


FIGURE 37. (*a*) and (*b*) *Gonodactylus chiragra* (Fabricius). (*c–e*) *Odontodactylus scyllarus* (Linnaeus). (*a*) *Gonodactylus* seen from the front, under water, with the central band of the right eye lined up with the camera. (*b*) the same animal with the eyes in a slightly different position. (*c*) *Odontodactylus*, right eye at 10°, 10°, from the acute zone. (*d*) at −15°, 0° from the acute zone (*e*) −1°, 0°, from the acute zone. Note the region of large facets at the three acute zones and that the axes of the centres of the three acute zones coincide. For illustration in colour see Horridge (1977*b*). (*c*), (*d*) and (*e*) are all at the same magnification.

*Hemicordulia* is found ranging far from water, as well as over lakes and reed beds: it hunts in bright sunlight but can carry on far into the evening when it can hardly be seen. The eye must therefore be adapted for a variety of tasks.

The eyes meet in the midline, but less so than in *Aeshna*, *Zyxomma* and many others. In the acute zones the facets are larger and facet lines more regular than elsewhere. They are also more regular on the equator of the eye but irregular behind the antenna, where facets are smaller. There is a region of sharp curvature along the horizontal axis at the back of the eye.

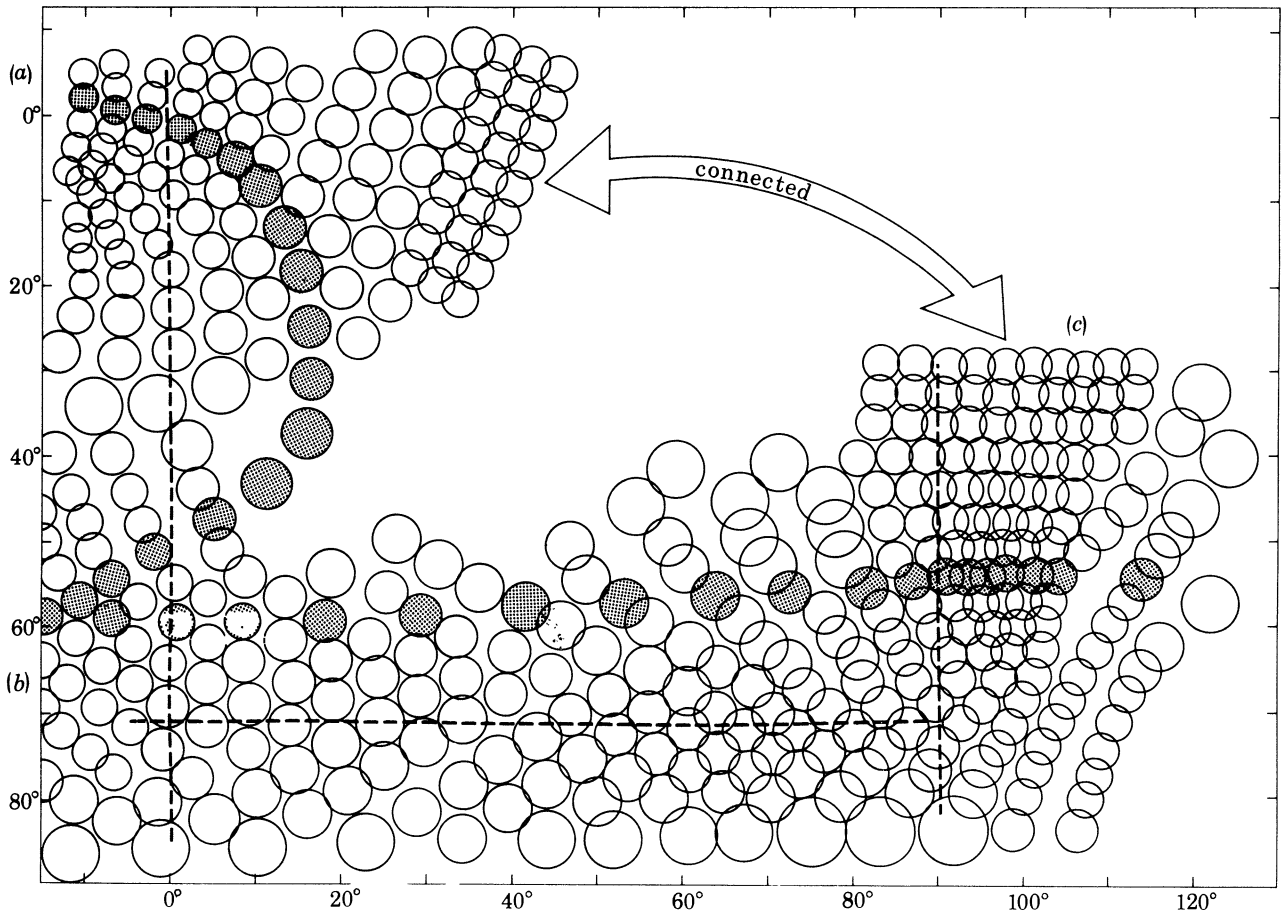


FIGURE 23. *Hemicordulia tau* Selys, (Corduliidae), Odonata, male. Type of map: every 5th ommatidial axis and its theoretical minimum visual field (magnified five times) in angular coordinates. Axes: zero near upward-looking acute zone. The dashed lines are the base lines of the map. Features: complexity of the eye; three acute zones (*a*) dorsal, (*b*) anterior and (*c*) lateral. Two lines of facets are shaded, one running from the anterior to the dorsal acute zone and the other from the anterior to the lateral one; large changes in inter-ommatidial angle, especially along the horizontal row of shaded circles. Habits: diverse species found near lakes and in dry areas and from mountains to coasts; active from sunlight to dusk; perching and cruising habits.

Maps of the eye (figures 22 and 23) show the three acute zones which have not previously been described in dragonflies, although the upward looking one can be inferred from figure 34 of del Portillo's paper. The acute zones differ in breadth and in depth. The upward looking zone is broad, extending over most of the top part of the eye and spreading down the side of the eye to form the lateral acute zone. This lateral acute zone is a feature that is well developed in *Hemicordulia* (figure 24, plate 5) but the forward looking acute zone is not so obvious as in many

insects which have only one zone. Possibly there is insufficient room for 3 deep acute zones in each eye, or *Hemicordulia* does not notably hover to examine stationary objects.

Along the equator of the eye there is a gradient of increasing $\Delta\phi_H$ from the front towards the side, until the lateral acute zone is reached. Here the interommatidial angle suddenly decreases. Posterior to the lateral acute zone the facets are very small and the eye extremely curved, as if little room can be spared for keeping a lookout behind.

The two dorsal acute zones are separable in *Hemicordulia*, but closer than in *Austrogomphus*. The binocular overlap across the top of the head is at most 10°. In contrast, in *Aeshna*, *Hemianax*, *Zyxomma* and several other large dragonflies which cruise in low intensity light, there is a continuous acute zone across the top of the head with no binocular overlap to speak of. This is shown by the sliding of the pseudopupil smoothly from one eye to the other as the head is rolled. Even in these enormous eyes there is evidently room for only one dorsal acute zone, which is shared between the two eyes (figure 25*a*).

The lateral acute zone is seen in many diurnal dragonflies as a tongue of large (and often darkly pigmented) ommatidia which spreads down the side of the eye (figure 24*c*, *d*). This is clearly seen in large corduliids, aeshnids, and libellulid dragonflies but not in Zygoptera or gomphids. It would be an interesting exercise to determine the function of the lateral acute zone, especially in relation to colour vision, as its pseudopupil is red, like that of the dorsal acute zone. From the smaller $D\Delta\phi$ values, one would expect it to be an acute zone with a spatial resolution that is fully utilized only in bright light.

The eye parameter $D\Delta\phi$ of *Hemicordulia* is different in different parts of the eye, ranging from 0.3 in the dorsal and lateral acute zones to more than 2.0 in a horizontal direction at the back of the eye. Over much of the intermediate regions $D\Delta\phi$ is near 0.5. There is a noticeable gradient of increasing $D\Delta\phi$ from front to back along the horizontal equatorial line. Along this line the ratio of $\Delta\phi_H$ to $\Delta\phi_V$ ranges from 2:1 to 3:1 which is seen as a vertical elongation of the pseudopupil (figure 24*a*, *b*).

(v) Zyxomma obtusum *Albarda*

Among dragonflies, many genera such as *Hemicordulia*, *Aeshna*, *Anax* and their relatives continue to hunt as the light fails in the evening, especially when mosquitoes are plentiful (Rau 1945). A few genera, notably the African *Anaciaeshna*, the SE Asian *Parazyxomma*, *Tholymis* and *Zyxomma*, and the Australian *Gynacantha* are truly crepuscular in that they avoid high intensities. In oriental countries *Zyxomma* has often been found deep down in wells during the day (Fraser 1960). In the garden of the Kuta Beach Club, Bali, Indonesia, I was fortunate to find *Z. obtusum* Albarda, and can confirm the report that it comes out to hunt over open water around sunset (Lieftinck 1954). The examples I collected preyed on mosquitoes at this time over a small freshwater pool surrounded and partially overhung by dark bushes.

Almost the whole head of *Zyxomma* is eye, and unlike diurnal dragonflies, the eye is light coloured so that the pseudopupil is obvious from any angle. At first sight the eyes of *Zyxomma* appear to have a larger number of small facets (figure 25, plate 6) but the scale shows that most of the facets of the top, front and sides of the eye are more than 50 μm diameter. Each eye has two acute zones, one looking directly ahead in level flight and the other inclined at about 50° above it looking upwards and forwards. Each acute zone is also a region where the facets are larger than elsewhere. The forward looking acute zone is a part of the band of facets that look in the direction of the horizon on each side of the head. The dorsal acute zone spreads

laterally down the side of the head, but to a lesser extent than in *Hemicordulia*. Comparison of the eye map of *Zyxomma* (figure 26) with those of *Austrogomphus* (figure 19), *Orthetrum* (figure 21) and *Hemicordulia* (figure 23) shows that the eye parameter $D\Delta\phi$ is much larger than in the diurnal dragonflies, i.e. circles of diameter $\lambda/D$ in the map of the eye in angular coordinates are separated by more than their diameter, and $D\Delta\phi$ lies in the range 1.0 to 1.5.

When we turn to the graph (figure 5) showing the optimum values of $D\Delta\phi$ for eyes that function at different ambient light intensities, we see that *Zyxomma* has eyes that are apparently best adapted for light intensities of about $10^{-4}$ of those in sunlight. Measurements with a Weston exposure meter showed that the intensity was in fact in this range, but exact values are useless because the twilight is bluer than sunlight. At any rate, the facets in *Zyxomma* have a


FIGURE 26. *Zyxomma obtusum* Albarda (Libellulidae), Odonata. Type of map: every 5th ommatidial axis and its theoretical visual field (magnified five times). Axes: zero near forward looking acute zone; vertical 0° line is the vertical plane parallel to midline of the head. The dashed lines are the base lines of the map. Features: $\lambda/D$ circles are far apart, with eye parameter $D\Delta\phi$ reasonably constant over the eye; acute zones shallow. Habits: crepuscular only, flies at limited range of light intensities, down wells, under trees; mosquito predator.

larger diameter ($D$) for a given value of the interommatidial angle ($\Delta\phi$) than they would have in a diurnal species and the values fit the theory that the cause is photon noise.

The larger value of $D\Delta\phi$ has been achieved in the following way. Firstly, in *Zyxomma* the whole head is large and most of the head is eye; secondly, the dorsal acute zone does not spread far down the side and its extent is reduced, making more room available on the eye; thirdly, the interommatidial angles are not sharply reduced in the acute zones. *Zyxomma* has eyes with relatively huge facets (see figure 25, plate 6) up to 75 μm in the upward looking acute zone and 65 μm in the forward looking zone. We can expect that the physiological field sizes, measured by the resolution in behavioural experiments or by microelectrode recording from the photoreceptor, will turn out to be much larger than the calculated minimum $\lambda/D$. To catch mosquitoes with the typical dragonfly power, flight speed, manoeuverability and grabbing equipment, and also perform successfully in dim light, the facets and rhabdoms have to be increased in size until the field width is similar to that for diurnal species. However, the increased sensitivity is retained, i.e. $D$ and $d$ and therefore $s$ are increased (figure 2*c–e*) but $\Delta\rho$ may turn out to be the same as in eyes with smaller $D$ and $d$ (equation (7)).

### (*d*) *Mantodea*

(i) *Previous work*

A confusing situation meets the researcher when he turns to mantid eyes. It has long been known that the ommatidia are larger and the interommatidial angles smaller in the centre of the front of the mantid eye (Hesse 1908; Friza 1928). In the S American mantid *Stagmatoptera* a region of large facets has been described as corresponding to a region of reduced angle between the interommatidial axes as measured from the pseudopupil (Maldonado & Barros-Pitá 1970). The 'fovea', however was defined as the region necessary for a successful strike and this was not the region of the greatest resolution, but a horseshoe shaped region around it. Before the strike this mantid was reported to centre its prey over an area extending more than 10° from the centre of widest spacing of the isopupil lines, and the angle relative to the centre of the acute zone depended consistently on the angle subtended by the prey to the head (Levin & Maldonado 1970). Possibly the explanation of these anomalies is that the acute zone was not effective at the experimental light intensity, or that the effective direction is not to the centre of the prey but to its boundary line. The extensive work of Mittelstaedt (reviewed in 1962) takes no acute zone into account, being concerned with the direction of the strike relative to the angle at which the head is held rather than with the choice of the region of the eye looking at the prey. Whether mantids gaze fixedly with their acute zones is in doubt from the literature but is obvious in several species, although the use of the acute zone has not been studied specifically. The behaviour related to binocular vision has not yet been analysed so it is impossible to say whether or not the eyes triangulate in the strike, or whether the reduced $\Delta\phi$ at the acute zone is significant for improved estimation of distance by disparity, for improved centring of the head for estimation of distance by either eye separately, as well as for improved resolution in general. The neurophysiology and neuroanatomy of binocular vision in mantids are as yet unopened subjects.

In the present context, mantid eyes unexpectedly turn out to have a large $D\Delta\phi$ value although these animals take a long time to stare at potential prey and they feed in bright light. There are also some curious differences between species. Possibly contrast discrimination is an important factor.

(ii) Orthodera ministralis (*F*) (*Orthoderinae*)

*Orthodera* is a green mantid 3–4 cm long, common in Canberra gardens during the summer, usually on flowering bushes in full sunlight, apparently lying in wait for prey to approach. The facets, marked in figure 27, look extremely homogeneous when seen from the front, with vertical rows of constant diameter (29–31 μm). The head is illustrated by Horridge (1977*b*).

Maps of the eye show a shallow acute zone with $D\Delta\phi$ decreasing to about 0.45, in contrast to the area around the acute zone where $D\Delta\phi$ is about 1.0 (figures 27 and 28).

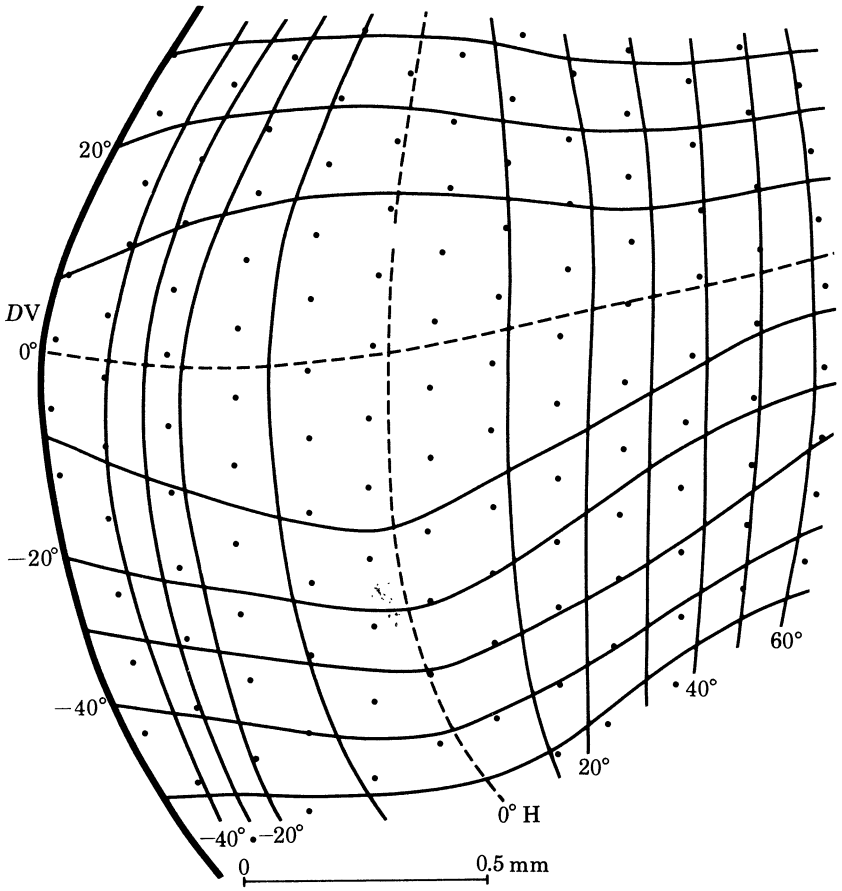


FIGURE 27. *Orthodera ministralis* (F) (Orthoderinae), Mantodea, left eye. Type of map: linear plot of the location of every 5th facet, and of the isopupil lines, taken from the photographs of pseudopupils. Axes: zero near centre of acute zone. The dashed lines are the base lines of the map. Features: no horizontal rows of facets; facet sizes similar over the front of the eye; binocular overlap of more than 45°. The head is illustrated by Horridge (1977*b*).

(iii) Archimantis latistyla (*Serv*) *and* Tenodera australasiae (*Mantinae*)

These two large mantids are similar in appearance, usually they are to be found resting in bushes, but *Archimantis* is common on tall thistles in one locality along the shores of Lake George, where it presumably feeds on mosquitoes. These large mantids have broad shallow acute zones that are obvious from the appearance of the pseudopupil but less obvious from the facet size. Maps of the front of the eye (figures 29 and 30) show that $D\Delta\phi$ ranges from 0.5 at the centre of the acute zone to more than 2.0 at the side and top of the eye. The acute zone

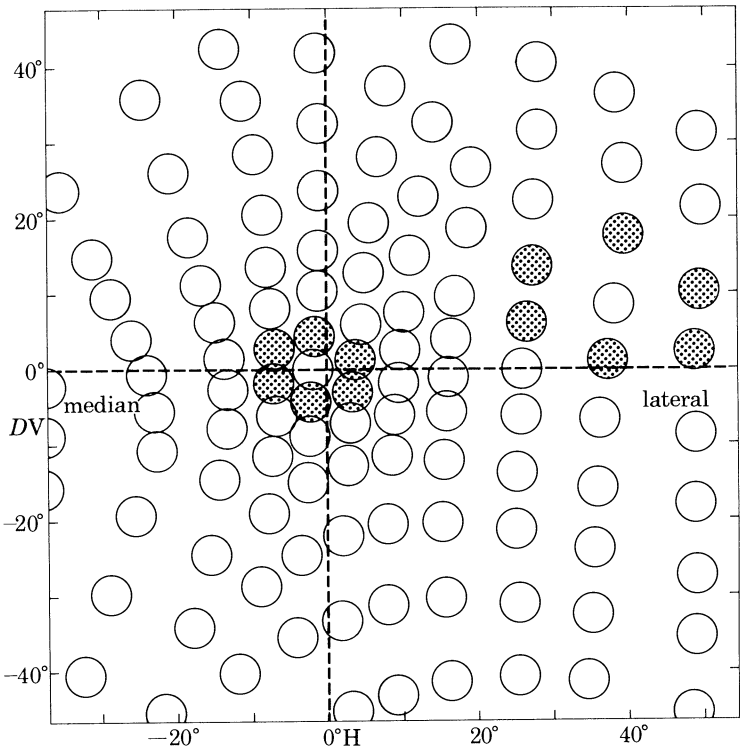


FIGURE 28. *Orthodera ministralis* (F) (Orthoderinae), Mantodea, left eye. Type of map: the location of every 5th ommatidial axis and its theoretical minimum visual field (magnified 5 times) in angular coordinates. Axes: horizontal and vertical with 0°, 0° near centre of acute zone. Features: the acute zone is formed by inward gathering of the rows of optical axes, with the hexagonal pattern of axes maintained; vertical rather than horizontal rows of axes; the eye parameter $D\Delta\phi$ decreases to less than 0.5 at the acute zone; binocular overlap of 45°; broad and shallow acute zone. Habits: lurks in wait for insects among flowers in bright sunlight.

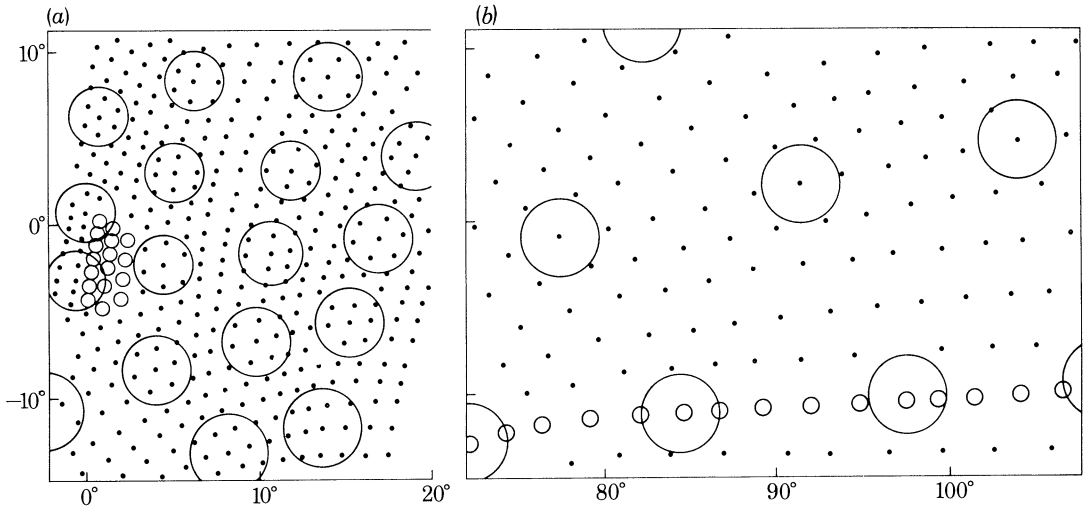


FIGURE 29. *Archimantis latistyla* (Serv.) (Mantinae), Mantodea, male, right eye. Type of map: the location of every individual ommatidial axis in angular coordinates is drawn as a dot and every fifth one is the centre of a large circle of diameter $5\lambda/D$. (*a*) region near the acute zone. (*b*) side of the eye in the same coordinates. Axes: zero near centre of the acute zone. Features: large values of the eye parameter $D\Delta\phi$, as shown by the separation of the circles. Even at the centre of the acute zone the eye parameter is not less than 0.5 μm. Habits: typical large mantid. The light intensity range of successful predation is not known; this species probably feeds on mosquitoes as well as diurnal insects.

in each case is formed by the simple inward bunching of the rows of the visual axes, which does not show from the rows of facets on the eye surface. The large values of $D\Delta\phi$ originate partly from the large diameter of the facets and partly from the large $\Delta\phi$ as a consequence of the binocular overlap of 45–50°. The interommatidial angles decrease to a little less than 1° in the acute zone.

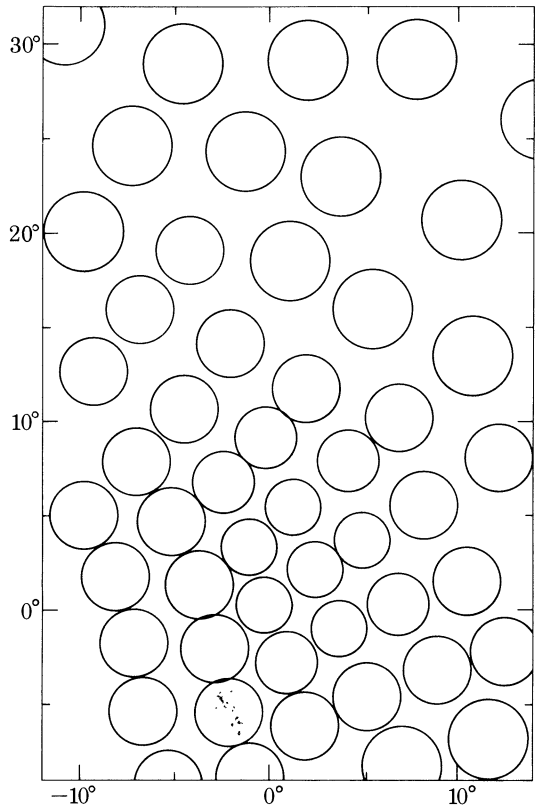


FIGURE 30. *Tenodera australasiae* (Mantinae), Mantodea, male left eye. Type of map: the location of every 5th ommatidial axis with its theoretical minimum visual field (magnified 5 times) in angular coordinates. Axes: zero near the centre of the acute zone. Features: Increased resolution and decreased eye parameter at the acute zone; hexagonal pattern maintained across the front of the eye, no horizontal rows of axes. Habits: typical large mantid; intensity range to which the eye is adapted is not known.

(iv) Ciulfina *sp. probably* C. biseriata (*Westwood*) (*Iridopteryginae, Mantidae*)

The most amazing mantid eyes are found in this group of narrow mantids with long thin legs that live on branches and trunks of trees in the N. Queensland rain forest. The eyes are almost spherical and far apart (figure 31, plate 2) with very regular rows of facets (figure 32). The black line across the centre of both eyes is camouflage pigment. The front of the eye is taken up by the enlarged facets of a forward looking acute zone, where the pseudopupil suddenly increases in size. One of the features of these mantids is that they can run very fast up or along tree trunks. Their feeding habits are unknown. A map of the eye (figure 33) shows a deep acute zone with $D\Delta\phi$ decreasing to 0.35. The acute zone is formed by the inward gathering of the oblique rows of optical axes, which is not indicated by the facet lines on the outside of the eye. There is about 25° of binocular overlap on each eye, which is less than in other mantids, and consistent with greater speed and smaller head.

(v) *Summary of observations on mantids*

The mantids proved to be so different from the other groups, in the large values of $D\Delta\phi$ and in the structure of the acute zone, that a special comment is invited. Mantids stalk towards their prey and often examine it visually for a long time before they strike, so that the values of $D\Delta\phi$ should be small as there is negligible relative velocity across the eye. In captivity mantids require bright light to feed. Apart from the acute zone, the mantid eyes have values of $D\Delta\phi$ and large facets that are typical of crepuscular animals. In mantids the value of $D\Delta\phi$ is large partly because the enormous binocular overlap of 30–55° makes it essential to have larger values of $\Delta\phi$ than in a typical insect with at most 10–15° of overlap. It would be of great interest to know the values of $\Delta\rho$ and $s$, and hence whether the large facets are an adaptation which increases the sensitivity or the resolving power.

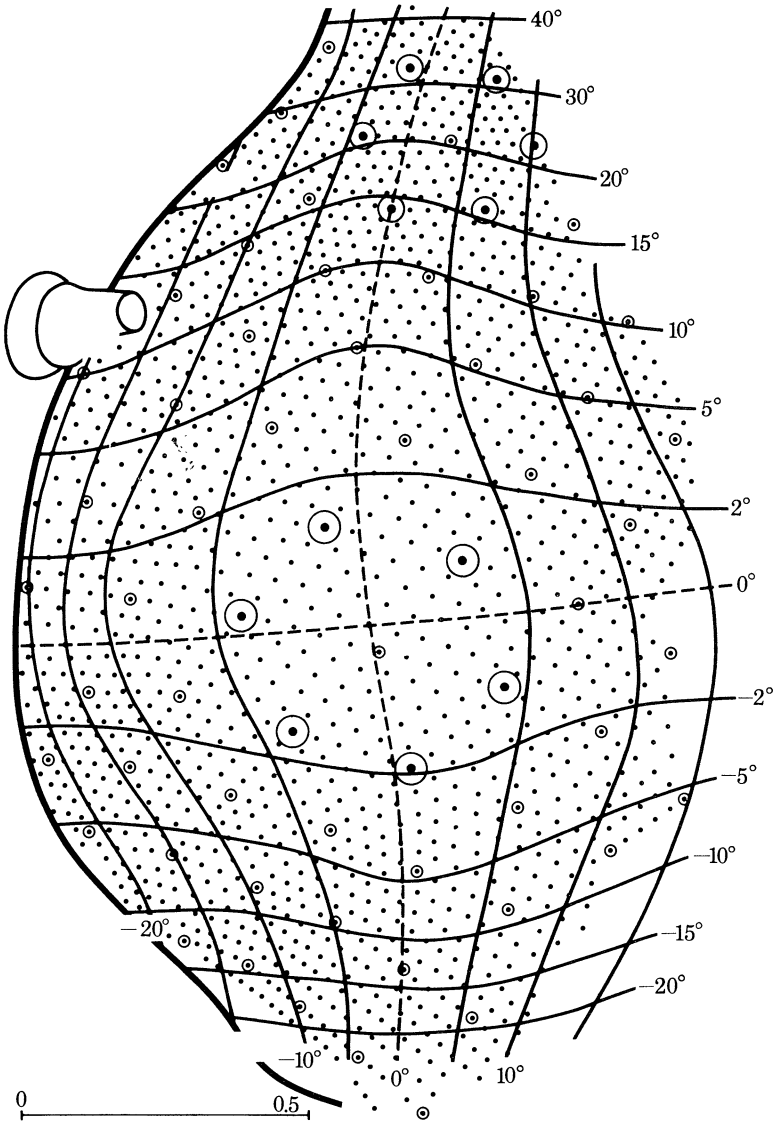


FIGURE 32. *Ciulfina* sp. (Iridopteryginae) Mantidae, male left eye. Type of map: linear plot of the location of every facet and of the isopupil lines taken from the photographs of pseudopupils. Axes: 0°, 0° near centre of acute zone. Features: regular rows of facets; larger facets at acute zone; hexagonal pattern with neither vertical nor horizontal rows of facets; more than 20° of binocular overlap. Scale in mm.

Secondly, studies of mantid behaviour in either stalking or the strike have not yet demonstrated that the acute zone is used in the strike at prey. The disadvantage of not having good resolution in all directions is reduced if the eye scans with the acute zone, as in primates, but we have no idea whether mantids scan.

Thirdly, the decreasing $D\Delta\phi$ towards the centre of the acute zone, in all four mantids studied, suggests that the acute zone is more useful in brighter light, so there may be an intensity threshold for the behaviour in which the acute zone is essential. As we know neither the function of the acute zone, nor its impact on the optic lobe, it is clear that a great deal remains to be done.

Finally the mantids have even more obvious differences from the other insects in lacking horizontal facet lines and in having a huge area of binocular overlap across the whole front of the head. For this reason, because it is said that mantids can strike successfully when not

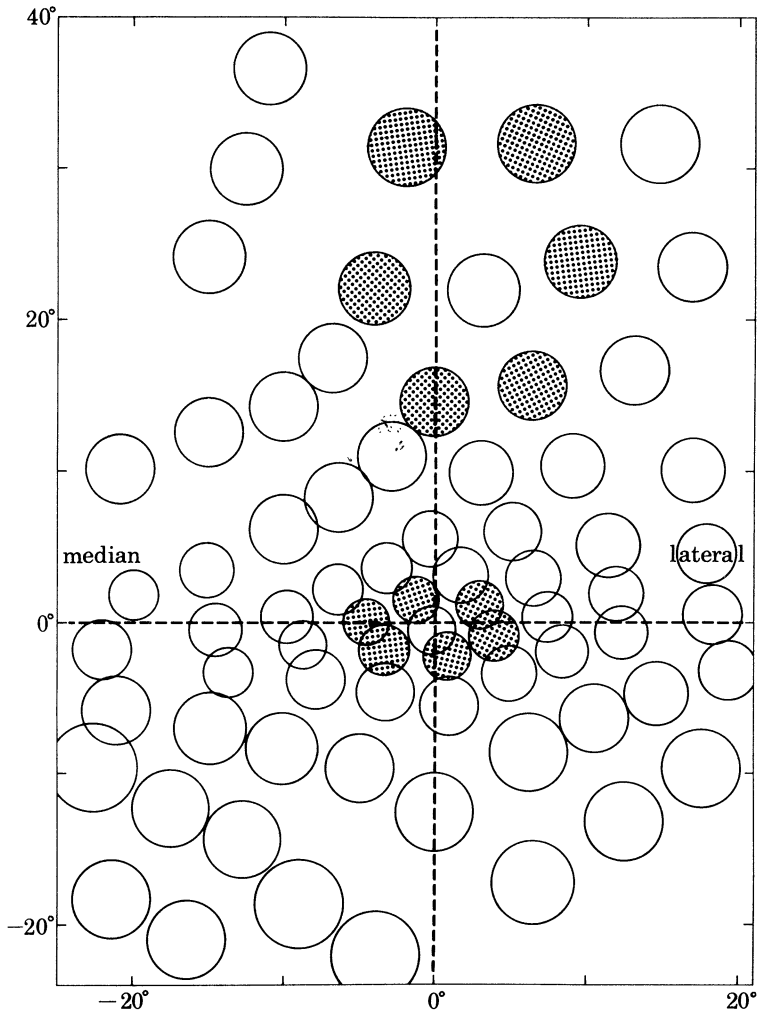


FIGURE 33. *Ciulfina* sp. (Iridopteryginae), Mantidae, male left eye. Type of map: the location of every 5th ommatidial optical axis and its theoretical minimum visual field (magnified 5 times). Axes: zero at centre of acute zone. The map was developed along the dashed lines, which are the isopupil lines at 0° H and 0° V in figure 32. Features: increased resolution and decreased eye parameter at the acute zone; some vertical compression of the hexagonal pattern of axes at the acute zone, as shown by the shaded circles; large gradient of eye parameter; large value of eye parameter outside the acute zone.

staring straight at their prey, and also because mantids, when blind in one eye, will not strike, it is possible that the mantids have a binocular vision which can detect *disparity* between the angles subtended by an object at each eye and that is why they sacrifice space on the eye for the sake of more binocular overlap. Again this has yet to be tested, and as pointed out by Pichka (1976) disparity detectors would require a set of retinotopic projections from the ommatidia to meet those from the other side, a state of affairs for which there is no evidence in insects. We are left with the paradox that mantids, as well as Zygoptera and many representatives of other groups, show no positive evidence or anatomical pathways for disparity detectors although with limited angular space they sacrifice resolution to make a binocular overlap.

### (*e*) *Diptera*

(i) *The situation in flies*

As *Musca*, *Calliphora* and several other flies have been studied intensively over the past decades, a good deal of scattered data is available. A map of the facet diameters of the *Calliphora* male was published by Kuiper (1962), and the interommatidial angles $\Delta\phi_V$ and $\Delta\phi_H$ were given for four regions of the eye by Burkhardt, de la Motte & Seitz (1966). A map of the optical axes of the housefly eye is given by Beersma *et al.* (1975). Although no maps of $D\Delta\phi$ are available, more is known of the differences between the optical system across the eye than in other insects. The optical requirement for the neural superposition is that the angle between adjacent rhabdomeres subtended at the posterior nodal point must be the same as the angle between corresponding adjacent ommatidia. In the housefly the distance between the rhabdom tip and the cornea is greater where the facet diameter is greater, at the front of the eye, in such a way that the ratio of these (not the $F$ value of the lens) is approximately constant at 1.9 over the eye. The facet diameter $D$ decreases from 24 μm at the front of the eye to 17 μm at the back, with a smooth gradient of increasing $\Delta\phi$ from the front to the back of the eye. The eye parameter $D\Delta\phi$ is approximately constant over the eye, at a surprisingly large value of 1.3. These data are from Stavenga (1975*a*), and the eye of *Musca* provided the best known example for the theoretical work of Snyder (1977). The large eye parameter is regarded as an adaptation to aerial acrobatics at moderate light intensity.

The pattern of facets is also the consequence of rigid geometrical constraints. At the side of the fly eye the hexagonal pattern of facets is turned through 90° relative to that at the front of the eye, and there are diamond shaped intermediate facets. This change in pattern fits in with the decreasing optical radius in the horizontal plane while the radius in the vertical plane does not change (Stavenga 1975*b*). This asymmetrical resolution in the lateral part of the fly eye is a factor to be reckoned with if, for example, the spatial frequency transfer function of the eye is measured by recording responses to striped patterns from interneurons that respond to movement in horizontal or alternatively in vertical planes across the eye.

Many groups of flies, especially those that hover, such as some Bibionidae, Simuliidae, Bombyliidae, Pipunculidae and Syrphidae have eyes which meet at the midline (often only in the male) in a region where the facets are larger than elsewhere. It is one of these, the hoverfly *Syritta* (Syrphidae) which provided the first clear example of a functional acute zone to be described in Diptera (Collett & Land 1975). In *Syritta*, an acute zone at the front of each eye, looking straight ahead with axis parallel to that in the other eye, extends over 5–10°. There is a binocular overlap (as defined here) of only 4–5°. Centre to centre separation of facets increases from 17–19 μm at 15° from the acute zone to 40 μm at its centre. Correspondingly,

$\Delta\phi$ decreases from 1.6 to 0.6° at the centre of the acute zone, so that $D\Delta\phi$ is reasonably constant at 0.43–0.48 along a horizontal row across the front of the eye. This is much less than in the housefly, presumably because the acute zone of the eye of *Syritta* is adapted for bright sunlight. The eye is still far from the diffraction limit, either because it is adapted for aerial pursuit of other flies, or possibly on account of the constraints imposed by neural superposition in a small eye (see below).

The dorsal part of the eye has enormously enlarged facets in male Simuliidae, in which the rhabdomeres are separate as in other flies but are greatly lengthened as if to increase sensitivity (Dietrich 1909). Recently Kirschfeld & Wenk (1977) have shown by behavioural tests that the male's ability to see the female in flight is limited by intensity in the range where the effect can be attributed to photon noise. It has long been known that at the lower intensity threshold of the optomotor response the vision of flies is limited by photon noise (Fermi & Reichardt 1963). Evidence is therefore accumulating that in flies the values of $D$ and $\Delta\phi$ are set by the compromise between sensitivity and resolution. The theory, however, which was worked out for fused rhabdomere apposition eyes, summarized in figure 5, does not necessarily apply when the rhabdomeres are separate, because $D$ and $\Delta\phi$ are set by the geometry of the neural superposition eye (Stavenga 1975*b*) and by the need to avoid optical coupling between adjacent rhabdomeres (Wijngaard & Stavenga 1975). Even with these constraints increasing the value of $D\Delta\phi$, the eye of *Musca* is more efficient over a limited but useful intensity range at transmitting information despite photon noise than is the optimum fused rhabdomere eye at each intensity, because the summation of the signal from sets of six retinula cells increases the ratio of signal to noise (Snyder, Stavenga & Laughlin 1977).

### (*f*) *Crustacea*

The ghost crab *Ocypode* has been included because it is the most extreme example of a nocturnal apposition eye that could be found, and at first sight the enormous number of facets suggest pooling of excitation to increase sensitivity. The mantid shrimp *Odontodactylus* is included because it has the most complicated eye structure encountered in this survey.

#### (i) Ocypode ceratophthalma (*Ocypodidae, Decapoda*)

When surprised out on the beach this crab rapidly returns to its burrow, reaching speeds of 3 m/s (Burrows & Hoyle 1973). The crabs emerge from the burrows to scavenge at night but are also commonly seen in bright sunlight if conditions are very peaceful. The only way to observe them is from a hide or with a telescope and undoubtedly a main function of the eye is to catch sight of seagulls and other predators, by night and day, before the crab itself is seen.

The eyes differ in the two sexes. The male has pointed eyestalk extensions beyond the eye proper, doubling the length of the eyestalk. The only possible function suggested for these structures is that they serve for visual intersex recognition, and the crabs are strongly territorial. The acute zone of the female also differs from that in the male. Only the situation in the female is described here, and no other studies are known. The eye which is held upright in normal posture, is elongated vertically and is almost a cylinder capped by a hemisphere (figure 34, plate 5). The field of view of each eye is almost 360°, the direction without ommatidia being that part of the visual field which is blocked by the other eye. For small angles of tilt the statocyst reflexes keep the eye angle constant relative to gravity with an error that is less than

10 % of the angle of tilt (for values in *Carcinus*, see Horridge 1966*b*). The significance of this stabilization depends on the function of the asymmetry of the optical axes of the ommatidia.

The rows of ommatidial axes are horizontal in the upper half of the eye but in the lower half they tilt progressively more and more. Facet diameters reach 43–45 μm in the acute zone and are remarkably homogeneous over large areas. At the top of the eye however, the diameter falls to 25 μm. At first sight the facets look small but this is a false impression caused by the enormous size of the eye (figure 35, plate 7).

A map of the visual axes shows a deep elongated acute zone along the equatorial line (figure 36). Because the facets are relatively constant in diameter, the acute zone is caused principally

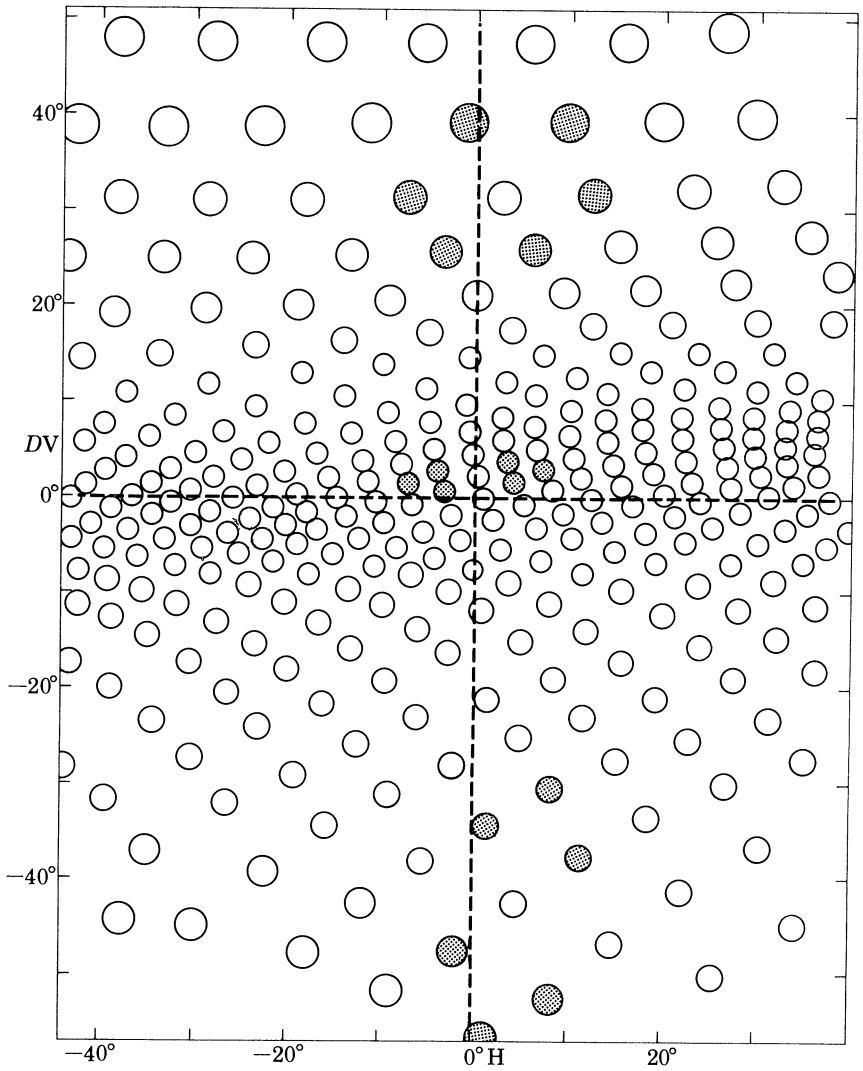


FIGURE 36. *Ocypode ceratophthalma*, female right eye. Type of map: location of the optical axis of every 5th ommatidium together with its minimum theoretical field width (magnified 5 times). Axes: vertical axis, zero near centre of the acute zone; horizontal axis arbitrary, but looking towards the front, as in figure 34. Features: strong gradient of $\Delta\phi$ and therefore of $D\Delta\phi$ along the vertical axis; central band of high resolution with crowding of axes near the horizontal plane; hexagonal pattern strongly compressed in angular space across the acute zone, as shown by the shaded circles; symmetrical hexagonal pattern at the top of the eye (round pseudopupil in figure 35*b*), vertical elongation at the bottom of the eye (flattened pseudopupil in figure 35*g*). Habits: Fast running on tropical beaches, emerges from burrow at any time of day or night; very wary of predators on the horizon.

by gradients of $\Delta\phi$. In the female there is little gradient along the equator at the front of the eye, and the back has not yet been mapped. The outstanding feature of the *Ocypode* eye is that it has a wide range of $D\Delta\phi$ along the vertical axis. At first sight the gradient of $D\Delta\phi$ is an adaptation for a wide range of intensities, as in the human eye, but a better explanation is that even such a large eye cannot cover a 360° visual field with sufficient sampling stations, and therefore only a critical horizontal band has the increased spatial resolution. The eye is large, with numerous large facets: interest is clearly centred on objects on the horizon, but from above, the seagull is an important predator for this crab, which must therefore be wary in all directions. In addition, a predator in the air moves rapidly whereas on the horizon the angular velocity is likely to be low. Whether the gradient of $D\Delta\phi$ is related to sensitivity and the *expected angular* velocity of objects of importance relative to the eye or merely to sampling density, will be seen when the field sizes ($\Delta\rho$) have been plotted.

(ii) Odontodactylus scyllarus (*Linnaeus*) *and* Gonodactylus chiragra (*Fabricius*)

*Odontodactylus* and *Gonodactylus* belong to a group of marine mantid shrimps called 'smashing stomatopods' because the heel of the dactyl is enlarged to form a club as an alternative weapon in addition to the sharp dagger-like end of the dactyl. These animals have a complex repertoire of visual behaviour which, with the aid of the antenna, is particularly important in the control of the aggressive strike of either dagger or club. To hit a hard object with the delicate dagger is a fatal mistake, but a strike at a fish requires success with the dagger at the first blow. These stomatopods normally rest in burrows from which they emerge to hunt for prey visually. They feed in daylight on crabs, molluscs or anything living and are strongly territorial. The eye is also important to spot the approach of a predator: walking over a reef flat one often sees *Gonodactylus* dart for cover. *Odontodactylus scyllarus* roams about fearlessly in water a few meters deep but usually scurries to its hole at the approach of a diver. Display, warning coloration and visual recognition of the social intentions of other members of the species form an important part of their behaviour (Caldwell & Dingle 1976). *Gonodactylus* is illustrated by Horridge (1977*b*). For visual behaviour of *Squilla*, see Schaller (1953).

The eye of *Odontodactylus* is huge for a compound eye, being 6 mm in diameter in a 15 cm animal. A band six facets wide, which divides the eye into two hemispheres (figure 37, plate 8) is normally orientated at approximately 45° to the horizontal. The eye is mobile in all axes with facets up to 120 μm at the acute zone. This is beyond the range of limitation by diffraction.

The eye has many optical features which are clearly related to behaviour. Primarily, in each hemisphere and in the central band there is a row of facets which all look in parallel planes (figure 38). Peripheral to these rows the optical axes diverge as in a typical compound eye, but central to these rows the axes fill the same angle in space as facets in the opposite hemisphere. Each eye therefore has a built in rangefinder, which is demonstrated by the appearance of the pseudopupils in figure 37, plate 8.

When either pole of the eye is observed, only one pseudopupil is visible, but when the eye is rotated and observed from a direction closer to the central band, two pseudopupils move across the eye until, as the symmetrical position is approached, the central band shows its own pseudopupil (figure 37*d*). In this plane there are three sets of facets with parallel optical axes. In Squillidae, as demonstrated long ago by Demoll (1909*a*), there are two such groups.

In each of the three parts of the eye of *Odontodactylus* but not *Gonodactylus*, the acute zone is superimposed on the system of intersecting axes described above. At one place on the central

band the facets are larger than on either side (figure 37). At the corresponding places on each hemisphere, sharing the same optical axis, a group of ommatidia also have larger facets. The three pseudopupils suddenly grow large and round when the eye is rotated so that these three regions are looking towards the observer (figure 37*e*). Maps of the eye made by the pseudopupil reveal that these are three deep acute zones, one in each part of the eye. In the acute zones of *Odontodactylus*, the facet sizes go up to 120 μm. The central band of the *Odontodactylus* eye is almost 1 mm wide and consists of only six rows of ommatidia which are 60 μm wide outside the acute zone, ranging up to 135 μm wide at the centre of the acute zone.

The map of the acute zone in angular coordinates (figure 39) is remarkable in that the values of $D\Delta\phi = 2$ are constant right across its centre, as the increase in $D$ towards the centre just keeps pace with the increase in $\Delta\phi$. The indication is that the acute zone is adapted to the same intensities as the rest of the eye. The actual value of $D\Delta\phi = 2$ and the maximum facet diameter up to 120 μm are also remarkable in being so large for an animal which hunts in bright light, and deserves further comment and experiment.

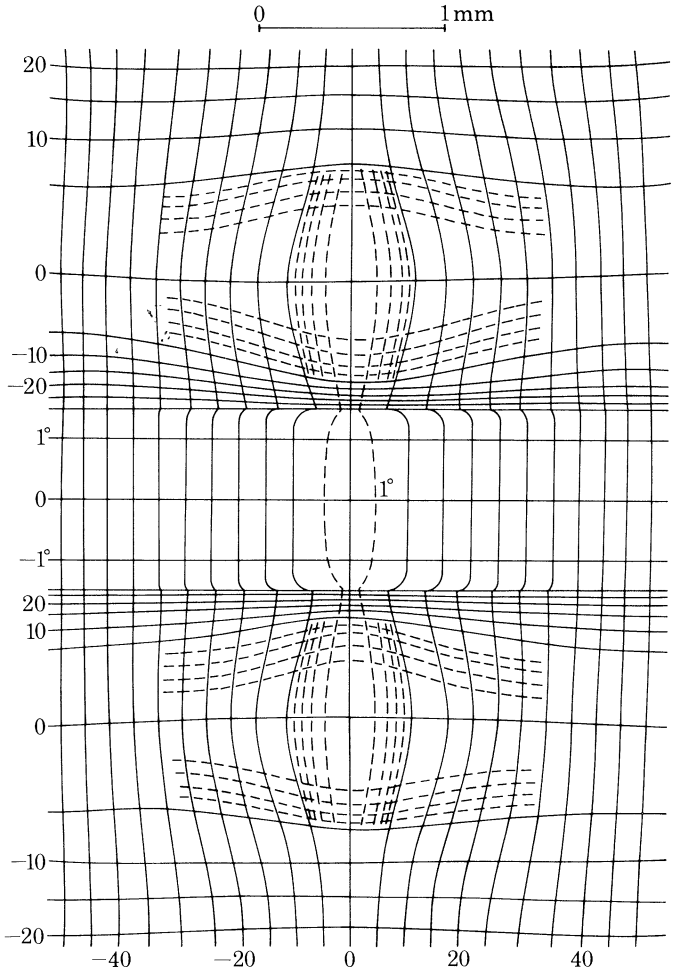


FIGURE 38. *Odontodactylus scyllarus*. Type of map: the foveal region in both hemispheres of one eye in linear coordinates, showing the locations of the isopupil lines. Features: three axes at 0°, 0°, sharing the same plane, which is held near 45° to the vertical in the living animal at rest (as illustrated for *Gonodactylus* in figure 37 *a*, *b*). Note the angular overlap of more than 20° between the two hemispheres of the eye and the two axes of symmetry, one along the central band and one along the line through the three acute zones.

The optical composition of the acute zone arises from an inward leaning of the optical axes of ommatidial rows which is not apparent from the superficial view of the eye. The facets are hexagonal except where rows are crowded together close to the central band to make room for the larger facets of the acute zone. The rows of facets are continuous through and all around the acute zone: no rows are crowded out in this region but between the acute zone and the central band the facets are distorted and the facets of a given row become separated from each other. As they approach the central band the facets rapidly diminish in size, down to 30 μm.

The functions of the three parts of the eye are not yet understood although clearly there is the possibility of one rangefinder in each eye and of another rangefinder between the central bands of the two eyes. The additional function of the acute zone, which does not occur in

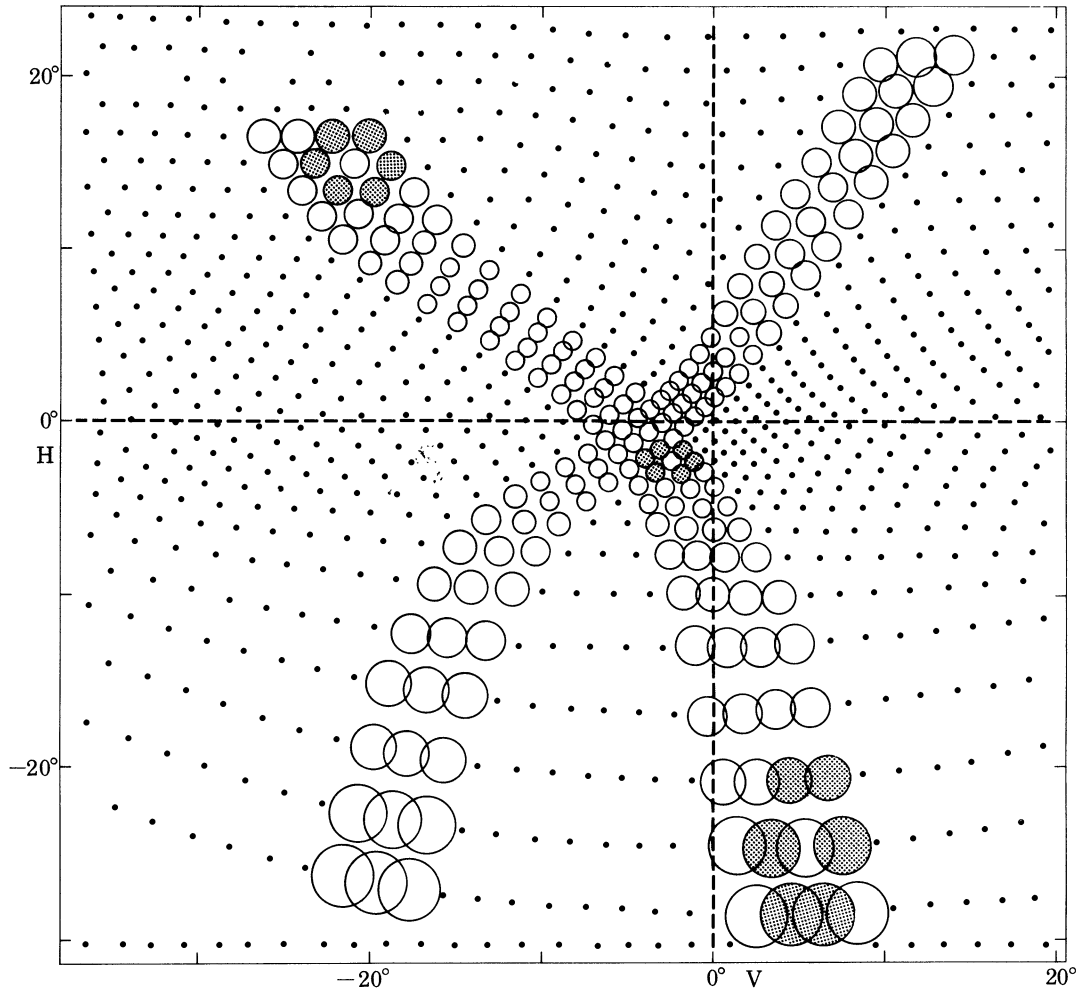


FIGURE 39. *Odontodactylus scyllarus*. Map in angular coordinates of the locations of visual axes of every ommatidium around one acute zone in one of the hemispheres of the eye. The lower part of this map is towards the central band. The circles have a diameter of $4\lambda/D$ in this map and therefore, in directions and in places where they touch, the eye parameter $D\Delta\phi = 2$. Axes: zeros near the centre of the acute zone. Features: the greatly enlarged facets of the acute zone have the consequence that the eye parameter is constant over large areas; the rows of visual axes are curved in such a way that the hexagonal pattern of facets (shaded circles) forms a hexagonal pattern of optical axes across the acute zone, but compressed in one direction along the horizontal zero axis and in the other direction near the central band of the eye (along −20° H to −30° H).

*Gonodactylus*, is also undescribed, but three features are clear. First, in life the eyestalks are rotated separately so that the acute zones are turned towards any novel object or movement in the visual field. Secondly, the three acute zones of one eye share the same axis, with the interommatidial angle decreasing towards those axes which converge at the greatest range. Thirdly, the central bands of the two eyes are crossed relative to each other, so that when the acute zones are fixated on objects of interest, the axes of the two eyes together are locked into positions which are different for every direction and range of the object. How all this fits in with the visual control of the two alternative strike patterns is yet to be described.

A factor which might contribute to the high value of $D\Delta\phi = 2$ for *Odontodactylus* is eye tremor. In an eye crowded by three acute zones and three regions duplicating the same axes, $\Delta\phi$ has to be large because there is insufficient room for more facets. Under these circumstances the number of sampling stations may possibly be effectively increased by eye tremor or scanning. In crabs there is a special muscle which maintains a tremor in the horizontal plane (Horridge & Sandeman 1964), which has the effect of accentuating edges in vision (Horridge 1966*a*) but the question of tremor remains open in other arthropods.

## Discussion

### (*a*) *General findings from the eye maps*

Maps of the distribution of visual axes show the maximum possible spatial resolution at each point and in each direction on the eye. They also show the directions and the regularity of the rows of axes, which are related to the directions and regularity of rows of facets. Maps of facet diameter show the maximum theoretical resolving power of individual ommatidia in each part of the eye.

Maps prepared, as here, with circles of diameter $\lambda/D$ at each optical axis show, in addition, the distribution of the eye parameter $D\Delta\phi$. We now have available a great deal of data for comparison of different species and different eye regions of each. The maps show that eye design does not depend entirely on diffraction.

Maps made from measurements of $\Delta\phi$ and $D$ are only a beginning in the analysis of regional differences and physiological differences between eyes. The next step is to prepare maps of the acceptance angle $\Delta\rho$, which would show the real overlap or separation of actual fields, rather than of theoretical minimum fields which is all that $\lambda/D$ shows. If values of $\Delta\rho$ are not available, maps of the subtense of the rhabdom ($d/f$, see figure 2) would indicate whether the rhabdom diameter (and therefore $\Delta\rho$) is increased as predicted in regions and in eyes where the eye parameter $D\Delta\phi$ is increased. Behavioural tests on regions of eyes would then show the consequences of the optical differences between eye regions, and study of the optic lobe neurons and their anatomy in known regions across the eye may show how the parts of the retina are integrated. Making maps of the optical system is therefore only a start.

#### (i) *Design*

At the outset it had better be stressed that descriptions of the form of organs that interact intimately with the environment are meaningless without reference to function. At the next stage of analysis, whether it be the optics which produces the field sizes, the physiology of retinula cells, or the straight description of anatomy and visual behaviour, we often omit, perhaps mistakenly, the apparent causative relation to the function of the whole eye that must

have arisen by natural selection. In particular, in mapping compound eyes, one cannot avoid considerations of the regional specializations in relation to function. The arrangement and spacing of visual axes, the size of individual facets and of the whole eye are related to the intensity and relative angular velocity at which the eye normally operates.

(ii) *Regional differences in interommatidial angle*

Maps of the visual axes of the compound eye in angular coordinates show that all studies of visual behaviour and eye function must be made on known and relevant eye regions. Over the past 20 years a great volume of work on the compound eye has paid little attention to this point. Secondly, the theory of spacing of the visual axes shows that the intensity at which normal functions are carried out is the most important factor determining the form of the eye. This is an aspect that has been overlooked: almost no electrophysiology of compound eye function has been carried out at normal ambient intensities.

Before the modern electrophysiological period a different outlook prevailed. Two papers which appeared 40 years ago related regional differences in the interommatidial angle to visual behaviour. Baumgärtner (1928) studied the bee and measured from sections the regional differences in the angles between ommatidia in vertical and horizontal planes, and demonstrated that the former is much smaller than the latter, data which has never been explained in functional terms. At about the same time Friederichs (1931) measured the interommatidial angles of the tiger beetle eye (*Cicindela*), and correlated the regional differences and binocular overlap with numerous experiments on the visual behaviour, mainly by painting over different parts of the eye. The result of both of the above pieces of work was an appreciation that the distribution of optical axes must be a large factor in visual behaviour, but no convincing correlations were demonstrated. One reason was that the interommatidial angles were measured from histological sections with the possibly erroneous result that the region of smallest interommatidial angle was thought to lie at the side of the eye. The lesson is that the visual axes should be observed optically in all experiments on the eye.

(iii) *Values of $D\Delta\phi$: sacrifice of resolution to sensitivity*

The present survey of eye types and arthropod groups, deliberately spread over several habitats, suggests that only in the acute zone of insects which hover to examine prey in brightest sunlight can we find values of $D\Delta\phi$ which approach the diffraction limit of 0.3 for hexagonal facets. The effect of photon noise is that no compound eyes have interommatidial angles small enough for the whole eye to reconstruct all the detail that could be resolved by the individual facets. In this sense there are no compound eyes that reach the diffraction limit set by $\lambda/D$, with rhabdoms of negligible diameter. In most parts of all the eyes studied the values of $D\Delta\phi$ suggest that even those that normally function by day have a spatial resolution matched to a facet size that is suitable for lower intensities than bright sunlight. The values of $D\Delta\phi$ are always greater than 0.3, and in many examples $D\Delta\phi$ can be correlated with the intensity at which selection may be most intense, or with the relative velocity of objects of interest across the eye. Although all of the data on $D\Delta\phi$ can be interpreted in terms of the theories of Snyder (1977) and Snyder, Stavenga & Laughlin (1977), some of the measurements are unexpected, e.g. that mantids have large values of $D\Delta\phi$, and that acute zones are of several different kinds. It is already clear that most of the detail of regional and eye differences is beyond the scope of the theory without more data on field sizes, absolute sensitivity and visual behaviour.

Most insects do not hover in bright sunshine and they have eyes that are too small to have space for regions which approach the diffraction limit. As seen from equation (7), the angular sensitivity function of diameter $\Delta\rho$ can be near the diffraction limit $\lambda/D$ only when the rhabdom is less than half the diameter of the Airy disk and then the absolute sensitivity is low (figure 2 *c*). Many large diurnal bees, dragonflies, grasshoppers, butterflies, crabs and others with fused rhabdomere apposition eyes have $D\Delta\phi$ values of about 0.5 over much of the eye, although they are frequently active in bright sunlight. The point is that an eye cannot be designed for just adequate modulation for stationary conditions in the brightest light encountered. Its owner must survive in shade and usually must see when in motion. With a range of $D\Delta\phi$ from 0.5 to 1.0, $\Delta\phi$ from 1 to 2° and $\Delta\rho_{LA}$ from 1 to 2°, it can be calculated from equation (9) that fractional modulation is across the working range from 0.15 to 0.8 at the threshold $\Delta\theta$ which the eye can reconstruct. From figure 5 it can be seen that an eye with $D\Delta\phi = 0.5$ will be reasonably adapted to a wide range of daylight intensities because the theoretical relation between $D\Delta\phi$ and intensity is flat in this region. Also many of these eyes are equipped with a mechanism for increase in $\Delta\rho$ on dark-adaptation, so that the fixed parameters $D$ and $\Delta\phi$ are adapted not only for bright light; $D\Delta\phi$ will therefore be larger than expected from the brightest intensity encountered.

Turning to the specialized examples of large apposition eyes with larger values of $D\Delta\phi$, we find three categories, the flies, the mantids and the true dim light visual predators. The fly eye has been discussed by Snyder (1977) and Snyder, Stavenga & Laughlin (1977). They conclude that values of $D\Delta\phi$ of about 1.3 agree with the aerobatic behaviour because the rapid turns in flight, acting via the trade off between sensitivity and exposure time, are equivalent to a reduced light intensity of about 2 log units. Small values of $\Delta\phi$ would not be compatible with the neural superposition eye because optical crosstalk occurs between rhabdomeres that are too close together (Wijngaard & Stavenga 1975). For exact summation without increase in field size, at lamina level, the angle subtended by adjacent rhabdomeres at the posterior nodal point must equal $\Delta\phi$. Possibly there are flies with deep acute zones in which the focal length of the lens is appropriately increased so that the rhabdomeres can be adequately separated. The very elongated cones of the dorsal eyes of simuliid flies (Dietrich 1909) indicate such a situation. This consideration does not apply to apposition eyes with fused rhabdomeres.

Secondly, the mantids, as discussed separately here, have $D\Delta\phi$ values ranging from less than 0.5 in the acute zone up to 1.5 in areas that still look to the front, and 2.0 or more at the side of the eye. There are three possible explanations for the high values of $D\Delta\phi$, (*a*) the eye although large, simply has insufficient room for a broad deep acute zone as well as 45° of binocular overlap, (*b*) the eye is adapted for a wide range of intensities, (*c*) the eye is adapted for making discriminations with small scanning movements.

Finally, predators which are active in dim light only are exemplified by the crepuscular dragonfly *Zyxomma* and the mantid shrimp *Odontodactylus*. The former has an exaggerated dragonfly eye with large facets, reduced acute zones and $D\Delta\phi$ of more than 1.0 in most areas: the mantid shrimp has deep acute zones with $D\Delta\phi = 2.0$ uniformly, even across the centre of the acute zone. Although the eye is huge, the compromise between the size of the acute zone and the spatial resolution of the rest of the eye is pushed to the limit because there is also strong selection pressure for larger facets. In *Zyxomma* the result is a single shallow acute zone, whereas in *Odontodactylus* sufficient angular space is found for the three acute zones by having an eye 5–6 mm in diameter.

(iv) *The gradient of interommatidial angle along the equator*

In some insects, and especially the rapid flying, diurnal ones, the interommatidial angle in the horizontal plane is least at the front of the eye, with a gradient of increasing angle from the front around the side of the head. Usually the interommatidial angle in the vertical plane is relatively constant along the equatorial region, with the result that the asymmetry of the resolution increases from front to back. The best documented eye is of the housefly (Stavenga 1975*a*, *b*) and the results can be correlated with the visual chasing behaviour of the female fly by the male, as described by Land & Collett (1974). Whether the properties of the optic lobe neurons confirm this explanation, and how it applies to the other types of compound eyes, awaits experiment.

In many arthropods, however, it is clear that other principles apply. Among Crabs, Orthoptera, Lepidoptera, Coleoptera and most slow moving arthropods there is little or no gradient of $\Delta\phi$ from front to back of the eye. Fast flying skipper butterflies with a diurnal superposition eye have remarkably symmetrical eyes: apparently an adaptation to a gradient of velocity is impossible in that type of eye. Once the correlation between rapid flight and gradient of $\Delta\phi$ has been noted, we can pick out the analomous cases for further investigation.

### (*b*) *Acute zones in compound eyes*

(i) *Previous work*

Apart from the isolated work of del Portillo (1936), the compound eye has for many years been treated as more homogeneous than is justified. From histological sections del Portillo found some independence between eye radius, facet diameter and interommatidial angle and suggested that particular regions of the eye are more important in vision than others. In a long paper, lost in undeserved obscurity, Friederichs (1931) demonstrated that regions of the eye of the tiger beetle differ in interommatidial angle, facet size and in effect upon turning, fleeing and approach behaviour.

Recently there have been three examples of a renewed interest in this area. First, the interommatidial angle, function and growth of the mantid eye regions were described by Maldonado and his associates in the early 1970s, but mantids have been regarded as different from other insects. Secondly, in a region at the front of the eye of the hoverfly, *Syritta*, with larger facets and smaller interommatidial angle than the rest of the eye, calculations suggested that on account of the limits set by diffraction 'the larger facets in the fovea are needed to match the reduced interommatidial angle' (Collett & Land 1975). To these authors the fovea meant a *region of best seeing* where the receptors are crowded more closely per unit solid angle, and where limiting angular resolving power is better than elsewhere on the eye. Thirdly, all of the commonly studied muscid flies have larger facets and greater radius of curvature at the front than at the side of the eye, with a smooth gradation between (Stavenga 1975*a*, *b*). Both flies and mantids are discussed separately in this paper: among crustaceans and other insects, references to acute zones of compound eyes are negligible.

(ii) *Types of acute zones*

First of all, a region of reduced interommatidial angle can be an elongated band, as occurs along the equator of the eye of dragonflies, many bees and wasps, flies and *Ocypode*. This situation is always related to the need to see the horizon particularly well.

The simplest type of acute zone encountered is where $\Delta\phi$ decreases locally with little change in facet size, illustrated by some mantids, the forward looking foveas of some dragonflies, some butterflies (e.g. *Vanessa*, not described here) *Ocypode*, and others.

The second type of acute zone has the facet diameter increasing in step with the reduction in interommatidial angle, so that $D\Delta\phi$ remains constant, as illustrated by *Syritta*, *Odontodactylus Austrogomphus* dorsal and *Amegilla* anterior acute zone.

The third type encountered is the intermediate situation in which the increase in facet size fails to keep pace with the reduction in $\Delta\phi$ so that $D\Delta\phi$ decreases towards the centre of the acute zone, as illustrated by dragonflies, mantids, *Bembix* and others.

One could interpret these differences in terms of the theory of Snyder, Stavenga & Laughlin (1977), in which larger $D\Delta\phi$ implies function at effectively lower light intensity. Certainly none of the data disproves the theory, and much of it is in line with the quantitative formulation, but there are so many factors and so many observable details that have now become of interest, that it would be unwise to explain too much too soon in terms of intensity alone. For example, the advantage conferred by an acute zone is increased if use can be made of eye or head movements. Hoverflies and man have the same strategy of eye movement in that the eye moves in large predetermined jerks to point the acute zone, and the position is stabilized to allow full use of the narrow fields and small angles between fields in the acute zone. All this is described for the hoverfly *Syritta* by Collett & Land (1975), but we have no theory of how eye tremor is used in arthropods, or of its effect on the sampling angle.

With reference to types of acute zones in particular, there are no measurements of field sizes, rhabdom sizes, or $F$ values of the ommatidia of acute zones, no observations on acute zones in relation to light intensity or possible collaboration between the two eyes. We have yet to demonstrate acute zones designed for staring in bright light, for accurate alignment of the head, for pursuit of moving targets and so on.

A deep and broad acute zone is obviously a more powerful specialization than one which is either shallow or small, but it takes up a large part of the eye so that only the very large eyes of some mantids, dragonflies and crustaceans have room for them. A small and deep acute zone is clearly ineffective for following a moving target, which is quickly lost from it, but is appropriate if the target is stationary. To explain the advantages of the different kinds of acute zones clearly requires more observation of their actual functions and how they are integrated in the optic lobes.

(iii) *Lateral areas of best seeing*

The two classical sets of measurements of the interommatidial angle from histological sections of compound eyes produced the now surprising result that the largest facets and the smallest interommatidial angles are about 60° from the front in the tiger beetle *Cicindela* (Friederichs 1931) and in the worker bee (Baumgärtner 1928). Probably these results were erroneous, for reasons already discussed. However, in many of the large dragonflies which fly in sunlight, notably corduliids and aeshnids, there is a deep acute zone looking out at 90° to the body axis. This lateral acute zone is much less extensive in dragonflies which have smaller heads or which fly in dim light, and it is clearly the least essential of the three acute zones.

Concerning the function of the side of the eye, Friedrichs provided one clue when he discovered that the tiger beetle flees from large moving objects when they are visible to the side. Similarly, Frazer-Rowell (1971) found that the sensitivity to small movements which acts as

an early warning visual mechanism in the locust is most sensitive at the side of the eye and ineffective in the forward looking regions. In the dragonfly the function of the lateral acute zone is quite unknown: one suggestion is that it is essential for visually stabilized hovering over water.

### (*c*) *The superficial pattern of facets*

(i) *Facet lines*

When we look closely at an insect eye, one of its obvious features is the direction of the rows of facets. When a wasp, grasshopper, dragonfly or crab is examined from the front, the obvious rows of facets are horizontal (figures 8, 14, 20, 25 and 35). In contrast, at the front of a fly eye the forward looking facets are in vertical rows. In dragonflies which have facets that look upwards as they fly, the rows of optical axes on the top of the eye run from front to back, but in mayflies and Simuliidae (not described here), the upward looking dorsal parts of the eyes have large facets in diagonal rows relative to the midline. On the other hand, in a nocturnal insect like a moth or an earwig the rows run in no particular direction. In mantids the forward looking facet rows are diagonal and curved.

A generalization that emerges is that where motion perception is important the rows of facets run along the expected direction of motion. Information on this point from a diverse assortment of compound eyes might validate such an idea, and studies of optic lobe neuron connectivity might confirm it. Expressed so simply as this, the principle might apply to eyes with reasonably uniform facet size and visual axes that look out at right angles to the surface of the eye. Where there is an acute zone, the situation is different because the pattern of axes does not necessarily correspond to the pattern of facet lines, as may be seen by comparing axes in angular coordinates with the facet pattern in the linear map of the same area.

(ii) *Dislocations in the hexagonal pattern*

A pattern of regular hexagons, even of graded diameter, cannot cover a hemispherical eye. When we examine compound eyes to see exactly how they solve this problem, we find remarkable regularities, which became obvious during the mapping procedure. The following generalizations emerge:

(*a*) Insects which depend on visual behaviour have regular facet rows and maximum geometrical perfection of the eye; others which clearly depend less on vision have irregular facet rows.

(*b*) Where the eyes are large, or complex with one or more acute zones, they are geometrically more perfect in the parts of the eye where vision matters most as judged by the behaviour or posture. The part of the eye behind the antenna is often the most irregular.

(*c*) Acute zones are almost always geometrically perfect. Extra facet lines are never interpolated in the acute zone but always start some way from it, where optical radius and facet diameter are already less than maximal. A deep acute zone can only be formed by squeezing some facet lines out of existence in the area surrounding the zone (see figure 8).

(*d*) Dislocations of the facet pattern do not occur on exactly the same row of facets in different individuals of the same species, but usually they occur in the same region, commonly behind the antenna.

(*e*) Square facets are rare among insects, for example in the dorsal eyes of some male mayflies, in special parts of the eye of many flies, and some mutants of *Drosophila*. Where they occur it is always as a definite specialization, the function of which is not understood. In Crustacea, by

contrast, square facets are quite common, and here they have a significance in that the mechanism of optical superposition by reflection depends upon having crystalline cones with flat reflecting sides (Land 1976).

### (*d*) *Collaboration between the two eyes*

The mapping procedure was not aimed at the elucidation of how the two eyes are used together where there is binocular overlap. However, several points can be made. When there are upward or forward looking acute zones they usually share the same axis, i.e. the centre of both acute zones looks in a direction parallel to the median plane through the head. At first sight the two acute zones could be used together for the estimation of the range of an object by the disparity between the two eyes (Demoll 1909). This is most unlikely, however, for several reasons. First, as pointed out by Pichka (1976) binocular depth perception by disparity requires a particular pattern of retinal projections for which there is no evidence in insects. Secondly, the estimation of distance is improved in proportion to the distance between the two eye centres (Burkhardt, Darnhofer-Demar & Fischer 1973), but in most of the advanced insects with forward or upward looking acute zones the separation between the two congruent regions is small. This is true for Diptera, Anisoptera and Hymenoptera and other insects which turn to look, or pursue prey in flight or which hover while examining an object visually. I have argued in more detail elsewhere that these insects estimate range by parallax as they move (Horridge 1977*b*), and the same point has also been mentioned by Collett & Land (1975, p. 32), but in no example is the issue settled.

Recently Frantsevich & Pichka (1976) have plotted binocular fields by the pseudopupil method and found three classes of overlap. (*a*) Short baseline and small overlap but large eyes, in insects which intercept in hunting, notably Odonata, Asilidae, Syrphidae and the drone bee. (*b*) Medium baseline and overlap looking in the landing direction, in pollinators such as the honeybee, Bombyliidae, Syrphidae and many Lepidoptera. (*c*) Large baseline and almost half the front of the eye taken up by binocular overlap, characteristic of predators which hunt among vegetation. The present review agrees with and extends these generalizations. Isotropic eyes (Burkhardt *et al.* 1973) do not occur.

Eyes with forward looking acute zones that are far apart are found in dragonfly larvae (Baldus 1926), damselflies and mantids. Even in these cases it is not clear that the eyes collaborate together in the estimation of range *by triangulation*. As a simpler alternative, let us suppose that the animal turns its head or body until the longitudinal axis is pointing directly at the object of interest. At each eye the range is then given by which facet is looking in the direction of the object. An acute zone in each eye would improve the accuracy of the initial lining up and also of the subsequent and quite separate estimation of range. If this is the mechanism, fewer nervous connections are needed than for the measurement by triangulation of an object, and either optic lobe can make the estimate. The mantids provide the only example with some evidence for estimation of range by triangulation (Maldonado & Rodriguez 1972), but even in mantids there is no evidence for triangulation over the whole of the binocular overlap. Clearly more facts must emerge before we understand why mantids and damselflies have such a large area of binocular overlap. No data is available relating to higher Crustacea, except that many have widely separated eyes and appear to have visual control when they bring the claw into action at the right range. In the case of the mantid shrimps, from the existence of a range finding mechanism *within each eye*, we still cannot infer a neural mechanism for measuring range by

triangulation, because the above mentioned method, by symmetry, is simpler and equally possible.

Effects of binocular vision on the eye parameter $D\Delta\phi$ are likely to be complex. If range finding is of advantage there will be selection pressure to reduce the interommatidial angle $\Delta\phi_H$. Then, if other factors are constant, either the acute zone will function only in brighter light than the rest of the eye or its integration time will have to increase. In either case $D\Delta\phi$ will be smaller in the acute zone. On the other hand, because binocular overlap implies that a solid angle of the field of view is sampled twice, the values of $D\Delta\phi$ for the eye as a whole are larger than would be otherwise required.

### (*e*) *Other strategies*

(i) *Pooling of visual axes*

Pooling of excitation in parallel channels improves the signal : noise ratio and can be either optical or neural. The two known forms of optical pooling have not been illustrated in the apposition eyes described. First, in neural superposition eyes of flies the separate rhabdomeres behind each facet have fields with different axes. Excitation from six retinula cells having the same optical axis in six neighbouring ommatidia is then summed neurally at the first synaptic layer of the optic lobe. Over a limited and rather low intensity range, the improvement in signal: noise ratio, by summation, more than compensates for the large value of $D\Delta\phi$ that is essential to prevent optical crosstalk between the separated rhabdomeres (Snyder *et al.* 1977, figure 14). The fly type of eye, despite its rigidly defined geometry, is clearly successful for medium intensities, but further increase in the size of the rhabdomeres to increase the sensitivity, as in figure 4*b*, is impossible if the parallel axes are in neighbouring ommatidia. In the bug *Lethocerus* this problem of a nocturnal open rhabdomere eye is solved by having each rhabdom on the same optical axis as six other rhabdoms which are 3–4 facets away in each direction. In *Lethocerus* the acceptance angle $\Delta\rho$ spreads to 10° in the dark adapted state. The sensitivity to large sources is therefore large and also the neural summation is available for further increase. The optimum is at a lower intensity level and lower spatial frequency than in the fly. Details of *Lethocerus* retinula cells are given by Ioannides & Horridge (1975).

The other way of pooling optically is by optical superposition in a clear zone eye. When only 120–150 facets collaborate, the superposition of images can be so good that the image of a point source covers no more than one rhabdom, as in the diurnal agaristid moths (Horridge *et al.* 1977). With recruitment of further ommatidia, however, the image is increasingly fuzzy, until in some beatles the threshold period of regular stripes must be more than 20° when the focal ratio of the optical system ($f/D$) is about 0.3. Such extremely wide apertures are found only in some nocturnal clear zone eyes. Because only large objects can be resolved and their images cover hundreds of receptors, such an eye realizes the increased sensitivity to large objects only if there is extensive neural summation within large adjacent areas of the optic lobe and correlation between them.

Besides optical pooling, a possible way of adjusting to low light intensities would be to have progressive pooling by larger and larger groups of optic lobe neurons, with corresponding loss of resolution. An apposition eye could then have the eye parameter $D\Delta\phi$ adapted to the brightest conditions typically encountered and neural pooling for those parts of the visual repertoire that have selective advantage in dim light. On this question Snyder *et al.* (1977) have pointed out that having larger facets preserves more information than increasing the sensitivity to the same

extent by neural pooling, because larger facets in addition give less diffraction. The point is, however, that facet sizes are fixed whereas the size of the neural pool can theoretically be adjusted almost instantaneously for any intensity. Evidence that this occurs comes from the effective increase in the field size (measured behaviourally) in the fly optomotor response as the mean pattern brightness is lowered (Eckert 1973, extended by Dvorak & Snyder 1977).

Pooling at the retinal level between retinula cells *with different optical axes* is not known in apposition eyes, except for an isolated case in the anterior part of the eye of the dronefly *Eristalis* where depolarization of one type of retinula cell causes depolarization of a particular neighbouring cell of different spectral sensitivity with its optical axis inclined at 1–2° to the first cell (Tsukahara & Horridge 1977*a*). Despite tests in many compound eyes, there is no fusion of excitation arising from different axes, as found in vertebrate dark adapted rods (Fain, Gold & Dowling 1976).

At the present time two comments may be made about neural pooling behind compound eyes. First, the perception of *differences* between the excitation of neighbouring ommatidia, including motion perception, must *precede* the summation which neural pooling presumes, therefore pooling cannot be complete. Secondly, convergence from many neurons in parallel to a few neurons at deeper levels is the standard pattern in all arthropod optic lobes, so that pooling of some kind is universal, with all degrees of convergence. What is not known is whether there are changes in the degree of convergence as the background intensity is altered.

(ii) *Eyes of maximum size*

The theory of eye parameters assumes that because of increased noise at lower light levels, the facet sizes and rhabdom diameters (and therefore field sizes and interommatidial angles) are larger than they need be according to the laws of diffraction. We might therefore ask why the eye does not cover a larger fraction of the head. In fact, in most dragonflies, flies, bees, butterflies, and especially in small insects, there are non-visual areas of cuticle on the top of the head whereas in the extreme examples the head is almost all eye.

The question is outside the scope of the theory presented, but on examination of insects where the head is all eye we find they have reduced jaw muscles. With more eye there must be less of something else, a heavier eye to carry, and more neurons and receptors to maintain. The balance of factors in the total design spreads beyond theories which explain the separation of optical axes.

(iii) *Discrepancy with behavioural tests*

A disconcerting finding of several detailed behavioural studies is that the apparent discrimination of patterns by small compound eyes with relatively few facets suggests that the spatial resolution is much better than would be expected from the interommatidial angle. The stick insect, for example, with $\Delta\phi = 6 \pm 0.5°$ has remarkable abilities to discriminate patterns resembling rough versus smooth twigs (Jander & Volk-Heinrichs 1970). For the water bug *Velia* black disks are the preferred size when 4° but white disks when 3.4°; *Velia* discriminates changes of 1° in the separation of disks although $\Delta\phi = 10°$ (Meyer 1974). Optomotor response of crabs can be recorded to movements of a striped pattern by less than 0.05° although the interommatidial angle is near 2° and the eye has a special muscle which causes it to tremor in the horizontal plane by 0.05–0.2° at 2–5 Hz (Horridge & Sandeman 1964). Even more extreme are the fly larvae which have a photoreceptor of wide field buried in their anterior end. This

swings from side to side as they crawl, and the larva turns towards the side which is shaded (Fraenkel & Gunn 1940).

If scanning or tremor by the eye or head is linked with a suitable coordinating system and a primitive memory of changes of intensity, then spatial resolution can be better than the interommatidial angle would otherwise allow. There is strong evidence that some such mechanism is at work in these examples, and maybe generally in arthropods. This does not disprove the sampling theory in equation (3): it shows that some highly organized visual behaviour requires a more elaborate theory because sequential sampling circumvents the restriction that there must be two sampling stations for each stripe period.

### (*f*) *Conclusion*

What has been presented is a general theory followed by eye maps which can be discussed in terms of the theory. Almost every step in the theory, however, needs to be refined: let us work through the steps. The question of focus is still doubtful in most apposition eyes: apart from the fly no examples have been described. The sampling criterion is applicable only if sampling is simultaneous and if regular stripes of all spatial frequencies are an adequate model of the visual world. Possible peculiar optical properties of the neck of the cone have been omitted in explaining the origin of the acceptance angle. Modulation as calculated from equation (9) is for fields of view which are Gaussian in sensitivity. Absolute sensitivity calculated from equation (10) omits factors such as the division of light between eight rhabdomeres of different sizes and absorption properties. The square root law for noise in equation (13) refers only to the intervals between photon arrivals and we have already found an additional transduction noise in the unequal amplitude of bumps caused by photons (Tsukahara & Horridge 1977*b*). In addition, factors such as receptor noise and modulation depend on the state of adaptation and the dynamic response of the retinula cell. The time over which the signal is integrated has not been studied but it presumably changes with adaptation and is perhaps different for different types of retinula cell. More serious, compound eyes are not necessarily adapted to see all possible patterns but may be adapted for their own particular sign stimuli. The eye maps therefore are a collection of data which at best can be sensibly discussed in terms of the eye parameter theory and they do not prove or refute it outright. Discrepancies can be investigated one by one. What has been done is to illustrate the differences between eye regions and eye types to validate the broad outlines of an elementary explanation and to point to the need for further observations on the origin, consequences and functions of these eye patterns. In fact, the measurements described in this paper should be done before, not after, other types of analysis.

I am indebted to many people who have contributed during the course of this work, notably to my collaborators A. Snyder, D. Stavenga and S. Laughlin for the stimulus provided by the theoretical background, to K. Key and T. Watson of CSIRO for identification of insects, to Tess Falconer and Ladina Ribi for typing and drawing respectively, to B. Ham, B. Igusti Raka, W. Huggins and W. Stephens for varied services including catching animals, and particularly to Maureen Whittaker for printing hundreds of prints in the surveys of eyes from different angles. The final draft was prepared during tenure of a Visiting Fellowship at Churchill College, Cambridge. The manuscript was kindly read by M. F. Land and H. B. Barlow. This project was initiated by the chance observation of the eye of *Odontodactylus* on the island of Banda, Moluccas, Indonesia, during the 1975 Alpha Helix expedition.

## References


Baldus, K. 1926 Experimentelle Untersuchungen über die Entfernungslokalisation der Libellen (*Aeschna cyanea*). *Z. vergl. Physiol.* **3**, 475–505.

Barlow, H. B. 1952 The size of ommatidia in apposition eyes. *J. exp. Biol.* **29**, 667–674.

Barlow, H. B. 1964 The physical limits of visual discrimination. In vol. 2 *Photophysiology* (ed. A. C. Giese), pp. 163–202. New York: Academic Press.

Barros-Pitá, J. C. & Maldonado, H. 1970 A fovea in the praying mantis eye. II. Some morphological characteristics. *Z. vergl. Physiol.* **67**, 79–92.

Baumgärtner, H 1928 Der Formensinn und die Sehschärfe der Bienen. *Z. vergl. Physiol.* **7**, 56–143.

Beersma, D. G. M., Stavenga, D. G. & Kuiper, J. W. 1975 Organization of visual axes in the compound eye of the fly *Musca domestica* L. and behavioural consequences. *J. Comp. Physiol.* **102**, 305–320.

Burkhardt, D., Darnhofer-Demar, B. & Fischer, K. 1973 Zum binokularen Entfernungssehen der Insekten. I. Die Struktur des Sehraums von Synsekten. *J. Comp. Physiol.* **87**, 165–188.

Burkhardt, D., de la Motte, I. & Seitz, G. 1966 Physiological optics of the compound eye of the blowfly. In *The functional organisation of the compound eye.* (ed. C. G. Bernhard), pp. 51–62. London: Pergamon Press.

Burrows, M. & Hoyle, G. 1973 The mechanism of rapid running in the ghost crab. *J. exp. Biol.* **58**, 327–349.

Caldwell, R. L. & Dingle, H. 1976 Stomatopods. *Sci. Am.* **234**, (1), 80–89.

Collett, T. S. & Land, M. F. 1975 Visual control of flight behaviour in the hoverfly *Syritta pipiens* L. *J. Comp. Physiol.* **99**, 1–66.

Demoll, R. 1909*a* Über die Augen und die Augenstielreflexe von *Squilla mantis*. *Zool. Jahrb. Abt. Anat. Ontog. Tiere* **27**, 171–212.

Demoll, R. 1909*b* Über die Beziehungen zwischen der Ausdehnung des binokularen Sehraumes und dem Nahrungserwerb bei einigen Insekten. *Zool. Jahrb. Abt. Syst. Geog. u. Biol. Tiere* **28**, 523–530.

Demoll, R. 1910 Die Physiologie des Facettenauges. *Ergebn. Fortsch. Zool.* **1910**, 431–516.

Dietrich, W. 1909 Die Facettenaugen der Dipteren. *Z. wiss. Zool.* **92**, 465–539.

Dvorak, D. & Snyder, A. 1978 The relationship between visual acuity and illumination in the fly, *Lucilia sericata*. *Zeit. Natur.* **33c**, 139–143.

Eckert, H. 1973 Optomotorische Untersuchungen am visuellen System der Stubenfliege *Musca domestica* L. *Kybernetik* **14**, 1–23.

Evans, H. E. & Matthews, R. W. 1973 Systematics and nesting behavior of Australian *Bembix* sand wasps (Hymenoptera, Sphecidae). *Mem. Am. Ent. Inst.* **20**, 1–387.

Exner, S. 1891 *Die Physiologie der facettirten Augen von Krebsen und Insekten.* Leipzig and Vienna: Franz Deuticke.

Fain, G. L., Gold, G. H. & Dowling, J. E. 1976 Receptor coupling in the toad retina. *Cold Spring Harb. Symp. quant. Biol.* **40**, 547–561.

Fermi, G. & Reichardt, W. 1963 Optomotorische Reaktionen der Fliege *Musca domestica*. *Kybernetik* **2**, 15–28.

Fraenkel, G. & Gunn, D. L. 1940 *The orientation of animals.* London: Oxford University Press.

Franceschini, N. & Kirschfeld, K. 1971 Les phénomènes de pseudopupille dans l'oeil composé de *Drosophila*. *Kybernetik* **9**, 159–182.

Frantsevich, L. I. & Pichka, V. E. 1976 The size of the binocular zone of the visual field in insects [in Russian]. *J. Evol. Biochem. and Physiol.* (U.S.S.R.) **12**, 461–465.

Fraser, F. C. 1960 *A handbook of the dragonflies of Australasia, with keys for the identification of all species.* (67 pages.) Sydney: Royal Zoological Society of New South Wales.

Frazer-Rowell, C. H. 1971 The orthopteran descending movement detector (D.M.D.) neurons: a characterization and a review. *Z. vergl. Physiol.* **73**, 167–194.

Friederichs, H. F. 1931 Beiträge zur Morphologie und Physiologie der Sehorgane der Cicindelliden (Col.) *Z. Morph. Ökol. Tiere* **21**, 1–172.

Friza, F. 1928 Zur Frage der Färbung und Zeichnung des facettierten Insektenauges. *Z. vergl. Physiol.* **8**, 289–336.

Götz, K. G. 1964 Optomotorische Untersuchung des visuellen Systems einiger Augenmutanten der Fruchtfliege *Drosophila*. *Kybernetik* **2**, 77–92.

Götz, K. G. 1965 Die optischen Übertragungeigenschaften der Komplexaugen von *Drosophila*. *Kybernetik* **2**, 215–221.

Hesse, R. 1908 *Das Sehen der niederen Tieren.* Jena.

Horridge, G. A. 1966*a* Perception of edges versus areas by the crab *Carcinus*. *J. exp. Biol.* **44**, 247–254.

Horridge, G. A. 1966*b* Direct response of the crab *Carcinus* to the movement of the sun. *J. exp. Biol.* **44**, 275–83.

Horridge, G. A. 1977*a* Looking at insect eyes. *Sci. Am.* **237**, 108–120.

Horridge, G. A. 1977*b* Insects which turn and look. *Endeavour* 1 (1), 7–17.

Horridge, G. A., McLean, M., Stange, G. & Lillywhite, P. G. 1977 A diurnal moth superposition eye with high resolution, *Phalaenoides tristifica* (Agaristidae). *Proc. R. Soc. Lond.*, B, **196**, 233–250.

Horridge, G. A., Mimura, K. & Hardie, R. 1976 Fly photoreceptors. III. Angular sensitivity as a function of wavelength and the limits of resolution. *Proc. R. Soc. Lond.*, B, **194**, 151–177.

Horridge, G. A. & Sandeman, D. C. 1964 Nervous control of the optokinetic responses of the crab *Carcinus*. *Proc. R. Soc. Lond*, B, **161**, 216–246.

Ioannides, A. C. & Horridge, G. A. 1975 The organisation of visual fields in the hemipteran acone eye. *Proc. R. Soc. Lond.*, B, **190**, 373–391.

Jander, R. & Volk-Heinrichs, I. 1970 Das strauschspezifische visuelle Perceptorsystem der Stabheuschrecke (*Carausius morosus*). *Z. vergl. Physiol.* **70**, 425–477.

Kemp, S. 1913 An account of the Stomatopoda of the Indo-Pacific region. *Mem. Indian Mus.* **4**, 1–218.

Kirschfeld, K. 1976 The resolution of lens and compound eyes. In *Neural principles in vision* (ed. F. Zettler and R. Weiler), pp. 354–370. Berlin: Springer Verlag.

Kirschfeld, K. & Wenk, P. 1976 The dorsal compound eye of simuliid flies. *Zeit. Natur.* **31c**, 764–765.

Kuiper, J. W. 1962 The optics of the compound eye. *Symp. Soc. exp. Biol.* **16**, 58–71.

Kuiper, J. W. 1966 On the image formation in a single ommatidium of the compound eye in Diptera. In *The functional organization of the compound eye* (ed. C. G. Bernhard), pp. 35–50. Oxford: Pergamon Press.

Land, M. F. 1976 Superposition images are formed by reflection in the eyes of some oceanic decapod Crustacea. *Nature, Lond.* **263**, 764–765.

Land, M. F. & Collett, T. S. 1974 Chasing behaviour of houseflies (*Fannia canicularis*). *J. Comp. Physiol.* **89**, 331–357.

Laughlin, S. B. 1976*a* The sensitivities of dragonfly photoreceptors and the voltage gain of transduction. *J. Comp. Physiol.* **111**, 221–247.

Laughlin, S. B. 1976*b* Adaptations of the dragonfly retina for contrast detection and the elucidation of neural principles in the peripheral visual system. In *Neural principles in vision* (ed. F. Zettler & R. Weiler), pp. 175–193. Berlin: Springer Verlag.

Levin, L. & Maldonado, H. 1970 A fovea in the praying mantis eye. III The centring of the prey. *Z. vergl. Physiol.* **67**, 93–101.

Lieftinck, M. A. 1954 Handlist of Malaysian Odonata. *Treubia Publ. Mus. Zool. Bogoriense.* **22**, Suppl. 1–92.

Maldonado, H. & Barros-Pitá, J. C. 1970 A fovea in the praying mantis eye. I. Estimation of the catching distance. *Z. vergl. Physiol.* **67**, 58–78.

Maldonado, H. & Rodriguez, E. 1972 Depth perception in the praying mantis. *Physiol. & Behav.* **8**, 751–759.

Mallock, A. 1894 Insect sight and the defining power of composite eyes. *Proc. R. Soc. Lond.*, B, **55**, 85–90.

Meyer, H. W. 1974 Geometrie und funktionelle Specialisierung des optischen Abtastrasters beim Bachwasserläufer (*Velia caprai*). *J. Comp. Physiol.* **92**, 85–103.

Miller, W. H. & Bernard, G. D. 1968 Butterfly Glow. *J. Ultrastruct. Res.* **24**, 286–294.

Mittelstaedt, H. 1962 Control systems of orientation in insects. *Annu. Rev. Entomol.* **7**, 177–198.

Pichka, V. E. 1976 Visual pathways in the protocerebrum of the dronefly *Eristalis tenax* [in Russian]. *J. Evol. Biochem. and Physiol.* (U.S.S.R.) **12**, 556–559.

Portillo, J. del. 1936 Beziehungen zwischen den Öffnungswinkeln der Ommatidien, Krümmung und Gestalt der Insektaugen und ihrer funktionellen Aufgabe. *Z. vergl. Physiol.* **23**, 100–145.

Pritchard, G. 1966 On the morphology of the compound eyes of dragonflies (Odonata: Anisoptera) with special reference to their rôle in prey capture. *Proc. R. Ent. Soc., Lond.*, A, **41**, 1–8.

Rau, P. 1945 The night habits of the dragonfly *Anax junis*. Dru. *J. Comp. Physiol.* **38**, 285–286.

Rose, A. 1973 Vision, human and electronic. New York and London: Plenum Press.

Schaller, F. 1953 Verhaltens und sinnesphysiologische Beobachtungen an *Squilla mantis*. *Zeit. Tierpsychol.* **10**, 1–12.

Smart, J. & Clifford, E. A. 1965 Simuliidae (Diptera) of the Territory of Papua and New Guinea. *Pacif. Insects* **7**, 505–619.

Snyder, A. W. 1977 Acuity of compound eyes. Physical limitations and design. *J. Comp. Physiol.* **116**, 161–182.

Snyder, A. W., Stavenga, D. G. & Laughlin, S. B. 1977 Spatial information capacity of compound eyes. *J. Comp. Physiol.* **116**, 183.

Stavenga, D. G. 1975*a* Optical qualities of the fly eye. An approach from the side of geometrical, physical and waveguide optics. In *Photoreceptor optics* (ed. A. W. Snyder & R. Menzel). pp. 126–144 Berlin: Springer.

Stavenga, D. G. 1975*b* The neural superposition eye and its optical demands. *J. Comp. Physiol.* **102**, 297–304.

Tillyard, R. J. 1917 *The biology of dragonflies* (*Odonata or Paraneuroptera*). Cambridge University Press.

Tillyard, R. J. 1926 *The insects of Australia and New Zealand*. Sydney: Angus & Robertson.

Tsukahara, Y. & Horridge, G. A. 1977*a* Interaction between two retinula cell types in the anterior eye of the dronefly *Eristalis*. *J. Comp. Physiol.* **115**, 287–298.

Tsukahara, Y. & Horridge, G. A. 1977*b* Miniature potentials, light adaptation and afterpotentials in locust retinula cells. *J. exp. Biol.* **68**, 137–150.

Wallace, G. K. 1959 Visual scanning in the desert locust *Schistocerca gregaria* Forskäl. *J. exp. Biol.* **36**, 512–525.

Wijngaard, W. & Stavenga, D. G. 1975 An optical crosstalk between fly rhabdomeres. *Biol. Cybernetics.* **18**, 61–67.

Wilson, M. 1975 Angular sensitivity of light and dark adapted locust retinula cells. *J. Comp. Physiol.* **97**, 323–328.

Zänkert, A. 1939 Vergleichend-morphologische und physiologischfunktionelle Untersuchungen an Augen beutefangender Insekten. *S.B. Ges. Natur. Freunde*. Berlin 1–3, 82–169.

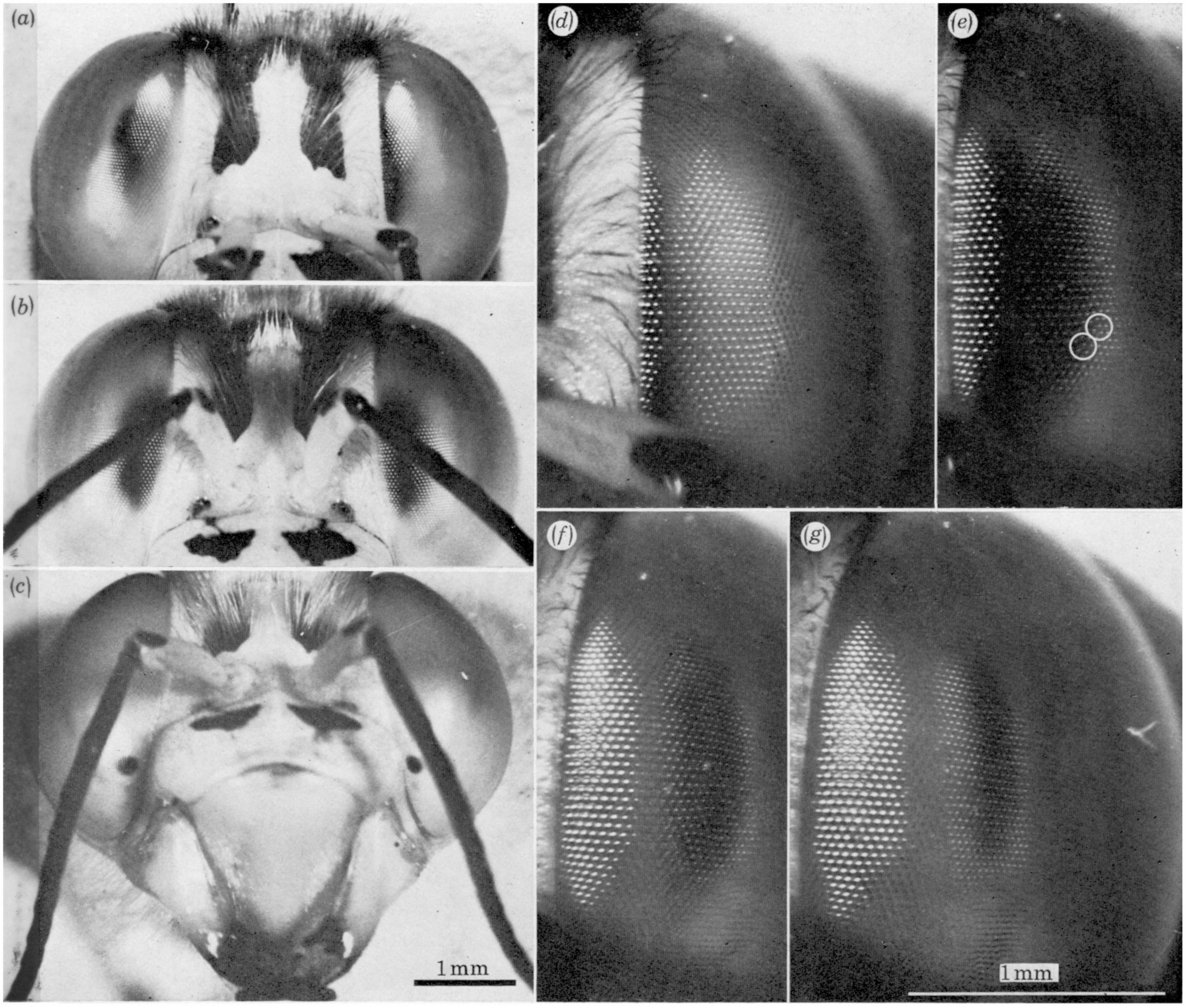


FIGURE 8. *Bembix palmata* Smith (sand wasp), Hymenoptera. (*a-c*) Living head seen from three angles: (*a*) from 5° to the side of the acute zone; (*b*) on the acute zone; (*c*) from 30° ventral to the acute zone. Features: large difference in size of the pseudopupil between (*b*) and (*c*); lateral shift of pseudopupil by about 8 facets for 5° horizontal shift; elongation of the pseudopupil in vertical direction at the level of the acute zone in (*a*) and (*b*) but not in (*c*); both acute zones look in the same direction, straight ahead. (*a*)–(*c*) are all the same magnification. (*d–g*) The pseudopupil at (*d*) −8°, (*e*) 0°, (*f*) 8°, (*g*) 16° relative to the acute zone, on the same horizontal line (the dashed line of figure 9). The circles show where additional facet lines begin, always *outside the acute zone*. (*d*)–(*g*) are all at the same magnification.

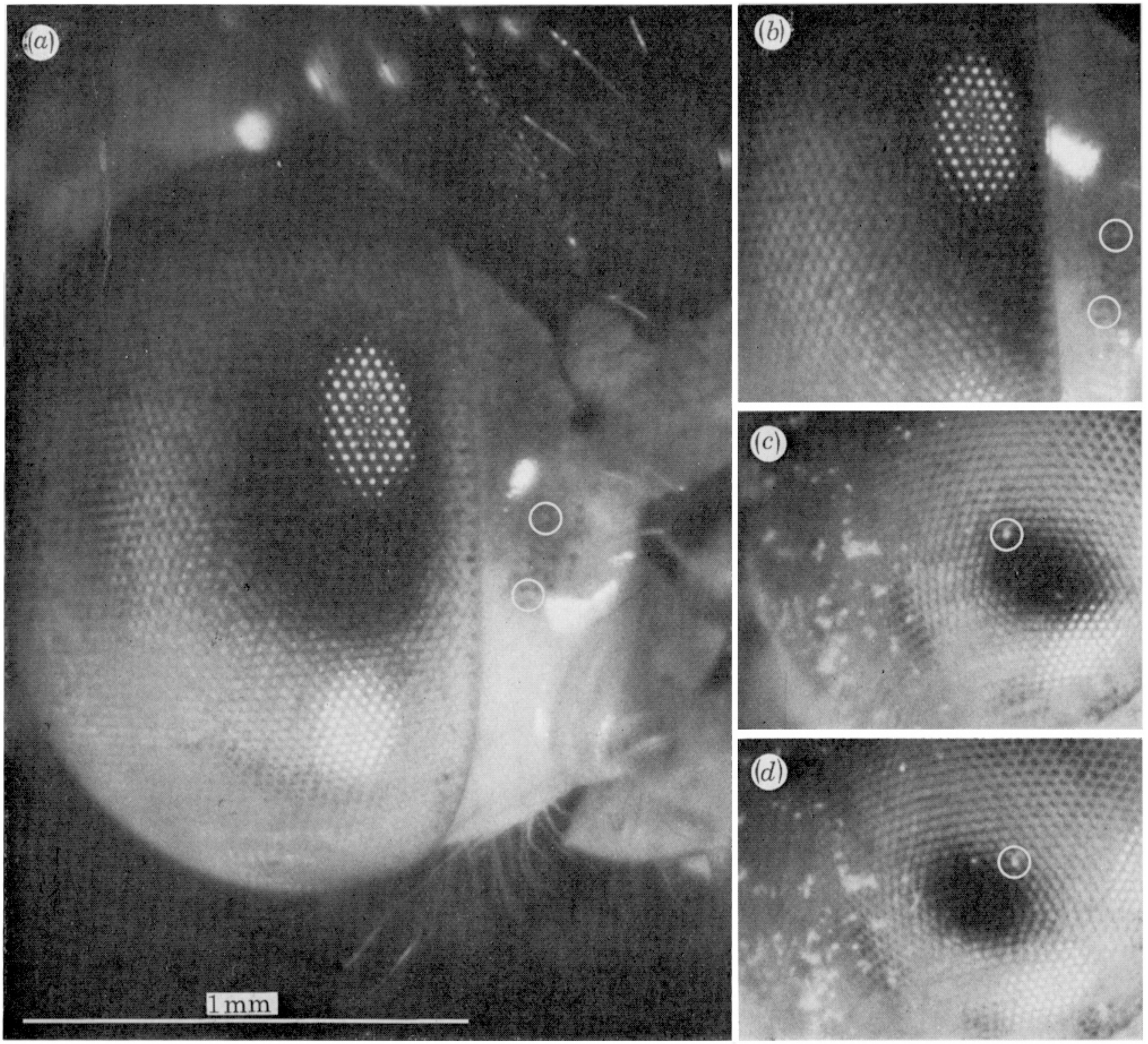


FIGURE 14. *Xanthagrion erythroneurum* Selys (damsel fly), Odonata. (*a*) The pseudopupil seen from the direction where it is largest, and axes are defined as 0°, 0°. Note the hemispherical eye, widely separated from its partner, which is characteristic of this group. (*b*) at 20° medial to (*a*) showing the large binocular overlap; axes 0° V, +20° H. (*c*) and (*d*) Movement of the pseudopupil relative to markers on the eye surface. Axes of (*c*) −15° V, 0° H: axes of (*d*) −15° V, +10° H. The coordinates are as in figure 16. Note the large differences in the size of the pseudopupil compared with the relatively small difference between the same regions on the map of the eye in figure 16. (*a*)–(*d*) are all at the same magnification.

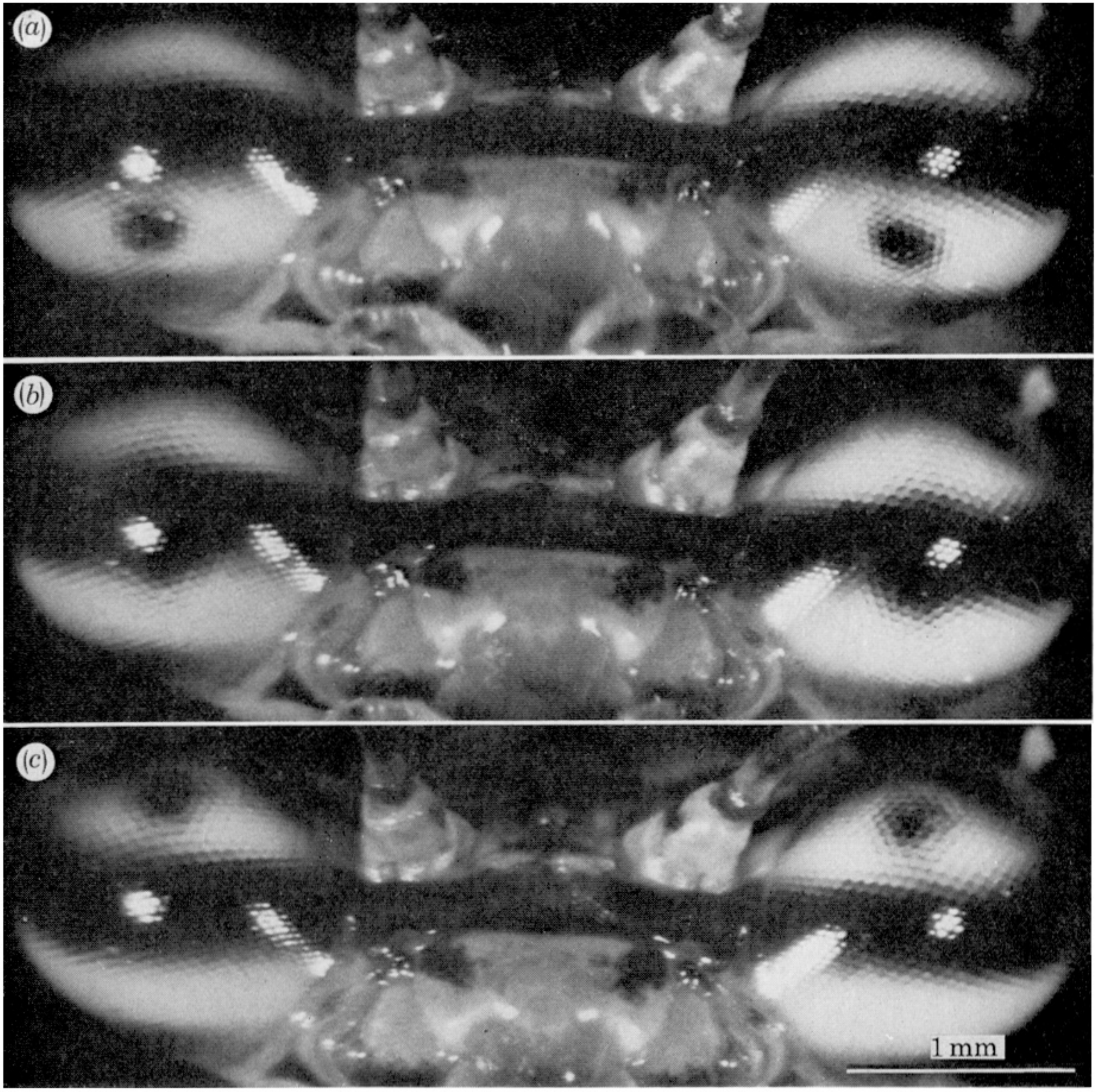


FIGURE 31. *Ciulfina* sp. probably *C. biseriata* (Westwood) (Iridopteryginae), Mantidae. Pseudopupils seen from the front at three inclinations of the head in the vertical plane; (*a*) 6° from fovea; (*b*) looking forwards; note pseudopupil extends beyond both sides of the line of pigment; (*c*) 6° below acute zone centre. Features: large binocular overlap and round, widely separated eyes, similar to those of Zygoptera (figure 14). (*a*), (*b*) and (*c*) are all the the same magnification.

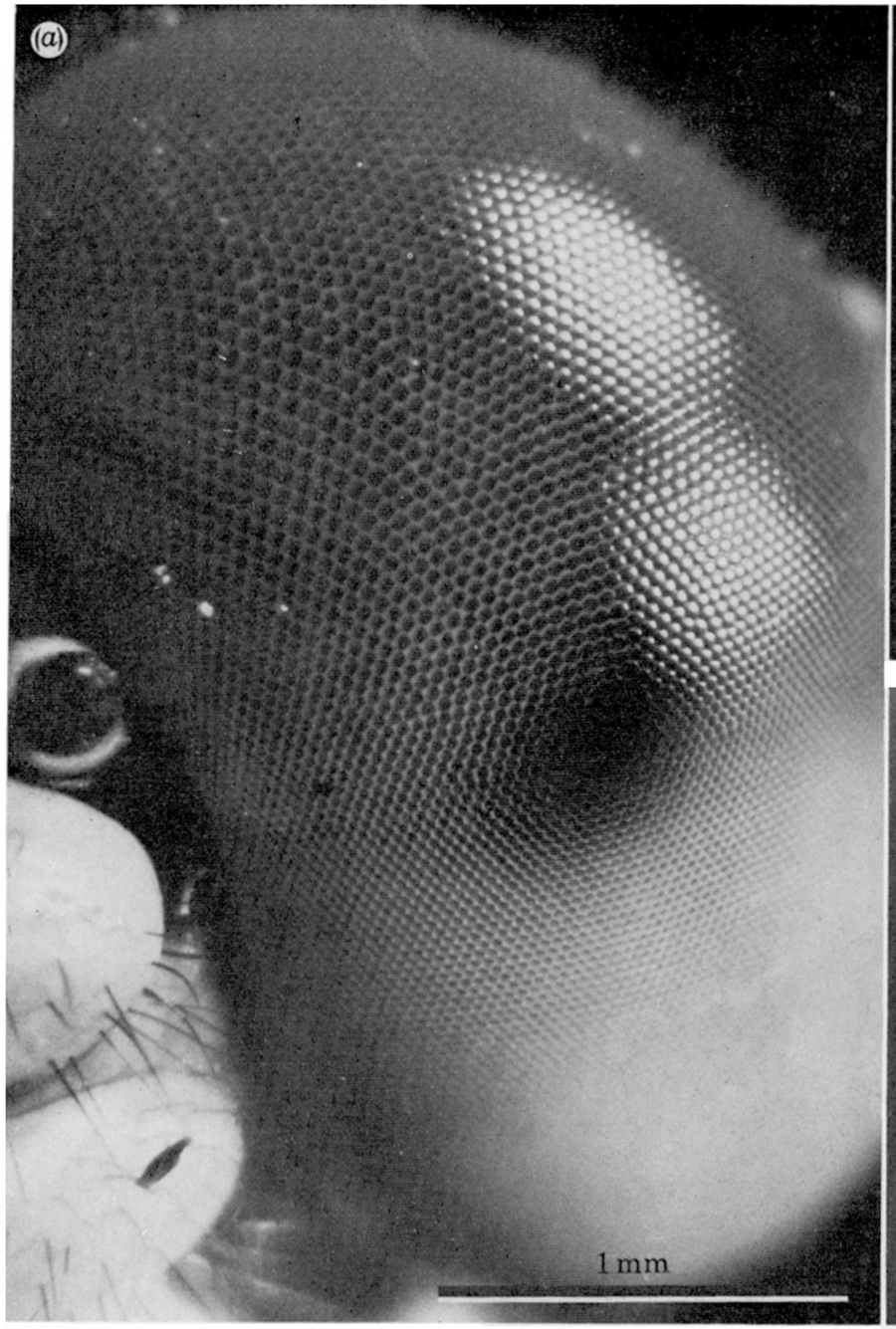


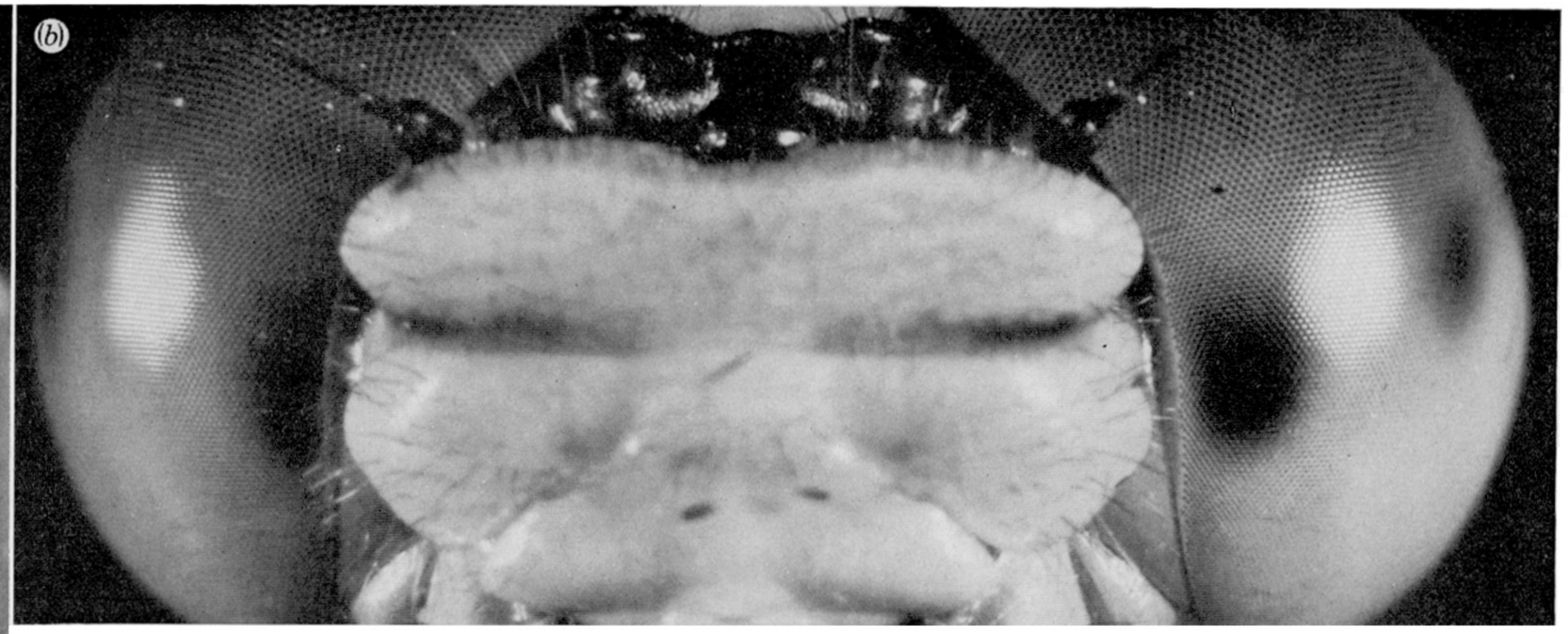


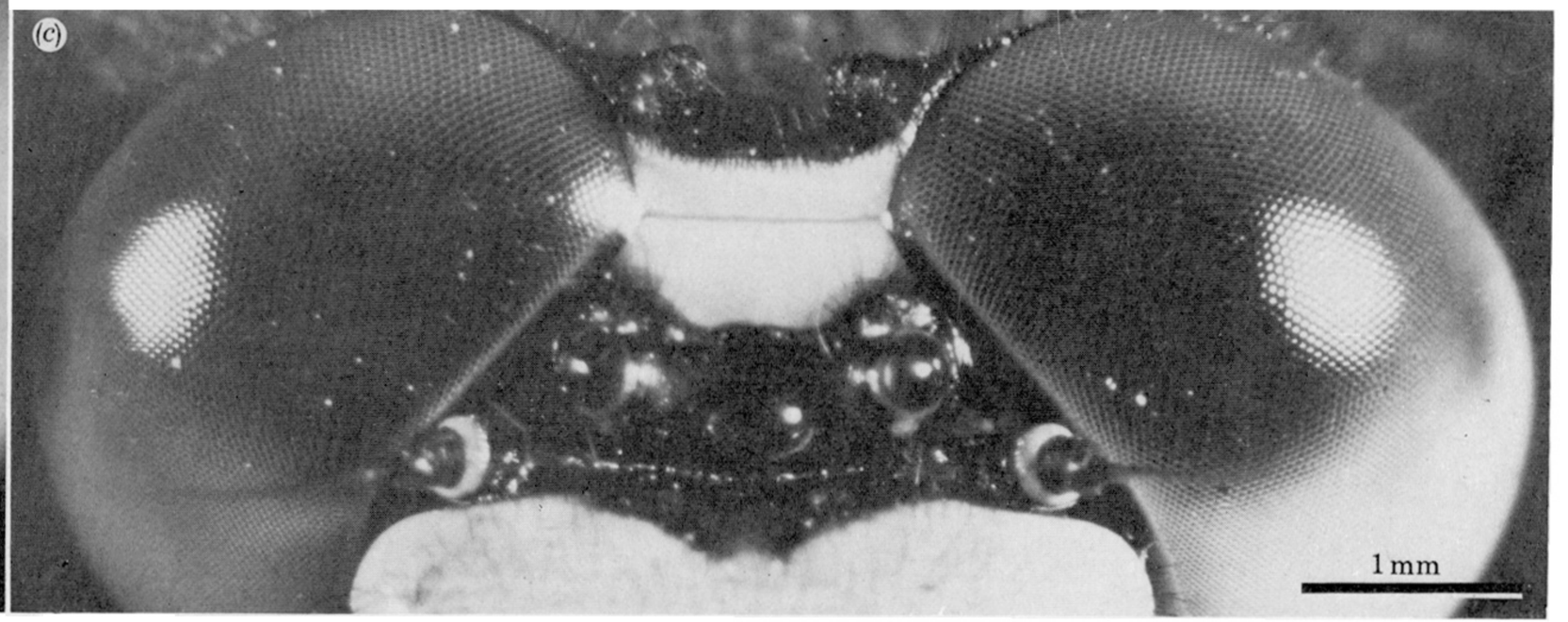


FIGURE 17. *Hemigomphus heteroclytus* Selys (gomphid), Odonata. (*a*) The great range of facet diameters, as in *Austrogomphus*. (*b*) The eyes, viewed from the front. The small forward looking acute zones are well separated, and the binocular overlap is small. (*c*) The large dorsal acute zones, which are also well separated, with at least 10° binocular overlap (see eye map, figure 18). Magnification of (*b*) the same as (*c*).

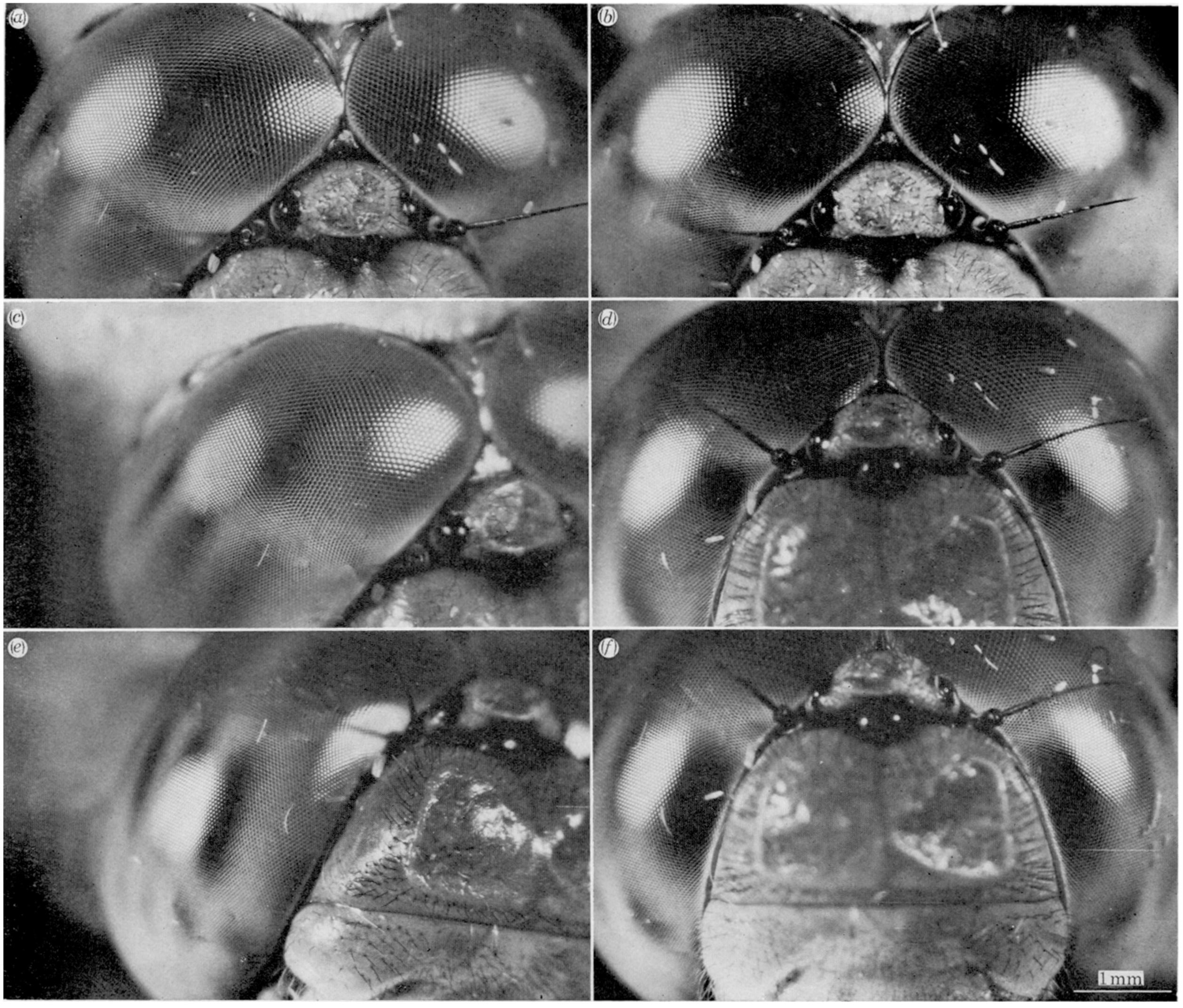


FIGURE 20. *Orthetrum caledonicum* (Brauer). The anterior regions of the eyes of a typical large dragonfly, photographed alive to show the different appearance of the pseudopupil and facets in different regions of the eye. (*a*), (*c*) and (*e*) are viewed from the right of the midline, (*b*), (*d*) and (*f*) are seen from on the midline. Axes as on figure 21; (*a*) 0° *D*V, 7.5° H (*b*) 0° *D*V, 0° H (*c*) 0° *D*V, 22.5° H (*d*) 25° *D*V, 0° H (*e*) 36° *D*V, 30° H (*f*) 36° *D*V, 0° H. (*a*)–(*f*) are all at the same magnification.

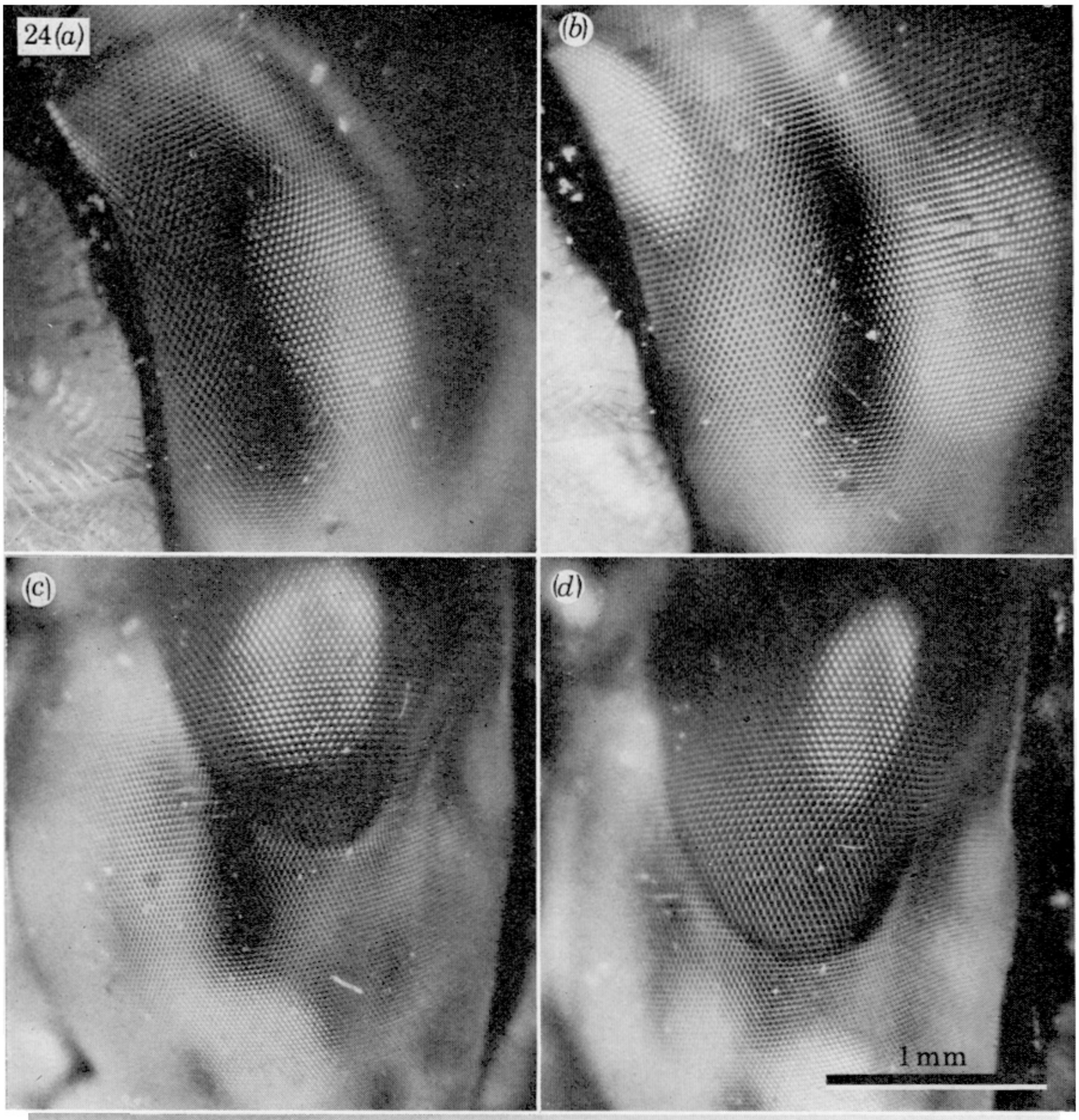


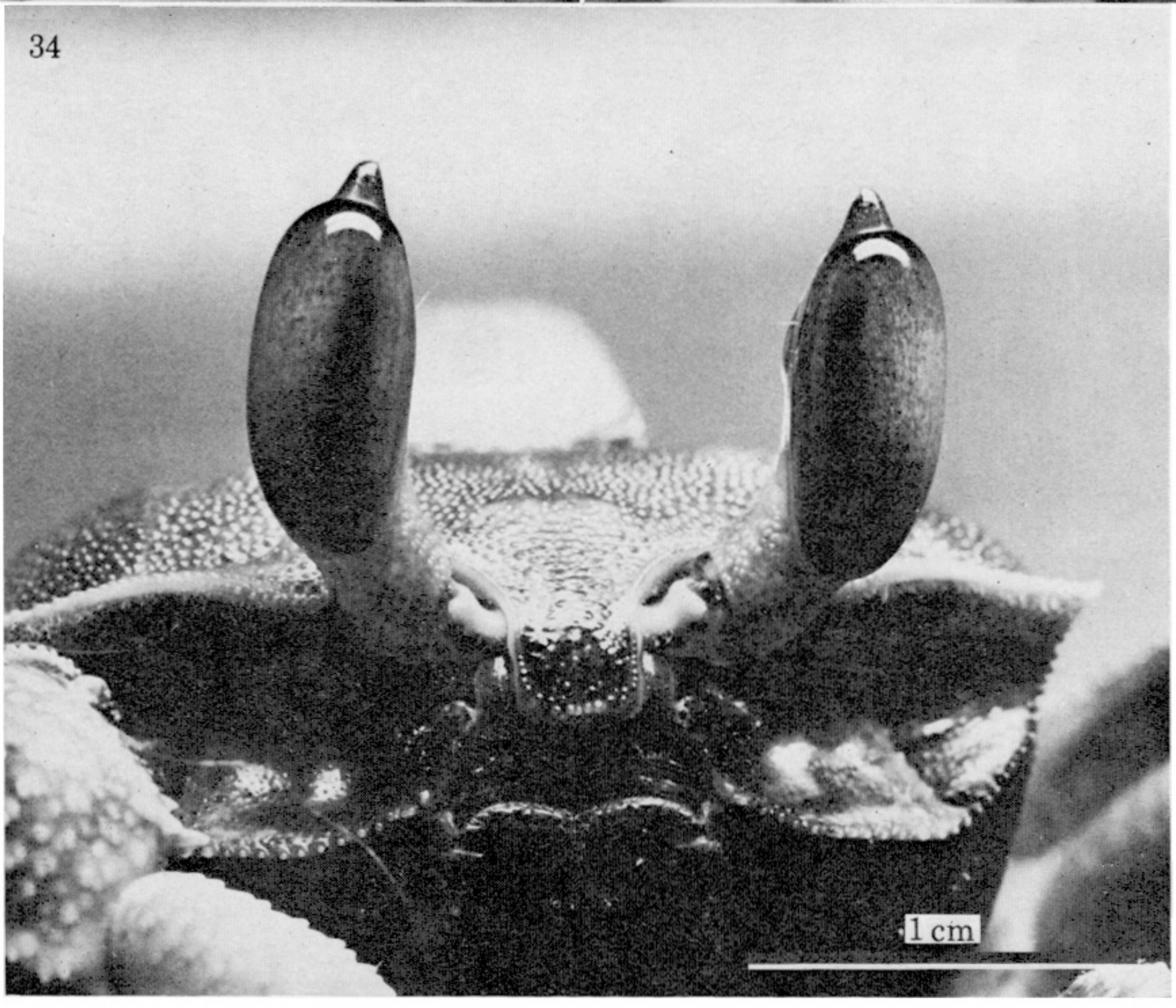


FIGURE 24. *Hemicordulia tau.* Selys (Corduliidae), Odonata, male. Change in shape of the pseudopupil as it moves along the part of the eye looking out at the horizon in level flight. (*a*) forward looking at 0° H, −60° V; (*b*) at 20° H, −60° V; (*c*) sideways looking at 90° H, −60° V, note the pseudopupil spreading across the lateral acute zone; (*d*) 100° H and −50° V, the pseudopupil is small, having now passed the acute zone. Note the changes in facet size. (*a*)–(*d*) are all at the same magnification. Angles as in figure 23.

FIGURE 34. *Ocypode ceratophthalma* female, from directly in front with the eyes erect and the camera on the same horizontal plane as the eyes. On this eye there are 160 horizontal rows of facets (Photograph W. Ribi).

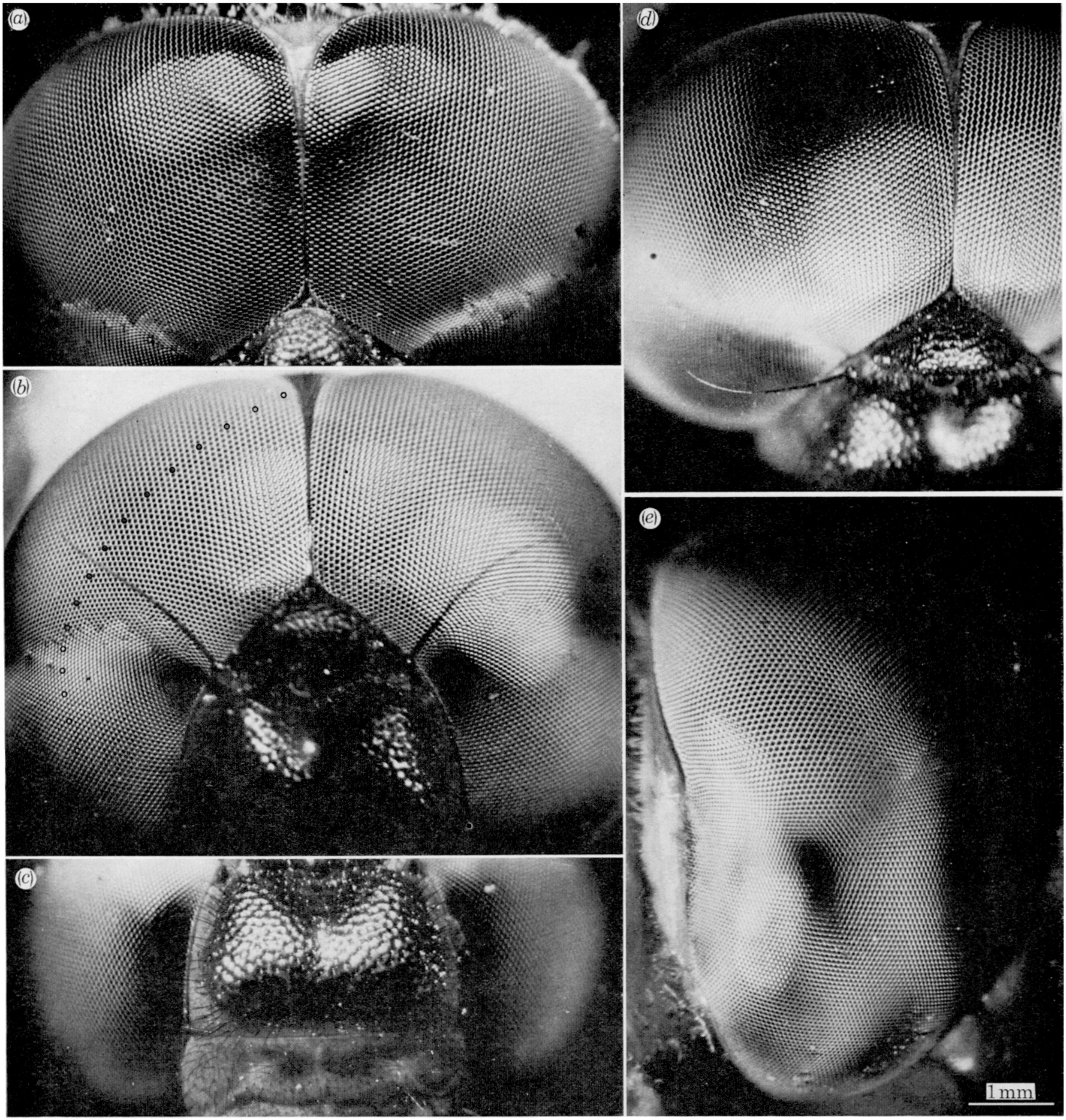


FIGURE 25. *Zyxomma obtusum* Albarda (Libellulidae), Odonata. The appearance of the pseudopupil in different regions of the living eye. Axes as figure 26; (*a*) lack of binocular overlap where the eyes meet dorsally, at 0° H, 55° *D*V; (*b*) the minimum pseudopupil at 0° H, 30° *D*V; (*c*) The forward looking pseudopupil near 0° H, 0° *D*V on the map; (*d*) part of the upward looking acute zone at 5° H, 60° *D*V; (*e*) the side of the eye lacks the sharply differentiated region of large facets, compare with *Hemicordulia*, figure 24). Features: eyes fused in the midline; facets large on absolute scale but no sharp gradients of facet size; region of obvious faults in the lines of facets behind the antenna in (*a*) and (*b*) but not on the side of the eye (*e*); uniform light colour of the eye, with pseudopupil visible in all regions. (*a*)–(*e*) are all at the same magnification.

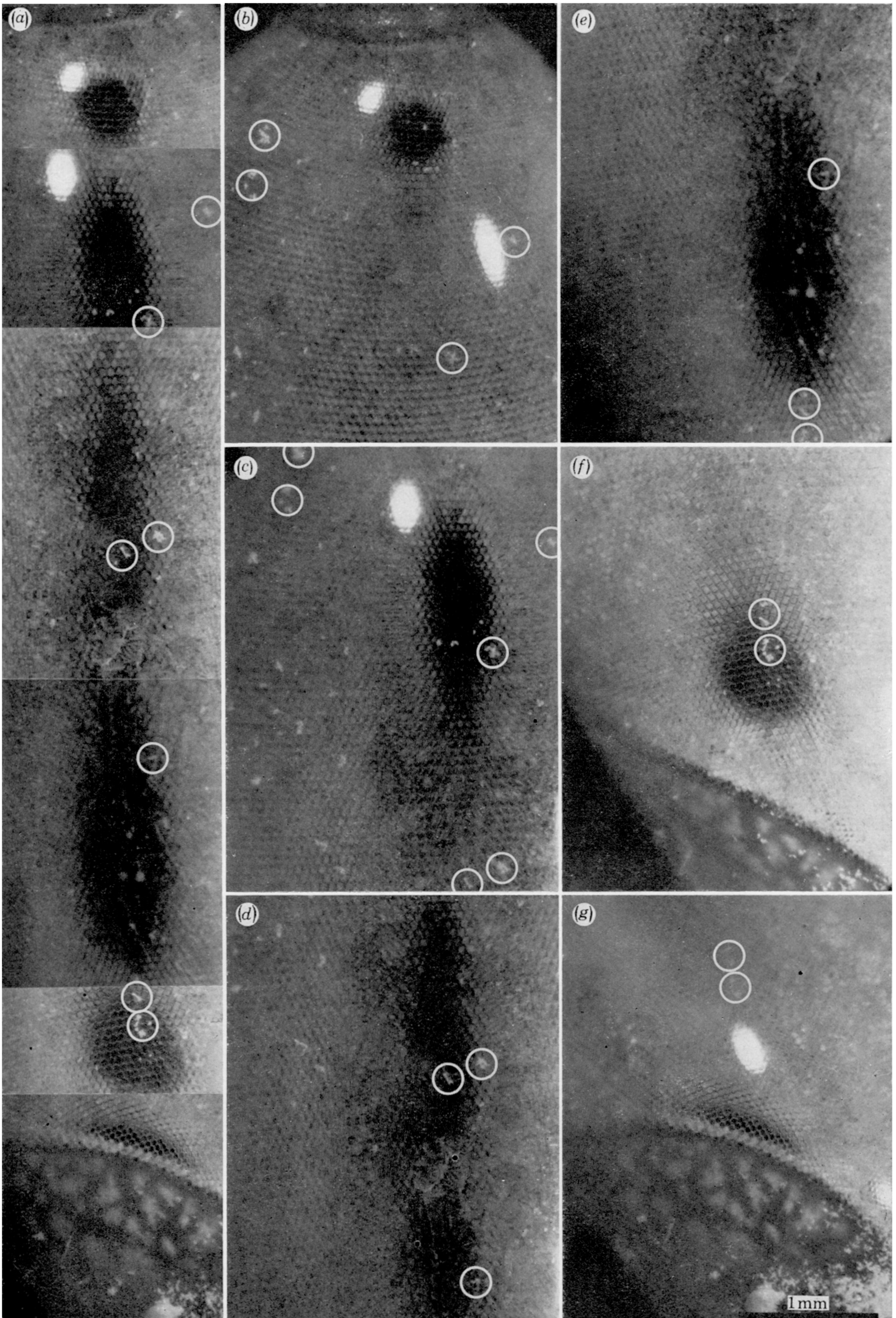


FIGURE 35. Pseudopupils of *Ocypode ceratophthalma*. (*a*) Assembled montage of 6 photographs of the eye at different angles, also shown in (*b*)–(*g*), along one vertical axis. (*b*) 30° above the acute zone, (*c*) 10° above the acute zone, (*d*) centred on the acute zone, (*e*) 5° below, (*f*) 30° below, (*g*) 60° below the acute zone. These pictures therefore cover a total of 90° in the vertical plane. Further axes, not shown, extend dorsally beyond an angle of 60° to the horizontal. Note that the facets are hexagonal, not square as in some crustaceans. (*a*)–(*g*) are all at the same magnification. The circles show the facet markers.

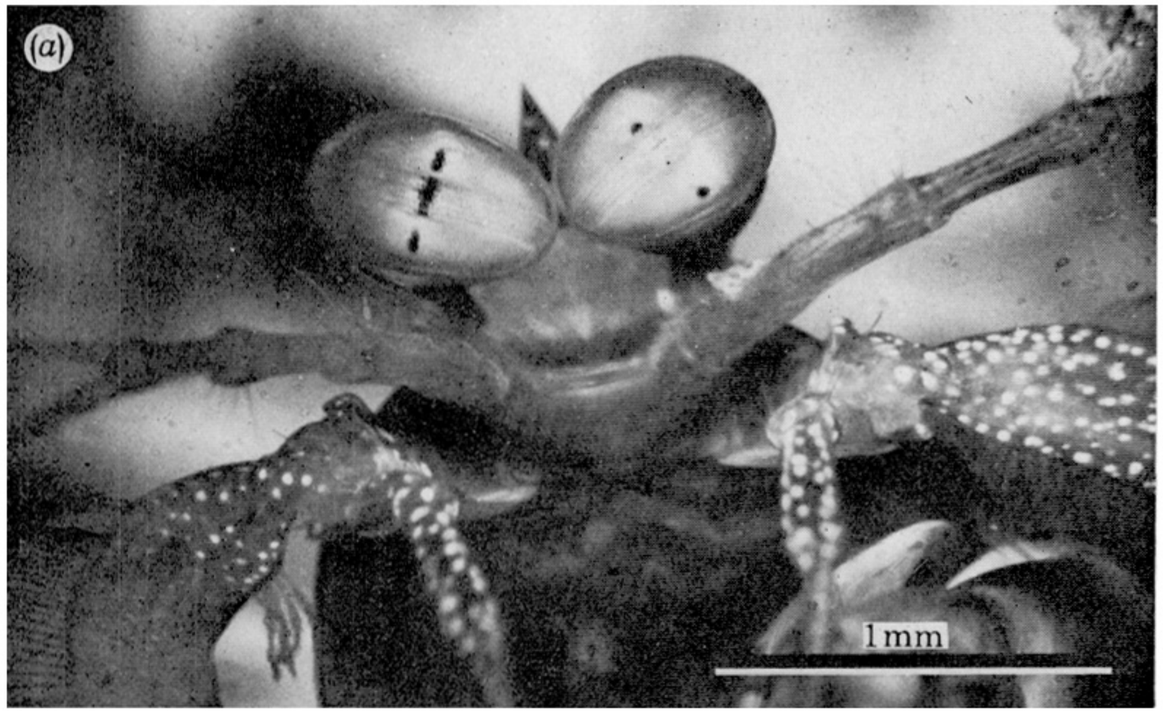


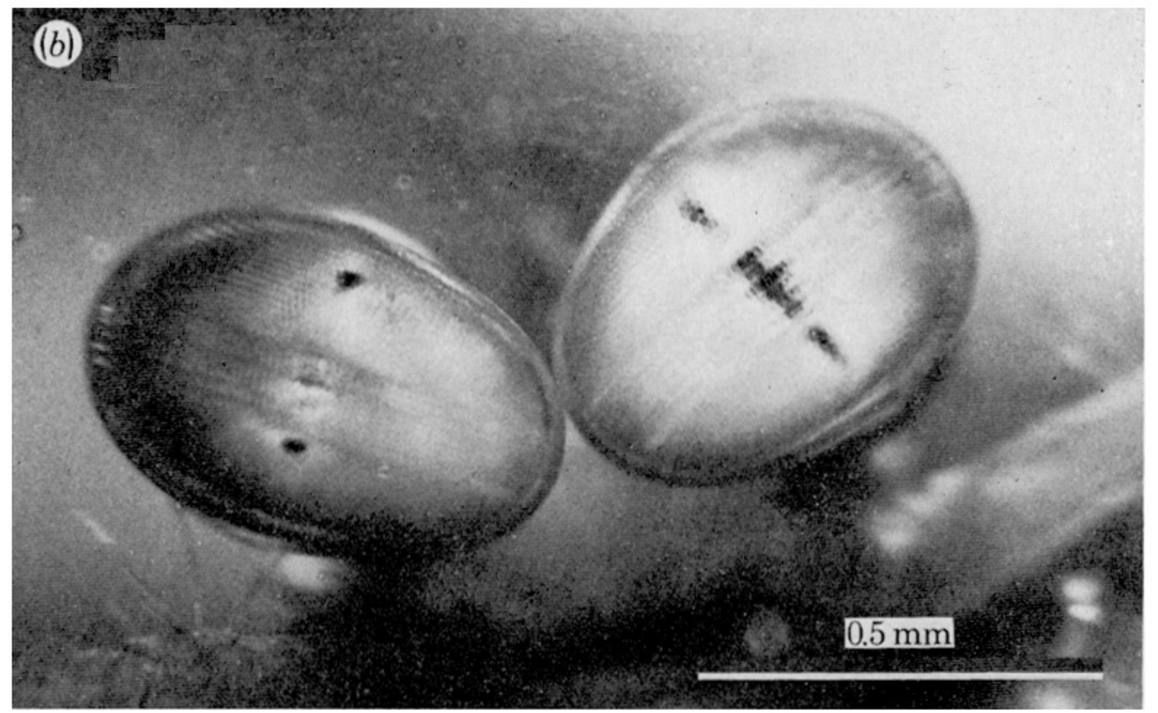


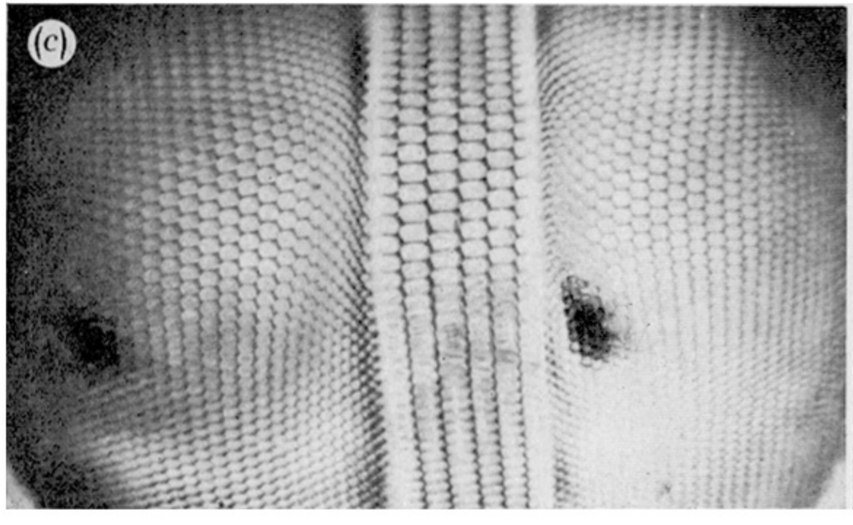


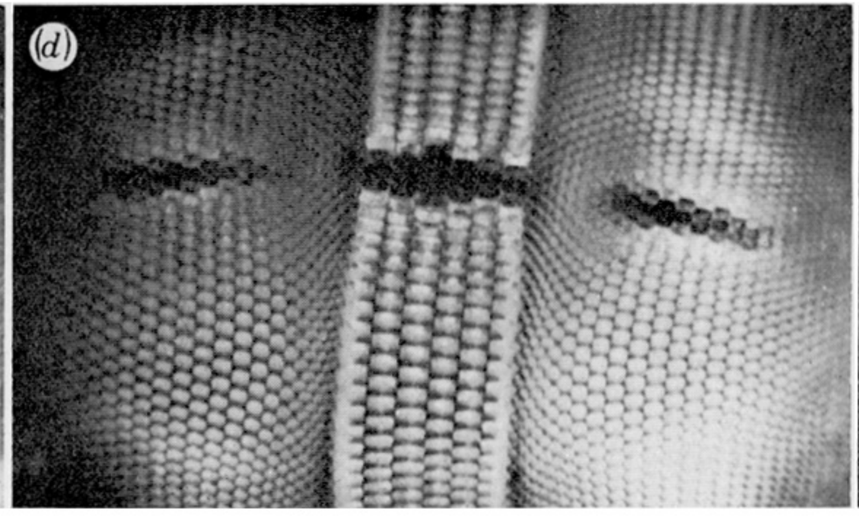


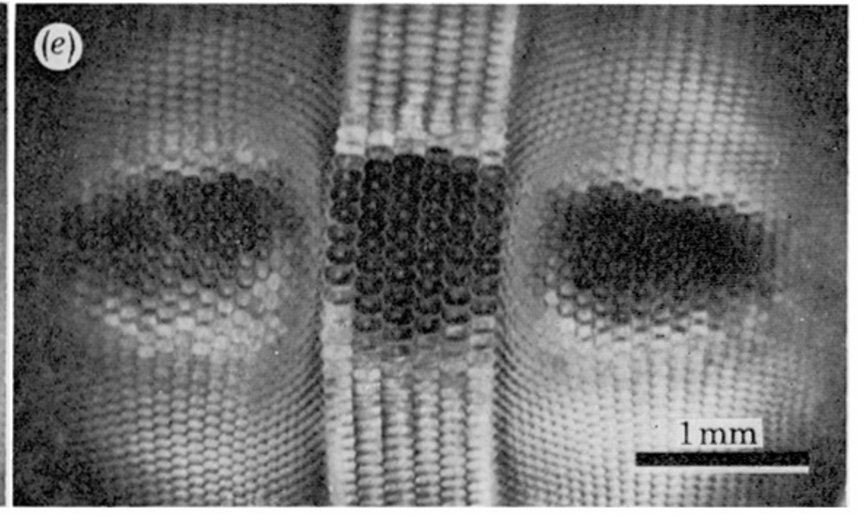


FIGURE 37. (*a*) and (*b*) *Gonodactylus chiragra* (Fabricius). (*c–e*) *Odontodactylus scyllarus* (Linnaeus). (*a*) *Gonodactylus* seen from the front, under water, with the central band of the right eye lined up with the camera. (*b*) the same animal with the eyes in a slightly different position. (*c*) *Odontodactylus*, right eye at 10°, 10°, from the acute zone. (*d*) at −15°, 0° from the acute zone (*e*) −1°, 0°, from the acute zone. Note the region of large facets at the three acute zones and that the axes of the centres of the three acute zones coincide. For illustration in colour see Horridge (1977*b*). (*c*), (*d*) and (*e*) are all at the same magnification.